



Project No. 037005



CECILIA

Central and Eastern Europe Climate Change Impact and Vulnerability Assessment

Specific targeted research project

1.1.6.3.I.3.2: Climate change impacts in central-eastern Europe

D4.2: Analysis of observational datasets and of a selection of pre-existing RCM data sets according to the decisions made in D4.1

Due date of deliverable: 1st December 2007

Actual submission date: 1st July 2008

Start date of project: 1st June 2006

Duration: 36 months

Lead contractor for this deliverable: Danish Meteorological Institute (DMI)

Revision [final]

Project co-funded by the European Commission within the Sixth Framework Programme (2002-2006)		
Dissemination Level		
PU	Public	X
PP	Restricted to other programme participants (including the	
RE	Restricted to a group specified by the consortium (including	
CO	Confidential, only for members of the consortium (including the Commission Services)	

CECILIA Deliverable 4.2: Analysis of observational datasets and of a selection of pre-existing RCM data sets according to the decisions made in D4.1

Lead partner for deliverable: DMI

Contributing partners: ETHZ, CUNI, CHMI, ELU, IAP, OMSZ, AUTH, NIMH, NMA

Final revision July 1st, 2008

D4.2.0 Overview

The present report contains sub-reports from the individual institutions contributing to CECILIA WP4. It has not been the intention at the present stage of the project to complete a systematic common analysis of extremes indices based on observations and model results. Rather, the main deliverable is the indices themselves, and this report serves as documentation for these indices.

During the calculation and documentation work aiming at the present report, some inconsistencies and ambiguities in the index list D4.1 were found. These have subsequently been discussed and resolved. As appendix A an updated list is enclosed.

A preliminary comparison of selected indices is presented as Appendix B. This consists of a collection of similar plots from the following sources: Observations from the Czech Republic (CHMI); observations from Hungary (OMSz); observations from Romania (NMA); the ECA&D database (ETHZ) and the reanalysis-based 25km-resolution regional climate simulation with the HIRHAM5 model from the ENSEMBLES project (DMI). The indices shown are 1, 2, 3, 76, 77, 78, 113 and 115 for both winter (DJF) and summer (JJA), and indices 58 and 66 for the entire year. All data correspond to the period 1961-1990. The amount of plots indicate the uniqueness of the present extensive collection of extremes indices for Central Europe.

D4.2.1 DMI

The Danish Meteorological Institute has been responsible for the calculation of D4.1 indices for regional climate model data stored in the PRUDENCE and ENSEMBLES-RT3 archives located at the DMI.

This has been done for the experiments where this was possible. Some of the ENSEMBLES RT3 experiments were missing monthly mean fields, or errors were found. In total, 10 PRUDENCE and 14 ENSEMBLES experiments were treated until now. The extended and updated list will lead to some recalculations being necessary, and some quality control still remains to be done.

As an example we show in Fig. 1.1 index 89, annual 99th wet-day precipitation percentile, for 8 ENSEMBLES simulations based on ERA-40 reanalysis boundaries in the period 1961-1990. The maps are quite similar with some exceptions: The SMHI model does not have as intense precipitation extremes at the Mediterranean coast as the other models. METNO in general has lower

values than most models. In the opposite end of the spectrum, the CHMI model exhibits the largest values in Northern Europe.

The present variable is just one out of more than 130 which have been calculated not just for the ENSEMBLES ERA-40 based simulations but also for the PRUDENCE time slices –30 years present-day climate and 30 years corresponding to 2071-2100 as simulated most commonly with the Hadley Centre models according to the SRES A2 scenario. These indices will at a later stage be calculated for the CECILIA high-resolution simulations.

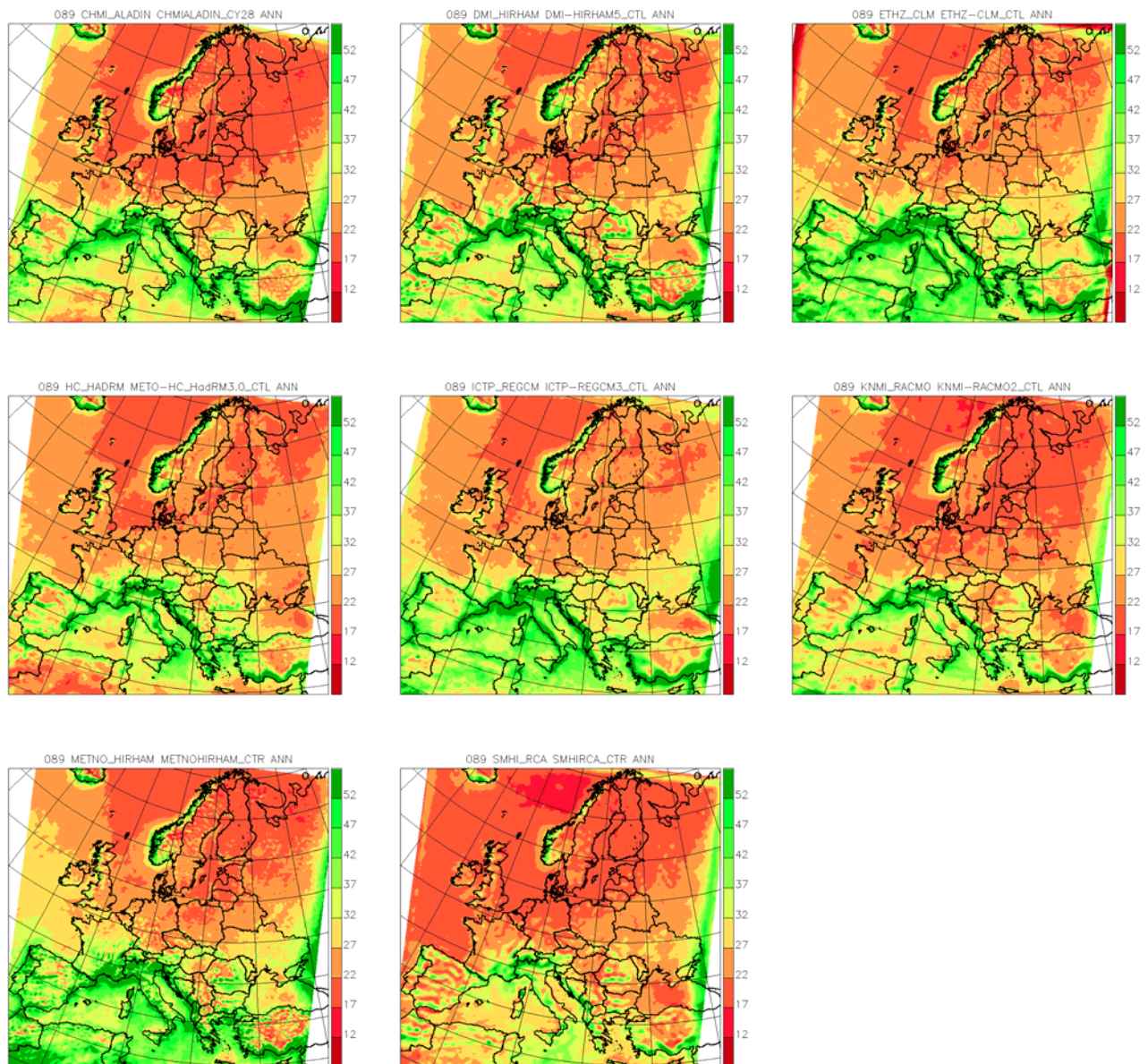


Figure 1.1 Annual 99th wet-day precipitation percentile for 8 ENSEMBLES simulations based on ERA-40 reanalysis boundaries in the period 1961-1990.

D4.2.2 ETH

Software testing

ETH was responsible for the testing of the software ProClimDB (Stepanek 2006), which is used in a batch job mode to process the indices for the daily station data by the WP4 members. This software was developed at the CHMI as part of CECILIA deliverable D4.2.

In parallel with the development of the batch job by CHMI, all 130 indices were also coded by ETH in the statistics environment R. Then the results from the two calculation procedures were successively compared and existing discrepancies were eliminated. As an example, Figure 2.1 shows a comparison of mean and heat wave duration indices computed with R and with the ProClimDB batch job. The color filled bars display the indices as calculated by R, and the hatched bars that are plotted over the filled bars refer to the ProClimDB results. The colors indicate the variable upon which the indices are based (TG: daily mean temperature; TX: daily maximum temperature; TN: daily minimum temperature; RR: daily precipitation; TXminusTN: daily temperature range). The indices from both calculation methods agree well in case of the mean (left panel). For the mean heat wave duration index, some minor discrepancies can be seen for the January, the DJF and the annual value, where ProClimDB shows slightly lower values than the R calculation.

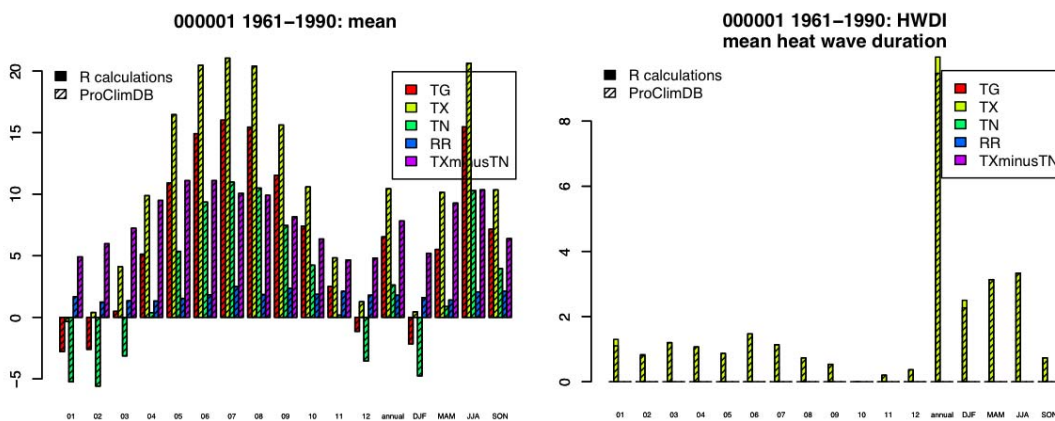


Figure 2.1: Example comparison of the indices calculation with ProClimDB and R for the period 1961–1990. (left) mean (indices 1–4 and 76); (right) mean heat wave duration (index 52). 000001 refers to the station number.

Index calculation

After the successful verification of the ProClimDB batch job, ETH was responsible for the calculation of the indices from the station data of the European Climate Assessment & Dataset (ECA&D) project (Klein Tank et al. 2002; <http://eca.knmi.nl/>). From the stations located in the Central and East European region, stations with at least 11 years of data and less than 20% of missing values have been selected. Almost 300 stations are fulfilling these criteria. For the daily time series of these stations, the indices were calculated using the ProClimDB batch job described above and will be submitted to the DMI data base after inclusion of the recent updates to index definitions (App. A).

Fig. 2.2 shows as an example the indices „heating degree days” and „percentage of wet days above 10 mm/day” calculated from ECA&D station data for the period 1961-1990 (annual time frame). It

can be seen that some parts of the CECILIA focus region have a relatively low station density in ECA&D. The additional observations from the local partners will help to fill these gaps.

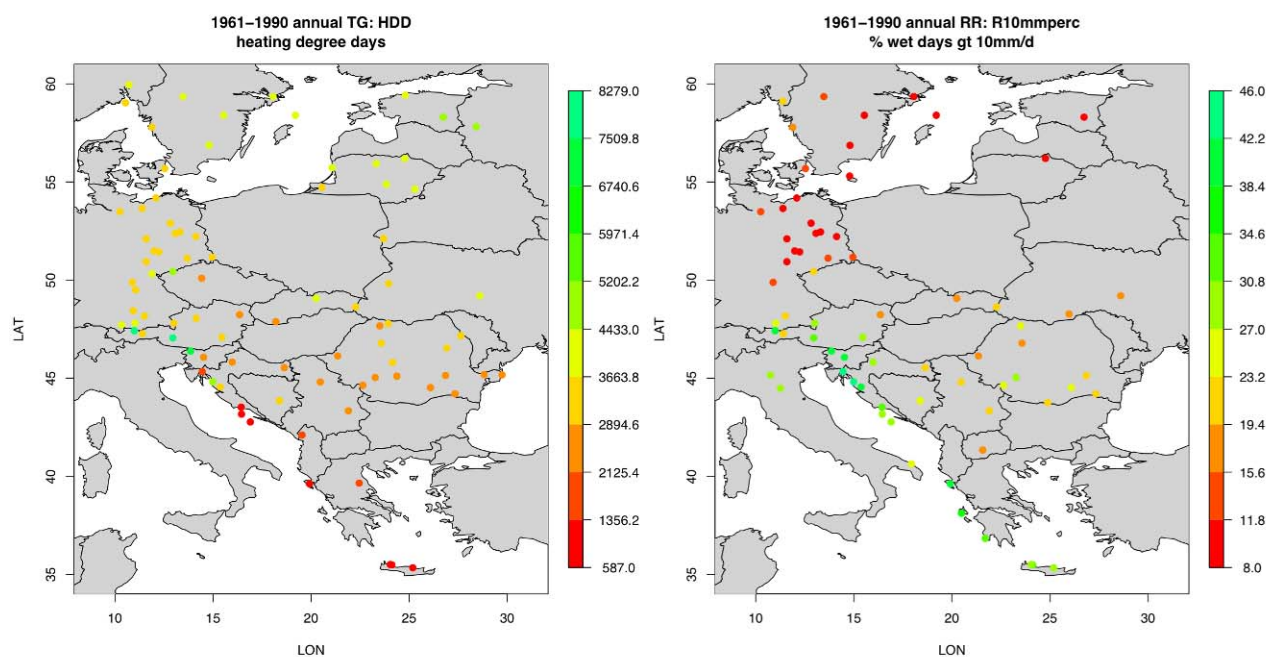


Figure 2.2: Indices „heating degree days” (left) and „percentage of wet days above 10 mm/day” (right) calculated from ECA&D daily station data for the period 1961-1990 (annual time frame).

References

Klein Tank, A., et al. (2002), Daily dataset of 20th-century surface air temperature and precipitation series for the European Climate Assessment, *Int. J. Climatol.*, **22**, 1441– 1453.
 Stepanek, P. (2006). ProClimDB – software for processing climatological datasets. CHMI, regional office Brno. <http://www.klimahom.com/software/ProcData.html>

D4.2.3 IAP and CHMI

The work at IAP concentrated on the development of extreme value models in existing regional climate model (RCM) outputs available from the PRUDENCE project database (16 control runs and 24 scenario runs of 10 RCMs; Table 3.1). The RCM outputs have a horizontal resolution of about 50 km; the only exceptions are the high-resolution runs of the HIRHAM model with a 25 km grid. A driving GCM for all RCM simulations was the Hadley Centre HadAM3 GCM; the RCAO RCM was driven also by the ECHAM4 GCM. The RCMs were run under SRES-A2 and SRES-B2 emission scenarios except for CLM, RACMO, CHRMs and REMO for which only SRES-A2 runs were available. We focused on extreme precipitation and a specific area of the Czech Republic where complex orography and an interaction of other factors governing the occurrence of heavy precipitation events result in patterns that cannot be captured by global models.

Table 3.1. RCMs examined and their basic characteristics. A2/B2 stands for the SRES emission scenarios.

RCM	Developed at	Resolution	Driving GCM	Examined runs
HadRM	Met. Office, Hadley Centre for Climate Prediction and Research	0.44°	HadAM3P	control (1960-90), 3 ensemble runs

HIRHAM	Danish Meteorological Institute (DMI)	0.44°	HadAM3H	A2 (2070-2100), 3 ensemble runs
				B2 (2070-2100) control (1961-90), 3 ensemble runs
CHRM	Swiss Federal Institute of Technology (ETH)	0.22°	HadAM3H	A2 (2071-2100), 3 ensemble runs
				B2 (2071-2100) control (1961-90)
PROMES	Complutense University of Madrid (UCM)	50 km	HadAM3H	A2 (2071-2100) control (1960-90)
				A2 (2071-2100)
RCAO	SMHI Rossby Centre	0.44°	HadAM3H	A2, B2 (2070-2100) control (1961-90)
				ECHAM4/OPYC control (1961-90)
ARPEGE	European Centre for Medium-Range Weather Forecasts (ECMWF)	50-70 km (in Europe)	observed SST	A2, B2 (2071-2100) control (1961-90)
				HadCM3 ARPEGE/OPA B2 (2071-2100)
CLM	GKSS Forschungszentrum	0.5°	HadAM3H	A2 (2071-2100) control (1961-90)
				A2 (2071-2100)
RegCM	Abdus Salam Int. Centre for Theoretical Physics (ICTP)	50 km	HadAM3H	A2 (2071-2100) control (1961-90)
				A2, B2 (2071-2100)
RACMO	Royal Dutch Meteorological Institute (KNMI)	0.44°	HadAM3H	A2 (2071-2100) control (1961-90)
				A2 (2071-2100)
REMO	Max Planck Institute (MPI)	0.5°	HadAM3H	A2 (2071-2100) control (1960-90)
				A2 (2071-2100)

The ‘peaks-over-threshold’ (POT) and ‘block-maxima’ approaches (e.g. Coles, 2001) to estimating probabilities and multi-year return levels of extreme daily precipitation were compared. Most up-to-now studies on extremes in RCM outputs over Europe have been confined to the block-maxima method (Booij, 2002; Huntingford et al., 2003; Semmler and Jacob, 2004; Ekström et al., 2005; Frei et al., 2006; Halenka et al., 2006; Beniston et al., 2007; Buonomo et al., 2007; Goubanova and Li, 2007); exceptions of using the POT approach were the studies of Paeth and Hense (2005) who examined daily extremes in the REMO model in the Mediterranean area, and May (2007) who analyzed daily extremes in the HIRHAM model over Europe.

We have found the POT method preferable since it leads to more robust estimates of distributions of extremes. It makes more efficient use of available data as all observations (cluster maxima) exceeding a sufficiently high threshold, respecting a given minimum distance between selected

events so that their independence is preserved, are taken into account. The method results in the Poisson process model for event arrivals, and utilizes the Generalized Pareto (GP) distribution for their magnitudes. Increasing threshold censoring (proposed by Begueria, 2005) was found particularly useful as the results do not depend on the (rather subjective) choice of the threshold used to delineate extremes. Minimum separation time ('deadtime') between events was determined from results of the test on the dispersion index (Cunnane, 1979) – for the deadtime of 1 day in JJA and 2 days in DJF the selected events were found usually independent in the RCM outputs. The fact that the deadtime of 1 day is not suitable in DJF points to the fact that the control RCM outputs reproduce the observation that precipitation extremes are more clustered in DJF than JJA.

We examined scenarios of changes in extreme daily precipitation for the late 21st century (2071-2100) in 24 future climate runs of the 10 RCMs, focusing on uncertainties related to the inter-model and within-ensemble variability and the use of the SRES-A2 and SRES-B2 emission scenarios (Table 3.2). The results show that

- heavy precipitation events are likely to increase in severity in DJF and (with less agreement among models) also in JJA;
- the inter-model and intra-model variability (and related uncertainties) in the pattern and magnitude of the change is large;
- in most scenario runs, the projected change in extreme precipitation in JJA is of the opposite sign than a change in mean seasonal totals, the latter pointing towards generally drier conditions in JJA; a combination of enhanced heavy precipitation amounts and reduced water infiltration capabilities of a dry soil may severely increase peak river discharges and flood-related risks in this region.

(see also Figures 3.1 and 3.2)

The projected changes were also compared with those observed over the recent decades (1961-2005) in the area under study. The climate change scenarios possess several basic features in common with the recently observed precipitation trends; this finding may contribute to credibility of the future projections (assuming that climate change has already been under way in recent decades). The observed changes over 1961-2005 that agree with climate change scenarios are mainly

- increasing trends in heavy precipitation indices as well as mean seasonal precipitation in DJF;
- increasing but weaker and spatially much less coherent trends in heavy precipitation indices in JJA;
- positive trends in heavy precipitation in JJA being stronger in the western part of the area.

Table 3.2. Mean relative changes of 50-yr return daily precipitation between the late 21st century scenario and control climate (1961-1990) in individual model runs, averaged over all grid boxes in the examined area. A2/B2 stands for the SRES emission scenarios; # denotes ensemble member. A driving GCM is given in parentheses if different from the HadAM/HadCM model.

RCM	JJA [%]	DJF [%]	RCM	JJA [%]	DJF [%]
HadRM, A2, #1	-4.8	19.2	RCAO (ECHAM), A2	-12.5	24.7
HadRM, A2, #2	5.6	24.3	RCAO (ECHAM), B2	3.1	45.6
HadRM, A2, #3	21.9	14.1	RCAO, A2	33.0	45.5
HadRM, B2	-7.1	-3.9	RCAO, B2	9.5	42.9

HIRHAM, A2, #1	36.8	21.3	ARPEGE, A2	6.6	19.7
HIRHAM, A2, #2	33.0	32.2	ARPEGE, B2	21.8	-1.7
			ARPEGE (ARPEGE/OPA),		
HIRHAM, A2, #3	17.3	26.9	B2	10.6	6.4
HIRHAM, B2	27.3	14.5	CLM, A2	16.4	16.6
HIRHAM, A2, high-res	39.6	17.5	RegCM, A2	18.3	28.9
CHRM, A2	47.8	20.7	RegCM, B2	18.4	35.2
PROMES, A2	43.5	20.4	RACMO, A2	35.6	18.9
PROMES, B2	22.5	24.9	REMO, A2	40.8	25.0

Main conclusions

The study shows that current RCM outputs should be interpreted with caution as regards changes in heavy precipitation at least in central Europe, since large inter-model differences appear in the future projections. The results for the late 21st century climate are much more model-dependent in JJA than DJF due to the enhanced role of the RCM formulation, particularly regarding parameterization of convective processes, on the simulated changes. Large differences in future scenarios of heavy precipitation appear also among ensemble members of a given RCM with a single emission scenario and the same driving GCM. Nevertheless, the basic features of the scenarios tend to agree with precipitation trends recently observed in the area, which may somewhat strengthen their credibility.

The magnitudes of the projected relative increases are comparable in JJA and DJF, the latter being the season when a relatively robust pattern of a positive change emerges in the RCM runs. Nevertheless, as increases are projected to be more likely also in JJA, which may severely impact on society and ecosystems due to related increases in the frequency and magnitude of floods, much attention should be paid to the further development of the RCMs (in terms of both increasing horizontal resolution in order to better reproduce orography and land use, and enhancing physical parameterizations employed) and a subsequent refinement of the future scenarios. In the current set of RCMs (except for the high-resolution HIRHAM), model orography fails to capture some important regional features, and the relatively narrow mountain chains in the southwest, north and northeast of the Czech Republic (reaching or exceeding 1400 m a.s.l.) are smoothed or even missing in some RCMs.

We also point out the fact that the increases in high quantiles of precipitation in summer are more coherent and statistically more significant in the high-resolution (25 km) HIRHAM model compared to any other (lower-resolution) RCM output under study, which may be related to a better representation of orography.

The POT approach has been found useful for estimating future changes in high quantiles of daily precipitation amounts (e.g. 50-year return levels), and could be applied also into simulations of RCMs with the very high resolution.

More details are given in a paper submitted to TAC:

Kyselý J., Beranová R.: Climate change effects on extreme precipitation in central Europe: uncertainties of scenarios based on regional climate models. *Theor. Appl. Climatol.* (accepted)

References

- Beguieria S (2005) Uncertainties in partial duration series modelling of extremes related to the choice of the threshold value. *J. Hydrol.* **303**: 215-230
- Beniston M, Stephenson DB, Christensen OB, Ferro CAT, Frei C, Goyette S, Halsnaes K, Holt T, Jylhä K, Koffi B, Palutikof J, Schöll R, Semmler T, Woth K (2007) Future extreme events in European climate: an exploration of regional climate model projections. *Clim. Change* **81**: 71–95
- Booij MJ (2002) Extreme daily precipitation in western Europe with climate change at appropriate spatial scales. *Int. J. Climatol.* **22**: 69-85
- Buonomo E, Jones R, Huntingford C, Hannaford J (2007) On the robustness of changes in extreme precipitation over Europe from two high resolution climate change simulation. *Q. J. R. Meteor. Soc.* **133**: 65-81
- Coles S (2001) An Introduction to Statistical Modeling of Extreme Values. London: Springer Verlag, 208 pp
- Cunnane C (1979) A note on the Poisson assumption in partial duration series models. *Water Res. Res.* **15**: 489-494
- Ekström M, Fowler HJ, Kilsby CG, Jones PD (2005) New estimates of future changes in extreme rainfall across the UK using regional climate model integrations. 2. Future estimates and use in impact studies. *J. Hydrol.* **300**: 234-251
- Frei C, Schöll R, Fukutome S, Schmidli J, Vidale PL (2006) Future change of precipitation extremes in Europe: Intercomparison of scenarios from regional climate models. *J. Geophys. Res.* **111**: D06105, doi:10.1029/2005JD005965
- Goubanova K, Li L (2007) Extremes in temperature and precipitation around the Mediterranean basin in an ensemble of future climate scenario simulations. *Glob. Planet. Change* **57**: 27–42
- Halenka T, Kalvova J, Chladova Z, Demeterova A, Zemankova K, Belda M (2006) On the capability of RegCM to capture extremes in long term regional climate simulation – comparison with the observations for Czech Republic. *Theor. Appl. Climatol.* **86**: 125-145
- Huntingford C, Jones RG, Prudhomme C, Lamb R, Gash JHC, Jones DA (2003) Regional climate model predictions of extreme rainfall for a changing climate. *Q. J. R. Meteorol. Soc.* **129**: 1607-1622
- May W (2007) The simulation of the variability and extremes of daily precipitation over Europe by the HIRHAM regional climate model. *Glob. Planet. Change* **57**: 59–82
- Paeth H, Hense A (2005) Mean versus extreme climate in the Mediterranean region and its sensitivity to future global warming conditions. *Meteorol. Z.* **14**:329-347
- Semmler T, Jacob D (2004) Modeling extreme precipitation events – a climate change simulation for Europe. *Glob. Planet. Change* **44**: 119-127

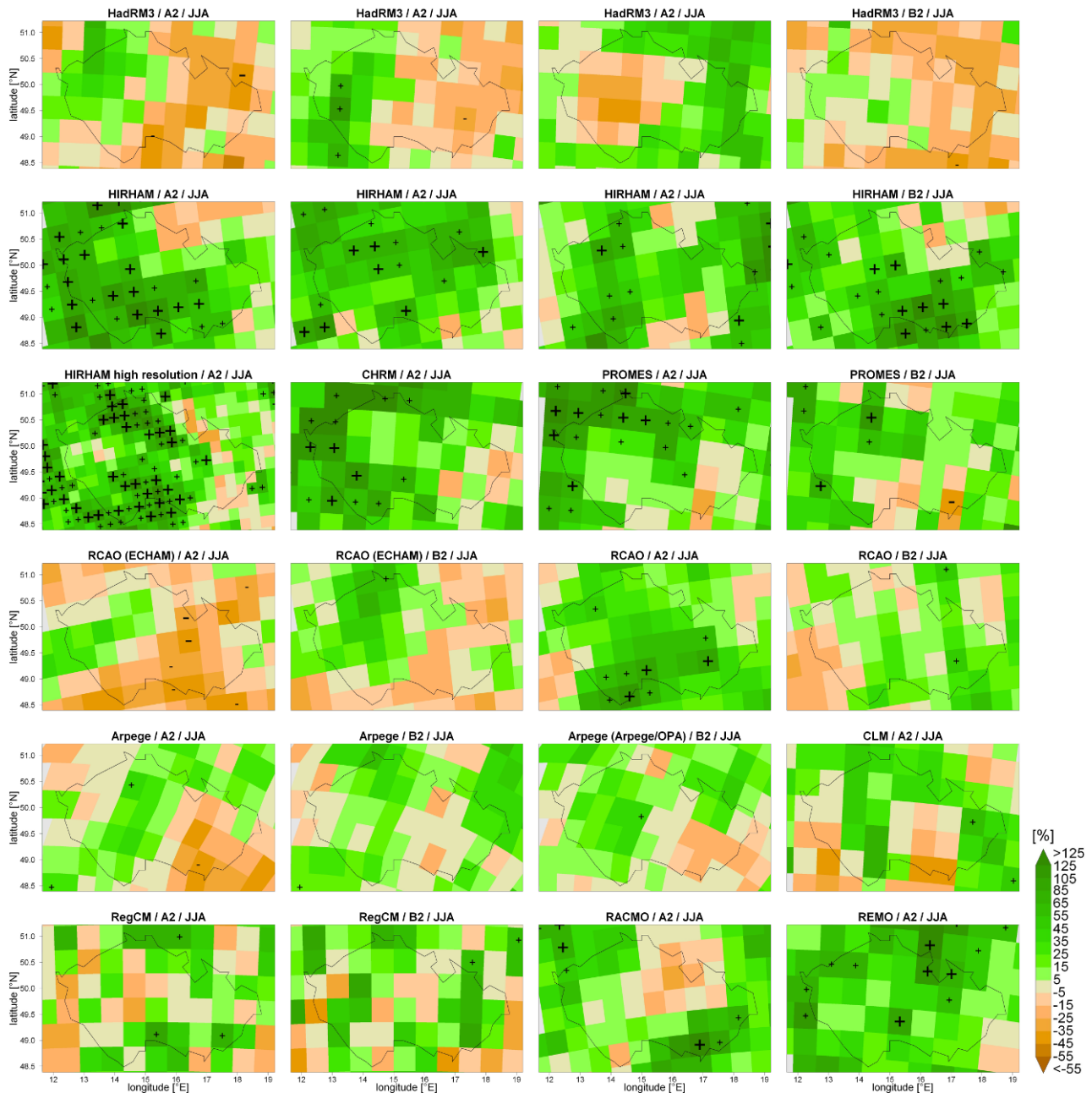


Figure 3.1 Relative changes (in %) of 50-yr return values of daily precipitation amounts between the late 21st century scenario and control climate (1961-1990) in summer (JJA). A2/B2 denotes the SRES emission scenarios; a driving GCM is given in the heading of panels if different from the HadAM/HadCM model (see also Table 3.1). Larger (smaller) crosses indicate gridboxes in which the estimated 90% (80%) confidence intervals of the 50-yr return values do not overlap, i.e. the change is statistically significant approximately at the 0.01 (0.07) level.

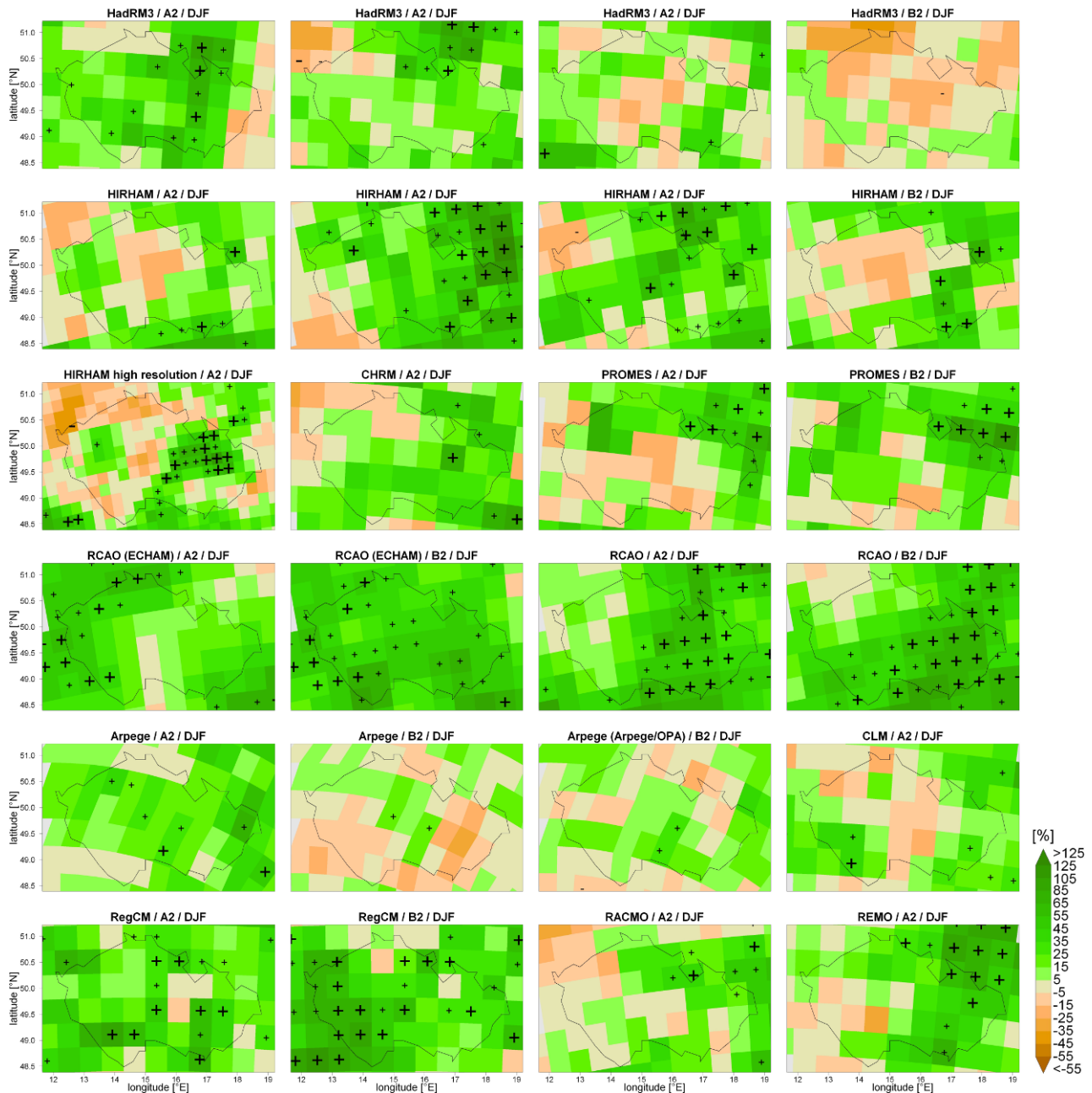


Figure 3.2. Same as in Fig. 3.1 except for winter (DJF).

D4.2.4 OMSz: Climate indices calculations on gridded data in Hungary

- List of indices:
 - Temperature: 1, 2, 3, 4, 46, 47, 58, 59, 66, 63, 65, 61, HWFI, 56, 60, 64
 - Precipitation: 76, 77, 78, 101, 102, 103, 104, 120, 122, 123, 118, 119
- Yearly and seasonal output
- Data covered the period 1901-2007

A list of climate indices to detect changes has been defined in the frame of Cecilia with using the experiences of several international projects on climate change. Climate index calculations require at least daily resolution of homogeneous time series, without inhomogeneities, such as transfer of stations, changes in observation practice. In many cases the characteristics of the estimated linear

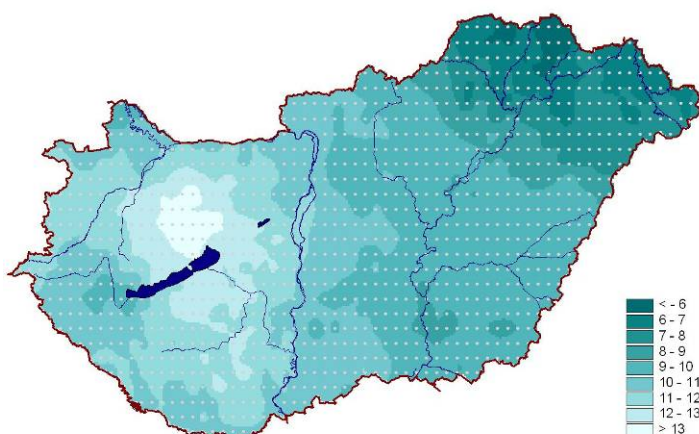
trends are unambiguously unlike to the original and homogenized time series (Lakatos, M. et al, 2007). Long time homogenized daily maximum, minimum and daily mean temperature data series and homogenized daily precipitation sums were examined. We present the result of climate index calculations on gridded (interpolated) daily data.

Trends of indices series

Temperature and precipitation indices calculations were extended on $0.1^\circ \times 0.1^\circ$ gridded (interpolated) daily data. This resolution matches to 10 km x 10 km approximately. Gridding of homogenized daily data series (Szentimrey, 2008) was carried out by method MISH (Meteorological Interpolation based on Surface Homogenized Data Basis; Szentimrey, Bihari, 2007) interpolation procedure. Note that the daily observations were interpolated, not the extreme indices, hereby the gridding not conflicts that the extreme events are local phenomena, interpolation of them is not suggested.

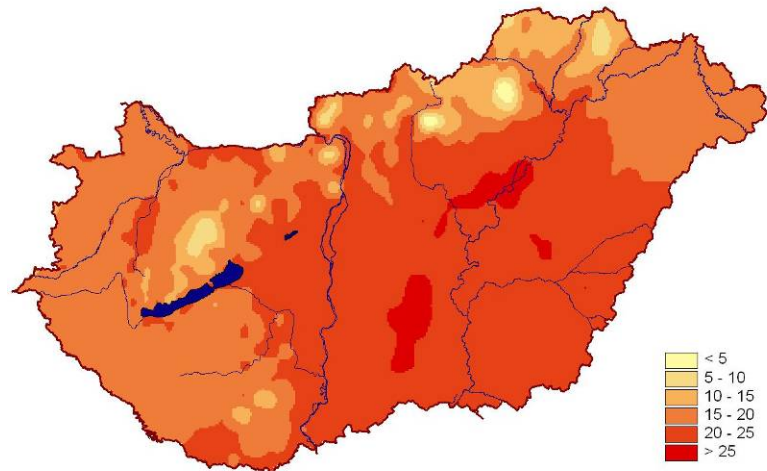
About 1000 grid points cover Hungary; therefore the technical implementation is more complex, than analysing station series. The indices series has to be calculated in every grid point at the first, and then follows the linear trend analysis of indices series. The method of climate indices calculations is illustrated on gridded (interpolated) daily data (*Figure 4.1*). The whole period change of the percentage of days with $T_{min} > 90$ th percentile, where 90th percentile is taken from all values for 5-day window around calendar day within base period from the middle of the last century is shown in grid points, and smoothed in the *Figure 4.1*. The grid point values of change calculated from the estimated linear trend, well demonstrate the method we have used and upon which we report.

Figure 4.1. Changes in the index 65 (D4.1) in 1961-2007 periods in grid points and smoothed



It can be seen in *Figure 4.1* that the percentage of days with high daily minimum notably increased, except in the north-east part of the country. The changes from 1976 in Hungary are substantial, because the warming tendencies came forward in parallel with the last most intensive global temperature increasing from the middle seventies.

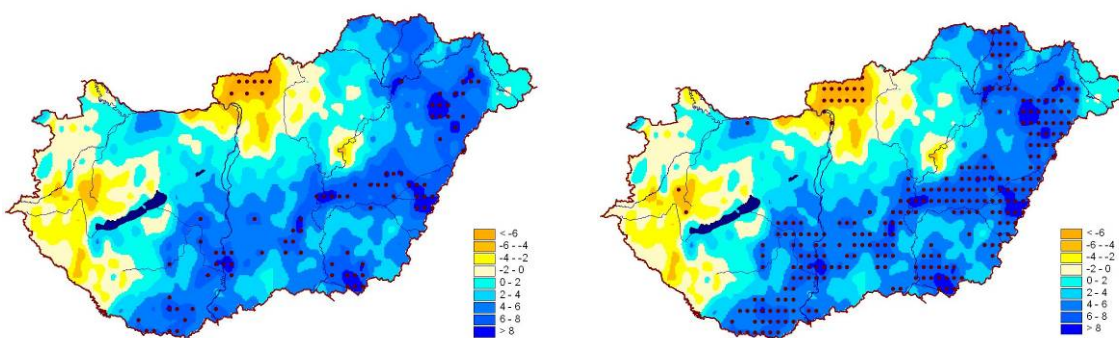
Figure 4.2. Change in the index 66 (D4.1) %age of days with $T_{max} \geq 30C$



South region of Kiskunság and in the division of Nagykunság considerably, some 25 % more hot days occur.

One of the precipitation index change, based on the gridded daily sum, is shown in *Figure 4.3*. In the East part of the country, in the Great plain region, and in the South-Transdanubian region we have to face more heavy rain. The dots show the significant change on 90% confidence level on the left, and on 80% confidence level on the right.

Figure 4.3. Change in the index 99 (D4.1) Fraction of total precipitation above annual 95th percentile



Remarkable, that using MISH interpolation we obtain a method to compare the observations and climate model simulations on a grid, in aspect of frequency and intensity of climate extremes.

Maps for the period 1961-90
Bihari Zita, Szentimrey Tamás

Homogenization procedure

The original MASH (Multiple Analysis of Series for Homogenization) procedure has been developed for homogenization of monthly series. MASH is a relative method and depending on the distribution of examined meteorological element additive (e.g. temperature) or multiplicative (e.g. precipitation) model can be applied. In the software the following subjects were elaborated for monthly data series: comparison of series, break point (change point) and outlier detection, correction of series, missing data complementing, automatic usage of metadata and a verification procedure to evaluate the homogenization results.

The new version MASHv3.01 (Szentimrey, 2006) has been developed also for homogenization of daily series as well as for quality control of daily data and missing data complementing. The present MASHv3.01 is suitable for daily temperature elements, since normal distribution is assumed and additive model can be applied in the procedure.

The procedure consists of the following steps.

1. Monthly means from daily data.
2. MASH homogenization procedure for monthly series, estimation of monthly inhomogeneities.
3. On the basis of estimated monthly inhomogeneities, continuous (smooth) estimation for daily inhomogeneities.
4. Homogenization of daily data.
5. Quality control for homogenized daily data.
6. Missing daily value complementing.
7. Monthly means from homogenized, controlled and complemented daily data.
8. Test of homogeneity for the new monthly series by MASH homogenization procedure. Repeating steps if it is necessary.

Besides the PC version of the MASH the daily data homogenization procedure and the ECA indices has been built into the Climate Database of the Hungarian Meteorological Service, as well.

MISH (Meteorological Interpolation based on Surface Homogenized Data Basis) interpolation procedure

The Main Features of MISHv1.01

I. Spatial Modelling Subsystem

1. Based on long homogenized data series and model variables.
2. Modelling procedure must be executed only once before the interpolation applications.

II. Spatial Interpolation System

3. Additive (e.g. temperature) or multiplicative (e.g. precipitation) model and interpolation formula can be used depending on the climate elements.
4. Daily, monthly, annual values and many years' means can be interpolated.
6. Few predictors are also sufficient for the interpolation.
7. The expected interpolation error is modelled too.
8. Capability for application of background information such as satellite, radar, forecast data.
10. gridding possibility.

Data

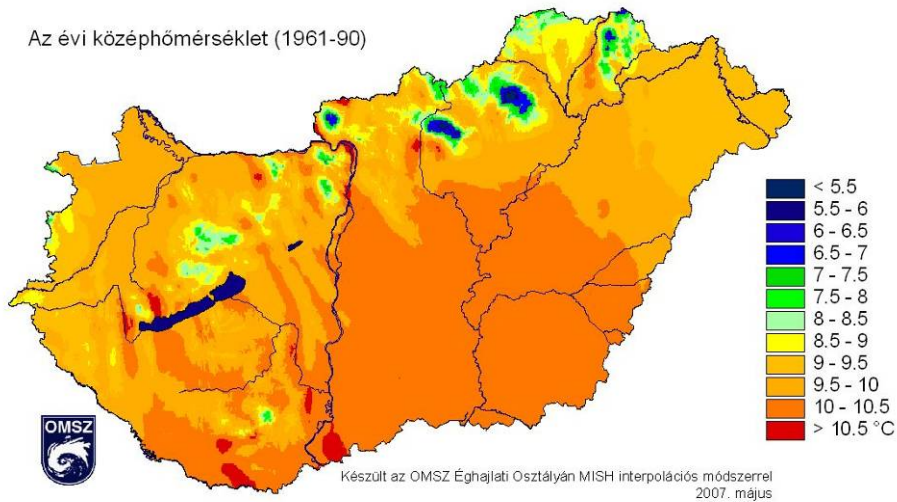
57 stations mean temperature 1961-90

72 stations maximum and minimum temperatures 1961-90

162 stations precipitation series 1961-90

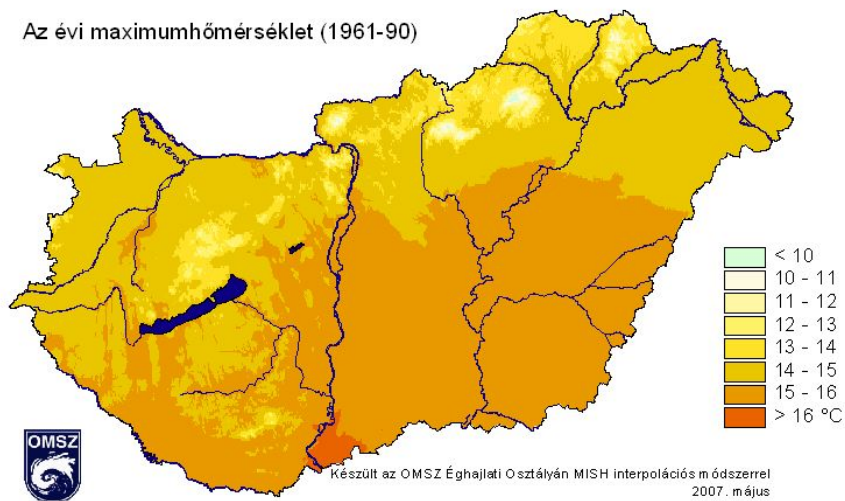
Annual mean 1961-1990

Az évi középhőmérséklet (1961-90)

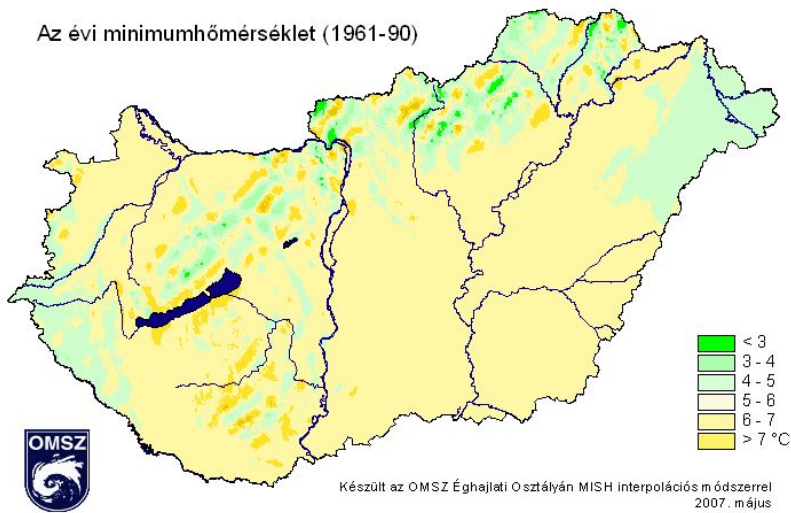


Annual maximum temperatures 1961-1990

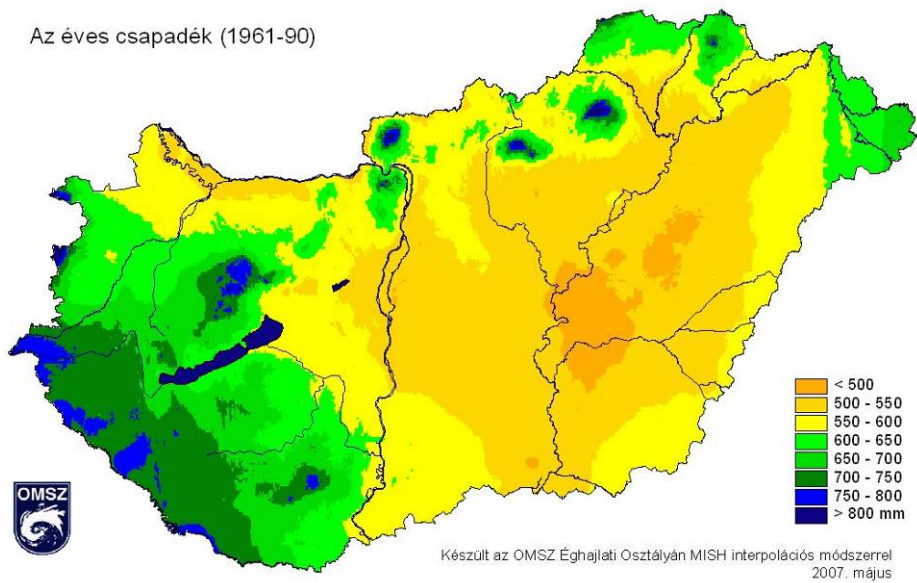
Az évi maximumhőmérséklet (1961-90)



Annual minimum temperatures 1961-1990



Annual mean precipitation 1961-1990



Trendmaps 1975-2004 period

Data

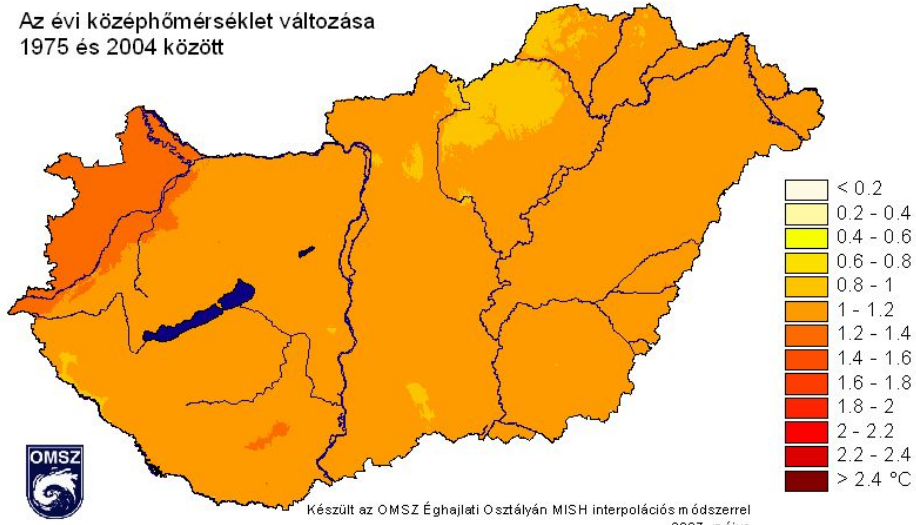
57 stations mean temperature 1975-2004

72 stations maximum and minimum temperatures 1975-2004

162 stations precipitation series 1975-2004

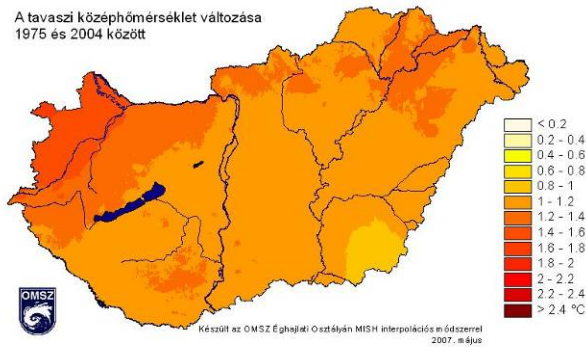
Change of the annual mean temperature 1975-2004

Az évi középhőmérséklet változása
1975 és 2004 között

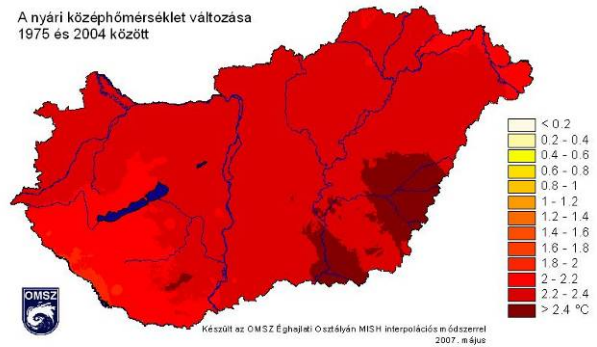


MAM, JJA, SON, DJF mean change 1975-2004

A tavaszi középhőmérséklet változása
1975 és 2004 között



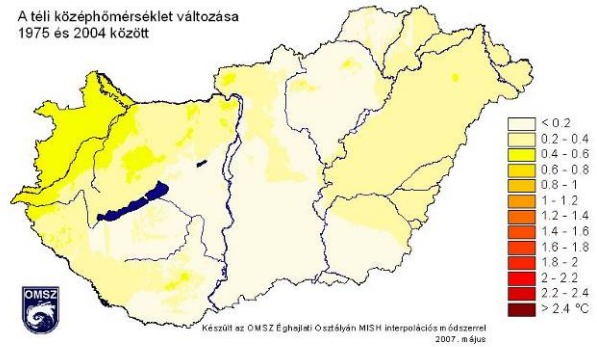
A nyári középhőmérséklet változása
1975 és 2004 között



Az őszi középhőmérséklet változása
1975 és 2004 között

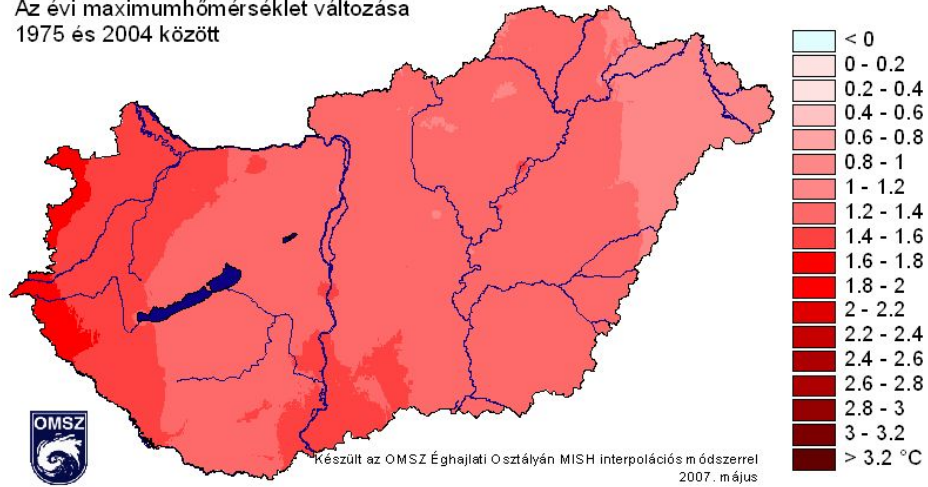


A téli középhőmérséklet változása
1975 és 2004 között



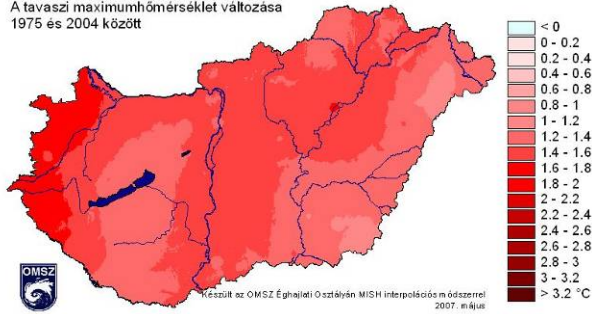
Change of the annual mean maximum temperature 1975-2004

Az évi maximumhőmérséklet változása
1975 és 2004 között

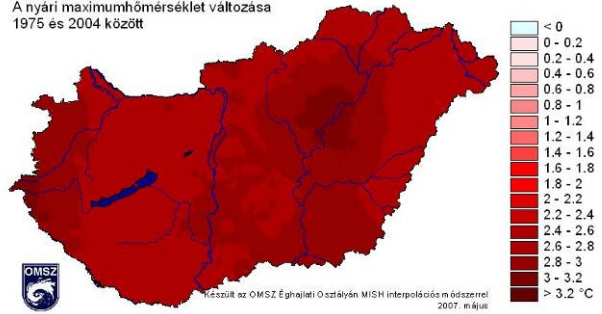


MAM, JJA, SON, DJF mean maximum change 1975-2004

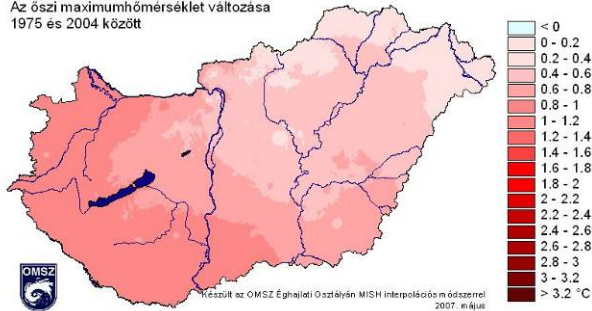
A tavaszi maximumhőmérséklet változása
1975 és 2004 között



A nyári maximumhőmérséklet változása
1975 és 2004 között



Az őszi maximumhőmérséklet változása
1975 és 2004 között

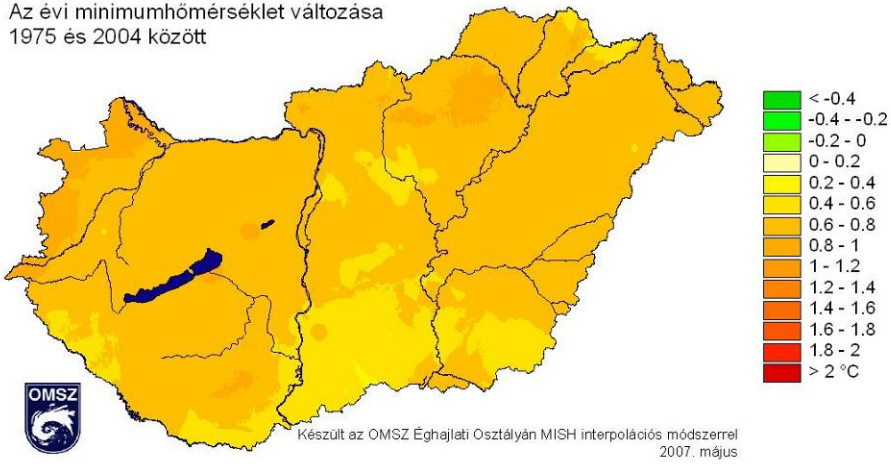


A téli maximumhőmérséklet változása
1975 és 2004 között



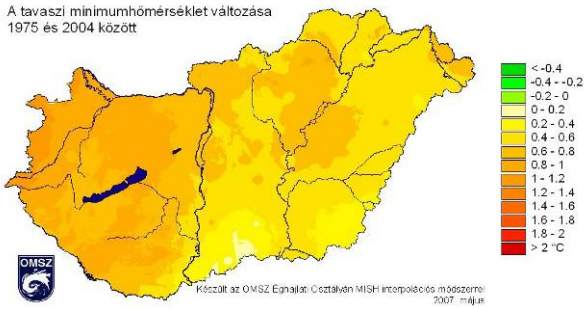
Change of the annual minimum temperature 1975-2004

Az évi minimumhőmérséklet változása
1975 és 2004 között

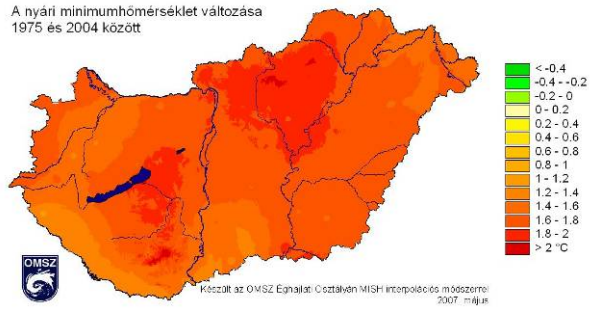


MAM, JJA, SON, DJF mean minimum change 1975-2004

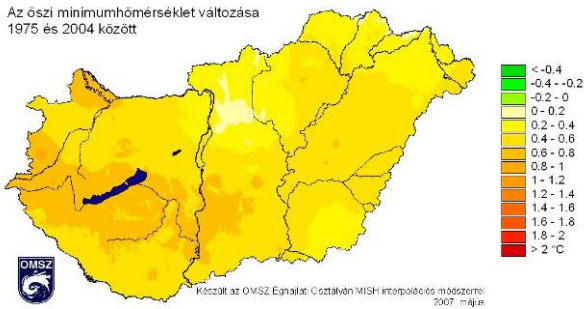
A tavaszi minimumhőmérséklet változása
1975 és 2004 között



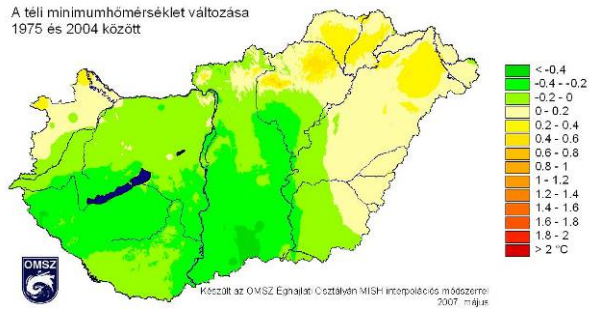
A nyári minimumhőmérséklet változása
1975 és 2004 között



Az őszi minimumhőmérséklet változása
1975 és 2004 között

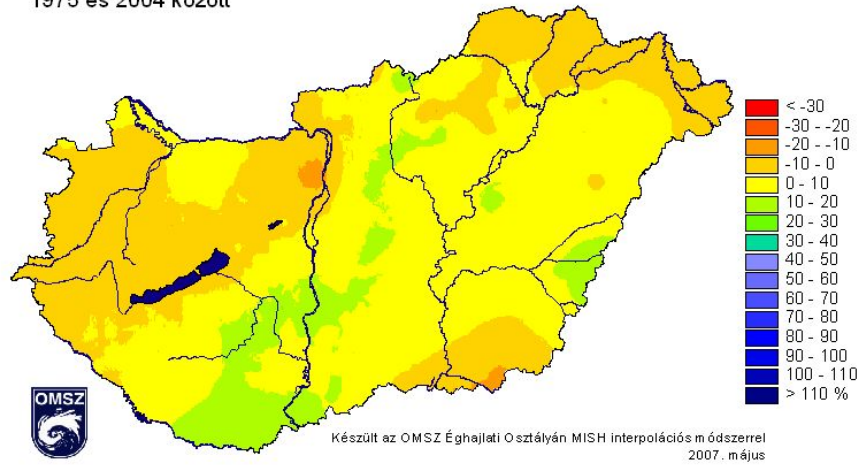


A téli minimumhőmérséklet változása
1975 és 2004 között



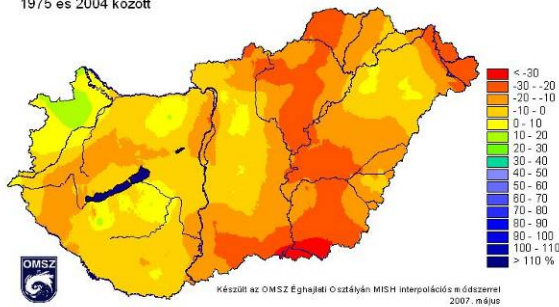
Change of the annual precipitation total 1975-2004

Az évi csapadék változása
1975 és 2004 között

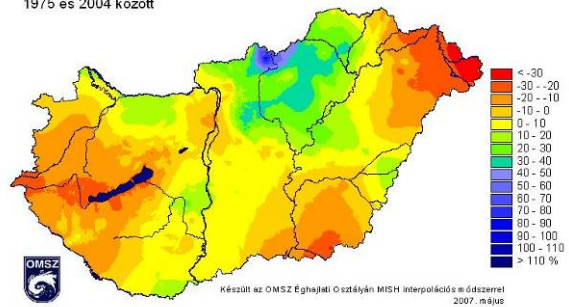


MAM, JJA, SON, DJF precipitation total change 1975-2004

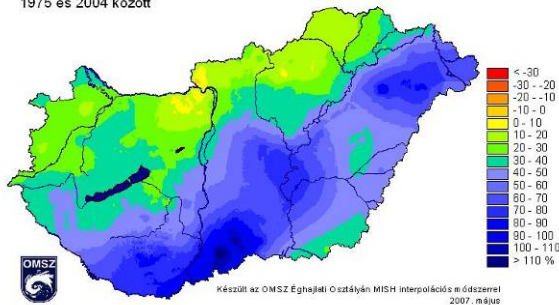
A tavaszi csapadék változása
1975 és 2004 között



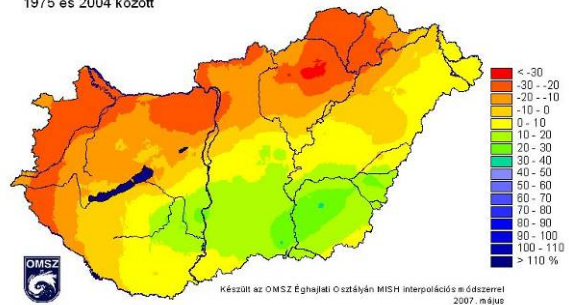
A nyári csapadék változása
1975 és 2004 között



Az őszi csapadék változása
1975 és 2004 között



A téli csapadék változása
1975 és 2004 között



References

- Lakatos, M., Szentimrey, T., Birszki, B., Kövér, B., Bihari, Z., Szalai, S.(2007): Changes of the Temperature and Precipitation Extremes following homogenization, *Acta Silv. Lign. Hung.*, Vol.3, pp. 87-95.
- Szentimrey, T. (2008): Development of MASH homogenization procedure for daily data. Proceedings of the Fifth Seminar for Homogenization and Quality Control in Climatological Databases, Budapest, Hungary (Budapest, Hungary, 29 May – 2 June 2006) WCDMP No. 68, WMO TD No. 1434) on CD.
- Szentimrey, T. (2006): Manual of homogenization software MASHv3.01 (<http://www.met.hu/pages/seminars/seeera/index.htm>)
- Szentimrey, T., Bihari, Z.,(2007): „Mathematical background of the spatial interpolation methods and the software MISH (Meteorological Interpolation based on Surface Homogenized Data Basis)”, Proceedings from the Conference on Spatial Interpolation in Climatology and Meteorology, Budapest, Hungary, 2004, COST Action 719, COST Office, 2007, pp. 17-27

D4.2.5 ELU: Expected Trends of Extreme Climate Indices for the Carpathian Basin

Regional climatological effects of global warming may be recognized not only in shifts of mean temperature and precipitation, but in the frequency and intensity changes of different climate extremes. A joint WMO-CCI (World Meteorological Organization Commission for Climatology) / CLIVAR (a project of the World Climate Research Programme addressing Climate Variability and Predictability) Working Group formed in 1998 on climate change detection (Karl et al., 1999); one of its task groups aimed to identify the climate extreme indices (Peterson et al., 2002) and completed a climate extreme analysis on all part of the world where appropriate data was available (Frich et al., 2002).

In order to compare the past and future trends of the extreme climate indices for the Carpathian basin, simulated daily values of meteorological variables are obtained from the regional climate model (RCM) outputs of the Swiss Federal Institute of Technology Zurich (Eidgenössische Technische Hochschule Zürich, ETHZ) in the frame of the completed EU-project PRUDENCE (Prediction of Regional scenarios and Uncertainties for Defining European Climate change risks and Effects). Results of the project PRUDENCE (Christensen, 2005) are disseminated widely via Internet and several other media. The primary objectives of PRUDENCE were to provide high resolution (50 km × 50 km) climate change scenarios for Europe for 2071-2100 (Christensen and Christensen, 2007) using dynamical downscaling methods with RCMs (using the reference period 1961-1990). ETHZ used the Climate High Resolution Model (CHRM) RCM (Vidale et al., 2003) with 50 km horizontal resolution, for which the boundary conditions were provided by the HadAM3H/HadCM3 (Rowell, 2005) global climate model of the UK Met Office. The simulations were accomplished for the period 2071-2100 using scenario A2, which describes a very heterogeneous world with preservation of local identities. According to this scenario, fertility patterns across regions converge very slowly resulting in continuously increasing world population. Economic development is primarily regionally oriented, per capita economic growth and technological changes are fragmented and slow. The projected CO₂ concentration may reach 850 ppm by the end of the 21st century (IPCC, 2007), which is about triple of the pre-industrial concentration level (280 ppm).

Extreme temperature indices are compared in Table 5.1 for the reference period and the last three decades of the 21st century. The annual values are calculated as an average of 10 representative grid points located in Hungary (Bartholy et al., 2007b).

Table 5.1: Comparison of extreme temperature indices in the reference period (1961-1990) and in case of the A2 scenario (2071-2100) based on the daily outputs of the regional climate model of ETHZ.

Extreme temperature index	Reference period (1961-1990)	A2 scenario (2071-2100)	Expected change	Detected trend (1961-2001)
Tx10: Cold days ($T_{\max} < T_{\max, 10\%, 1961-90}$)	36 days/year	10 days/year	-72%	-
Tx90: Warm days ($T_{\max} > T_{\max, 90\%, 1961-90}$)	36 days/year	78 days/year	+116%	+
Tn10: Cold nights ($T_{\min} < T_{\min, 10\%, 1961-90}$)	36 days/year	9 days/year	-76%	-
Tn90: Warm nights ($T_{\min} > T_{\min, 90\%, 1961-90}$)	36 days/year	79 days/year	+120%	+
FD: Frost days ($T_{\min} < 0$ °C)	74 days/year	26 days/year	-65%	-
SU: Summer days ($T_{\max} > 25$ °C)	98 DAYS/YEAR	136 DAYS/YEAR	+39%	+
Tx30GE: Hot days ($T_{\max} \geq 30$ °C)	47 DAYS/YEAR	90 DAYS/YEAR	+91%	+
Tx35GE: Extremely hot days ($T_{\max} \geq 35$ °C)	13 DAYS/YEAR	45 DAYS/YEAR	+250%	+
Tn20GT: Hot nights ($T_{\min} > 20$ °C)	5 days/year	36 days/year	+625%	+
Tx0LT: Winter days ($T_{\max} < 0$ °C)	24 DAYS/YEAR	6 DAYS/YEAR	-75%	-
Tn-10LT: Severe cold days ($T_{\min} < -10$ °C)	8 DAYS/YEAR	1 DAYS/YEAR	-83%	-

It can be seen that negative extremes are expected to decrease while positive extremes tend to increase significantly. Both imply regional warming in the Carpathian basin. The largest increase due to this warming trend can be expected in case of hot days (Tx30GE), warm days (Tx90), warm nights (Tn90), extremely hot days (Tx35GE), and hot nights (Tn20GT) by +91%, +116%, +120%, +250%, and +625%, respectively. Expected changes of all the temperature indices are completely consistent with the detected trend in the 1961-2001 period (Bartholy and Pongrácz, 2007).

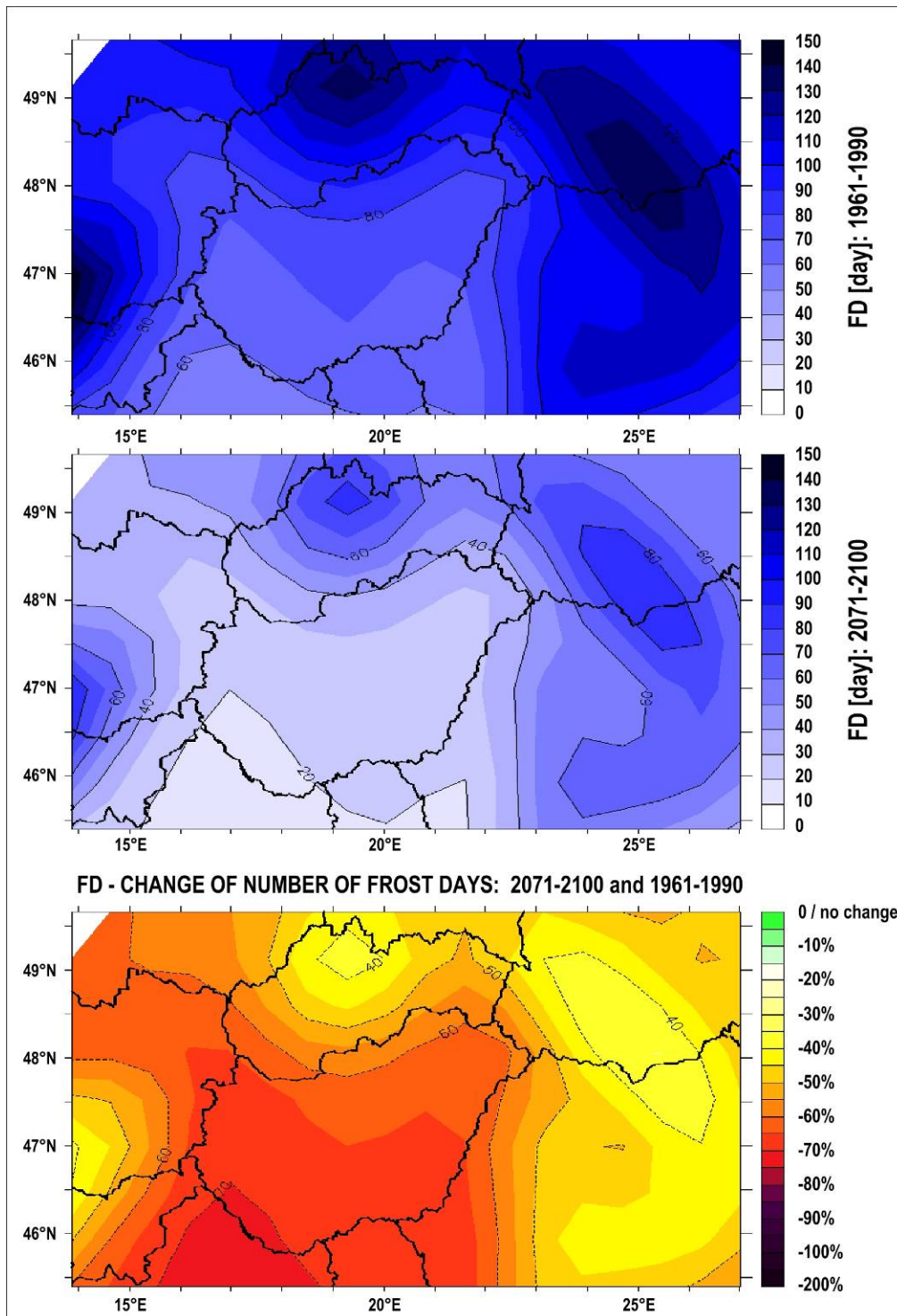


Figure 5.1. Expected change of annual number of frost days (FD) in case of the A2 scenario (2071-2100) compared to the reference period (1961-1990), maps are determined using daily minimum temperature values of the regional climate model of ETHZ.

Among the extreme temperature indices, the number of frost days (FD) and the number of summer days (SU) are selected to illustrate the spatial distribution of the index values both in the reference period (upper map) and in the last three decades of the 21st century (center map) in Figs. 5.1 and 5.2, respectively. In both cases the orography is the main factor determining the spatial patterns of

the extreme indices. In the higher elevated mountainous areas (in the range of the Carpathes and in the eastern foothills of the Alpes), the annual number of frost days exceeds 120 in the reference period, while it is expected to decrease to only about 80 days per year. In the lower elevated areas of Hungary, FD was about 60-80 days in each year on average, which is likely to decrease to 10-40 days by the end of the 21st century resulting in a decrease by 60-70% in the country (lower map of Fig. 5.1). According to the ETHZ model simulations, the decrease of FD is expected to be smaller in the northern part of Hungary (about 60%) than in the southern subregions (about 70%).

In case of the annual number of summer days (SU) similar patterns can be identified. In 1961-1990, SU was about 80-105 days per year on average in Hungary, and it is expected to increase to 120-145 days by 2071-2100 in case of A2 scenario. The smallest increase (35%) is projected in the southeastern part of the country, while in the northwestern border the increase may exceed 60% (lower map of Fig. 5.2). In the higher elevated mountainous subregions, the expected increase of SU is larger than 150%.

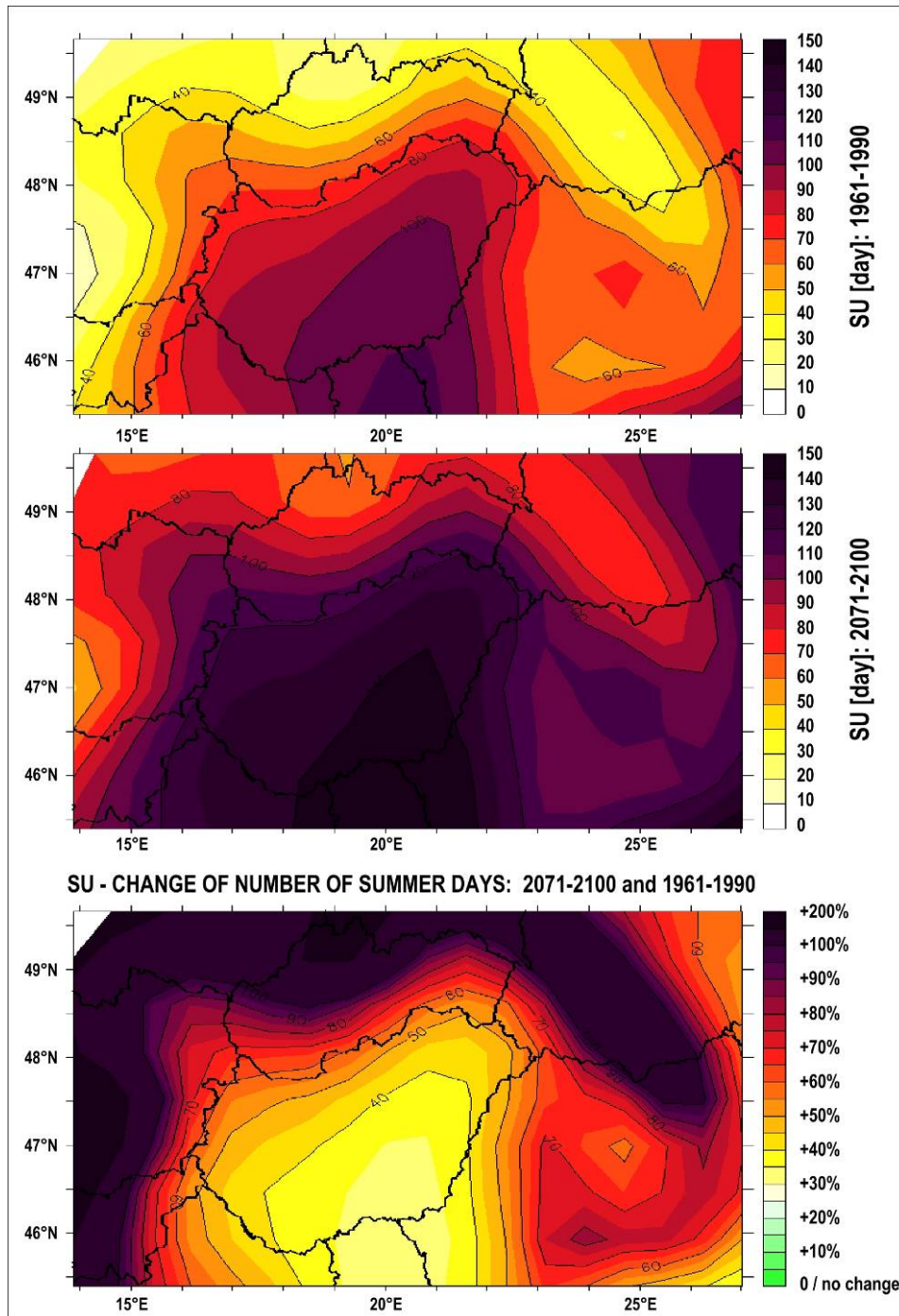


Figure 5.2. Expected change of annual number of summer days (SU) in case of the A2 scenario (2071-2100) compared to the reference period (1961-1990), maps are determined using daily maximum temperature values of the regional climate model of ETHZ.

Table 5.2: Comparison of extreme precipitation indices in the reference period (1961-1990) and in case of the A2 scenario (2071-2100) based on the daily outputs of the regional climate model of ETHZ. In case of the detected trends, signs in parentheses indicate regional mean coefficients being not significant at 95% level.

Extreme	Reference	A2	Expected change	Detected
---------	-----------	----	-----------------	----------

precipitation index	period (1961–1990)	scenario (2071– 2100)	Annual	January	July	trend (1976– 2001)
CDD ($R_{\text{day}} < 1 \text{ mm}$)	159 days/year	176 days/year	+10%	-27%	+26%	-
Rx1 (R_{max})	147 mm	156 mm	+6%	+27%	-17%	-
Rx5 ($R_{\text{max}, 5 \text{ days}}$)	251 mm	252 mm	+0.3%	+18%	-24%	+
SDII ($R_{\text{year}}/RR1$)	68 mm	72 mm	+7%	+15%	-5%	(+)
R95 ($R_{\text{day}} \geq R_{95\%, 1961-90}$)	18 days/year	19 days/year	+6%	+55%	-39%	+
R75 ($R_{\text{day}} \geq R_{75\%, 1961-90}$)	90 days/year	77 days/year	-14%	+13%	-46%	+
RR20 ($R_{\text{day}} \geq 20 \text{ mm}$)	2 days/year	3 days/year	+37%	+308%	-5%	+
RR10 ($R_{\text{day}} \geq 10 \text{ mm}$)	11 days/year	12 days/year	+13%	+89%	-28%	+
RR5 ($R_{\text{day}} \geq 5 \text{ mm}$)	29 days/year	28 days/year	-2%	+38%	-39%	(-)
RR1 ($R_{\text{day}} \geq 1 \text{ mm}$)	77 days/year	67 days/year	-13%	+13%	-45%	-
RR0.1 ($R_{\text{day}} \geq 0.1 \text{ mm}$)	133 days/year	114 days/year	-15%	+9%	-47%	-

Similar analysis is presented in Table 5.2 for the extreme precipitation indices. Expected changes of annual indices are generally consistent with the detected trends in the last quarter of the 20th century (Bartholyí and Pongrácz, 2007). However, the expected regional increase or decrease is usually small (not exceeding 15% in absolute value). Much larger positive and negative changes are projected in January and in July, respectively, on the base of the RCM simulations in case of A2 scenario. The only exception is CDD (consecutive dry days) but this is the only precipitation index, which is related to drought instead of rainfall. Therefore, the opposite signs of the projected CDD changes are consistent with the expected regional changes of the other precipitation indices. These results suggest that the climate tends to be wetter in January and drier in July in the Carpathian basin (Bartholy et al., 2007a). Since the projected increases of RR20, RR10, and R95 (these indices describe very extreme precipitation events) exceed 50% in January, and the expected increases of RR0.1 or RR1 (these indices are not related to extreme precipitation) do not reach 15%, the extreme precipitation events are expected to become more intense and more frequent in January. Furthermore, drought is projected to become more intense in July by the end of the 21st century. This can be derived from the robust decrease of precipitation indices and the increase of CDD. The largest decrease rates (exceeding 35%) in July are expected in case of RR0.1, RR1, R75, R95, and RR5.

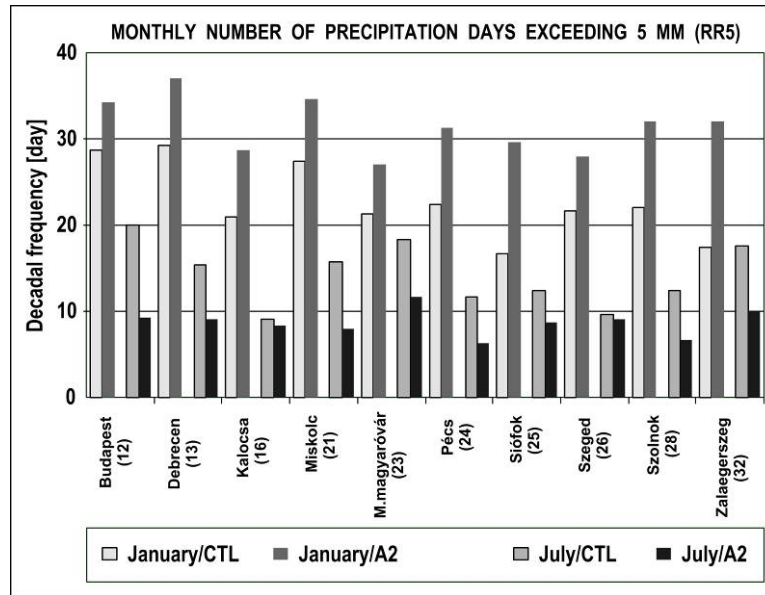


Figure 5.3. Comparison of monthly number of precipitation days exceeding 5 mm (RR5) in January and in July, in the reference period (1961-1990, CTL) and in case of the A2 scenario (2071-2100) based on the daily precipitation outputs of the regional climate model of ETHZ.

Detailed comparison of the decadal monthly numbers of precipitation days exceeding 5 mm (RR5) in the periods 1961-1990 and 2071-2100 is shown in Fig. 5.3 for January and for July using the index values determined for the 10 selected grid points (each of them is assigned to one of the meteorological stations located in the vicinity of the grid point). Regional average changes of RR5 are -2% (in case of the entire year), +38% (in January), and -39% (in July). Although the annual number is not expected to change significantly in any grid point, but the seasonal distribution of RR5 may change very much. RR5 in January is projected to become about 3-4 times of RR5 in July.

The difference between the expected changes of RR1 and RR10 is illustrated in Fig. 5.4 using annual and monthly (January and July) grid point values of the indices. Blue circles in the maps indicate expected decrease, while yellow and red circles imply expected increase. The size of the circles corresponds to the magnitude of the expected changes. In case of the annual change, the expected decreasing rate in the country is about 10-20% in RR1, while the increasing rate of RR10 between 2071-2100 and 1961-1990 is expected to vary between 0 and 40% in Hungary. The largest changes of RR1 are projected in July, namely, 40-60% increase by the end of the 21st century. Opposite changes (0-40% increase) can be expected in January. The largest changes of RR10 are expected in January, the projected decrease exceeds 60% in most of the grid points. In July, in general, about 10-60% decrease is expected, except the southeastern part of the country where the expected increase exceeds 40%.

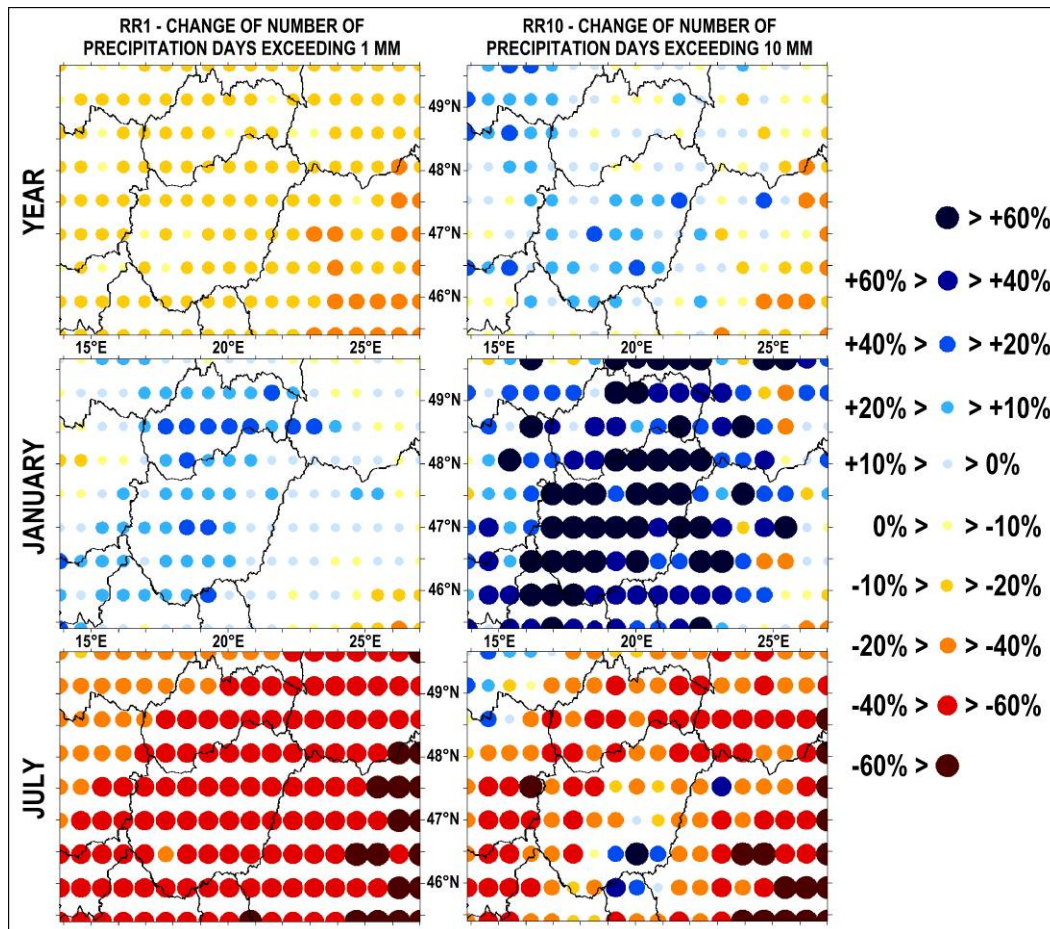


Figure 5.4. Expected change of annual and monthly number of precipitation days exceeding 1 mm and 10 mm (RR1 and RR10, respectively) in case of the A2 scenario (2071-2100) compared to the reference period (1961-1990). Maps are determined using simulated daily precipitation amounts of the regional climate model of ETHZ.

Acknowledgements. Research leading to this paper has been supported by the following sources: the Hungarian Academy of Sciences under the program 2006/TKI/246 titled Adaptation to climate change, the Hungarian National Research Development Program under grants NKFP-3A/082/2004 and NKFP-6/079/2005, the Hungarian National Science Research Foundation under grants T-049824, K-67626, and K-69164, the Hungarian Academy of Science and the Hungarian Prime Minister's Office under grant 10.025-MeH-IV/3.1/2006, the Hungarian Ministry of Environment and Water under the National Climate Strategy Development project, and the CECILIA project of the European Union Nr. 6 program (contract no. GOCE-037005). Climate change data have been provided through the PRUDENCE data archive, funded by the EU through contract EVK2-CT2001-00132.

References

Bartholy, J., Pongrácz, R., 2007: Regional analysis of extreme temperature and precipitation indices for the Carpathian Basin from 1946 to 2001. *Global and Planetary Change*, 57, 83-95. doi:10.1016/j.gloplacha.2006.11.002

- Bartholy, J., Pongrácz, R., Gelybó, Gy., 2007a: Regional climate change expected in Hungary for 2071-2100. *Applied Ecology and Environmental Research*, 5, 1-17.
- Bartholy, J., Pongrácz, R., Gelybó, Gy., Szabó, P., 2007b: Expected change of temperature extremes in the Carpathian basin by the end of the 21st century. (in Hungarian) *Klíma-21*. 51, 3-17.
- Christensen, J.H., 2005: Prediction of Regional scenarios and Uncertainties for Defining European Climate change risks and Effects. Final Report. DMI, Copenhagen.
- Christensen, J.H., Christensen, O.B., 2007: A summary of of the PRUDENCE model projections of changes in European climate by the end of this century. *Climatic Change* 81, 7-30.
- Frich, P., Alexander, L.V., Della-Marta, P., Gleason, B., Haylock, M., Klein Tank, A.M.G., Peterson, T., 2002: Observed coherent changes in climatic extremes during the second half of the twentieth century. *Climate Research* 19, 193-212.
- IPCC, 2007: *Climate Change 2007: The Physical Science Basis*. Working Group I Contribution to the Fourth Assessment Report of the IPCC. Intergovernmental Panel on Climate Change, Cambridge University Press, New York.
- Karl, T.R., Nicholls, N., Ghazi, A., 1999: Clivar/GCOS/WMO Workshop on Indices and Indicators for Climate Extremes Workshop Summary. *Climatic Change* 42, 3-7.
- Peterson, T., Folland, C.K., Gruza, G., Hogg, W., Mokssit, A., Plummer, N., 2002: Report on the Activities of the Working Group on Climate Change Detection and Related Rapporteurs, 1998-2001. World Meteorological Organisation Rep. WCDMP-47. WMO-TD 1071. Geneva, Switzerland. 143p.
- Rowell, D.P., 2005: A scenario of European climate change for the late 21st century: seasonal means and interannual variability. *Clim. Dyn.* 25, 837-849.
- Vidale, P.L., Lüthi, D., Frei, C., Seneviratne, S.I., Schär, C., 2003: Predictability and uncertainty in a regional climate model. *J. Geophys. Res.* 108 (D18), 4586, doi:10.1029/2002JD002810.

D4.2.6 NIMH: A case study on Utilization of Precipitation Indices in Bulgaria

Abstract

Various climate indices are widely used across the world in order to assess climate as well as its variability and change in a given location, region, etc. Many climate indices including precipitation ones have been already applied in Bulgaria. This case study also aimed to explore some precipitation indices throughout the country. Several precipitation indices were selected, calculated and analyzed for different weather stations in Bulgaria. The selected precipitation indices are based on the STARDEX project and hence represent a sub-sample of the final list of indices chosen for WP4 (see App. A)..

Introduction

Substantial work has been completed in recent years in the area of climate trend research (e.g., Houghton et al., 2001). Most analyses of long-term global climate changes have focused on changes in mean values. This is largely due to the lack of availability of high quality daily resolution data required for monitoring, detection and attribution of changes in climate extremes. However, any change in the frequency or severity of extreme climate events could have profound impacts on nature and society. It is thus very important to analyze extreme events (Zhang et al., 2005). The compilation, provision, and updating of a globally complete and readily available full resolution daily data set is difficult. In the absence of daily data-sets, the wide-areas trend studies on extremes needed to rely on combining the results of different analyses from different areas. For example, the global analysis of climate extreme indices by Frich et al. (2002) does not cover large areas of land.

In addition, the analyses conducted by different researchers in different countries may not seamlessly merge together to form a global map because the analyses might have been conducted on different indices (e.g., Bonsal et al., 2001) and/or using different methods.

Various climate indices are widely used across the world in order to assess climate as well as its variability and change in a given location, region, etc. Unfortunately, the exact definition of the measures that were used to characterize the extremes in the tails of the distribution differed from one study to the other. To gain a uniform perspective on observed changes in climate extremes, a core set of standardized indices was recently defined by the joint Working Group on Climate Change Detection of the World Meteorological Organization – Commission for Climatology (WMO–CCL) and the Research Programme on Climate Variability and Predictability (e.g., Peterson et al., 2001). Each index describes particular aspects of climate extremes. An example is the maximum rainfall amount observed in any period of 5 consecutive days. These indices are calculated by different individuals in different countries and regions, using exactly the same formula. The analyses of those indices can thus fit seamlessly into the global picture (e.g., Easterling et al., 2003; Karl et al., 1999; Peterson et al., 2002). It is considered that this effort will result in an improved monitoring of climate extreme change with much broader spatial coverage than currently available. Using the standardized indices, the trends in the extremes, for example of Europe's climate of the past, can be analyzed unambiguously.

Many climate indices including precipitation ones have been already applied in Bulgaria (e.g., Koleva et al., 2004). However, this case study aimed to explore different standardized precipitation indices throughout the country. Several standardized precipitation indices were selected, calculated and analyzed for different weather stations in Bulgaria. The selected standardized precipitation indices are based on the STARDEX project.

Data and methods

Data

Long-term monthly and daily precipitation data were collected from near 40 weather stations (Fig. 6.1) across the country. The precipitation data, used in this study were provided by the weather network of the National Institute of Meteorology and Hydrology in Sofia.

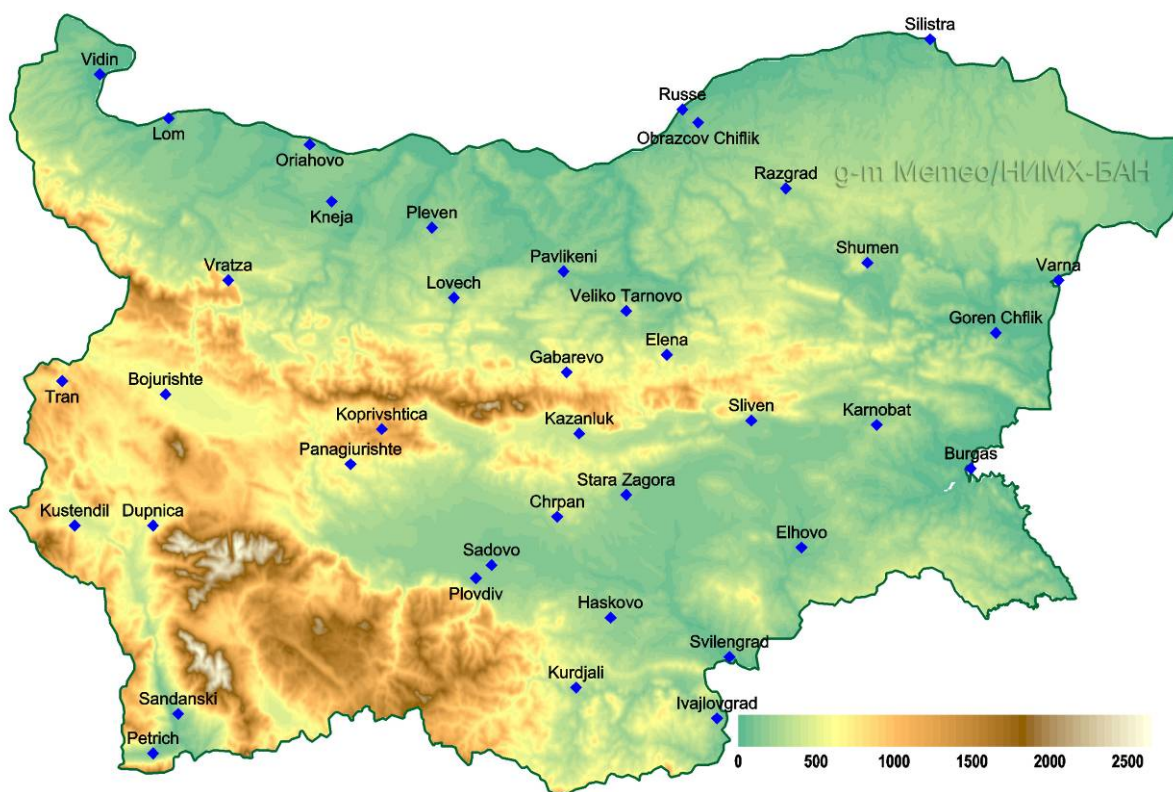


Figure 6.1. Weather stations, used in the study

Methods

Precipitation indices

The indices from the STARDEX project and the ones additionally incorporated by Météo-France were explored in this study. The STARDEX climate indices were collected and developed from the program Climate Indices originally written at the US National Climatic Data Centre (NCDC) in 1999. The first version included about 20 climate indices. A further 20 indices were added in 2000. A further dozen indices were added later. Météo-France has adapted and used the STARDEX extreme indices for the objectives of the IMFREX project (e.g., Bessemoulin and Moisselin, 2005). The multidisciplinary IMFREX (Impacts of Anthropogenetic Changes on Frequency of Extremes of Wind, Temperature and Precipitation) project aimed to characterize and forecast the evolution of climate extremes in France and their impacts to some end-users. Now the STARDEX package consists of around 80 indices, related to precipitation (Table 6.1) and air temperature.

Table 6.1. Precipitation indices, applied within the study

<i>index</i>	unit	meaning
cumulRR	mm	Cumulative precipitation
RR1	days	Number of days with precipitation ≥ 1.0 mm
prec20	mm/day	20th percentile of rainday amounts
prec40	mm/day	40th percentile of rainday amounts

prec50	mm/day	50th percentile of rainday amounts
prec60	mm/day	60th percentile of rainday amounts
prec80	mm/day	80th percentile of rainday amounts
prec90	mm/day	90th percentile of rainday amounts
prec95	mm/day	95th percentile of rainday amounts
Frac20p	%	Fraction of total precipitation above annual 20th percentile
Frac40p	%	Fraction of total precipitation above annual 40th percentile
Frac50p	%	Fraction of total precipitation above annual 50th percentile
Frac60p	%	Fraction of total precipitation above annual 60th percentile
Frac80p	%	Fraction of total precipitation above annual 80th percentile
Frac90p	%	Fraction of total precipitation above annual 90th percentile
Frac95p	%	Fraction of total precipitation above annual 95th percentile
R10	days	Numbers of days with precipitation ≥ 10 mm
R20	days	Numbers of days with precipitation ≥ 20 mm
CDD	days	Max number consecutive dry days
CWD	days	Max number consecutive wet days
pww	%	Mean wet-day persistence
Pdd	%	Mean dry-day persistence
Wet_spell_mean	days	Mean wet spell lengths
Wet_spell_perc	days	Median wet spell lengths
Wet_spell_sd	days	Standard deviation wet spell lengths
Dry_spell_mean	days	Mean dry spell lengths
Dry_spell_perc	days	Median dry spell lengths
Dry_spell_sd	days	Standard deviation dry spell lengths
R1d	mm	Greatest 1-day total rainfall
R3d	mm	Greatest 3-day total rainfall
R5d	mm	Greatest 5-day total rainfall
R10d	mm	Greatest 10-day total rainfall
SDII	mm/day	Simple Daily Intensity
R75T	%	% of total rainfall from events $>$ long-term 75th percentile
R75N	days	Numbers of events $>$ long-term 75th percentile
R90T	%	% of total rainfall from events $>$ long-term 90th percentile
R90N	days	Numbers of events $>$ long-term 90th percentile
R95T	%	% of total rainfall from events $>$ long-term 95th percentile
R95N	days	Numbers of events $>$ long-term 95th percentile
R99T	%	% of total rainfall from events $>$ long-term 99th percentile
R99N	days	Numbers of events $>$ long-term 99th percentile
coeff_varia	%	Coefficient of precipitation variation

Data control and homogenization

The first important activity in this study was to carry out a quality data control and a homogenization procedure of monthly precipitation series. The major goal was to detect possible breaks due to the necessity to constitute as longer as possible reference daily weather series. In case of less breaks for a weather station, the opportunity for a longer reference period, after applying the respective criteria, was higher.

The Caussinus-Mestre method, applied within this study, simultaneously accounts for the detection of unknown number of multiple breaks and generating reference series. It is based on the premise that between two breaks, a time series is homogeneous and these homogeneous sections can be used as reference series. Each single series is compared with others with the same climatic area by making ratios series. These ratios series are tested for discontinuities. When a detected break remains constant throughout the set of comparisons of a candidate station with its neighbours, the break is attributed to the candidate station time series (e.g., Caussinus and Mestre, 1997; Mestre, 1999, 2000; Peterson et al., 1998)

Detection of breaks and outliers

For detection purposes, the formulation described by Caussinus and Lyazrhi (1997) is used. It allows the determination in a normal linear model of an unknown number of breaks and outliers. They formulated it is a problem of testing multiple hypotheses. Let us give now the formulation of this procedure in the case of a normal sample (e.g., Moisselin and Mestre, 2002). We consider n normal random variables Y_i ($i=1, \dots, n$) and let Y denote the column vector of the Y_i 's. We assume that the probability distribution of Y is n -dimensional normal, with covariance matrix I_n (identity matrix of order $n \times n$) up to the unknown variance σ^2 .

Let k be the number of breaks and l - the number of outliers. Let $\tau_1, \tau_2, \dots, \tau_k$ be the positions of the k breaks, and let $\delta_1, \delta_2, \dots, \delta_l$ be the positions of the l outliers. Let

$K = (\{\tau_1, \tau_2, \dots, \tau_k\}, \{\delta_1, \delta_2, \dots, \delta_l\})$ be the set of breaks and outliers. To simplify the notation, we will set $\tau_0=0$ and $\tau_{k+1}=n$. Finally, let $\Delta = \{\delta_1, \delta_2, \dots, \delta_l\}$ and

$n_j = \tau_j - \tau_{j-1} - \text{Card}\{\{\tau_{j-1} + 1, \tau_{j-1} + 2, \dots, \tau_j\} \cap \Delta\}$, i.e. n_j is equal to the length of the period $[\tau_{j-1} + 1, \tau_j]$ minus the number of outliers within this period.

We denote:

$$\bar{Y} = \frac{1}{n} \sum_{i=1}^n Y_i, \quad \bar{Y}_j = \frac{1}{n_j} \sum_{i=\tau_{j-1}+1}^{\tau_j} Y_i, \quad j=1, \dots, k+1; i \notin \Delta \quad (1)$$

Let:

$$C_{\emptyset}(Y) = 0$$

$$C_K(Y) = \ln \left[1 - \frac{\sum_{j=1}^{k+1} n_j (\bar{Y}_j - \bar{Y})^2}{\sum_{i=1}^{k+1} (\bar{Y}_i - \bar{Y})^2} \right] + \frac{2(k+1)}{n-1} \ln(n) \quad (2)$$

The penalized log-likelihood procedure proposed by Caussinus and Lyazrhi (1997) is:

$$\text{select } H_{K^*} \text{ such that } K^* = \text{Argmin}_K(C_K(Y)) \quad (3)$$

The variance σ^2 is estimated by $\frac{1}{n-k-l-1} \sum_{j=1}^{k+l} \sum_{i=\tau_{j-1}+1}^{\tau_j} (Y - \bar{Y}_j)^2$, where the number and positions of outliers and breaks are those given by (3).

The procedure (3) has been proved to be asymptotically Bayes invariant optimal under a set of assumptions, which turn out to be realistic (e.g., Mestre, 2000) in the problem we are dealing with. For the particular problem of breaks in a Gaussian sample, the chosen penalty term gives much better results than Akaike's or Schwartz's criteria (e.g., Moisselin and Mestre, 2002).

The natural way to compute the procedure is to calculate $C_K(Y)$ for every possible hypothesis H_K (complete procedure). Nevertheless, this approach suffers from a major drawback: the number of hypotheses to examine rises very fast with n (length of the series) and $k+l$ the number of accidents to be detected. When detection is only performed for breaks, a dynamic programming algorithm (e.g. Hawkins, 2001; Lavielle, 1998) can be used. The computation time then becomes only linear in k , and quadratic in n . To enable the detection of outliers at a reasonable computing cost, a slightly different algorithm (Mestre, 2000) is used.

At each step, one or two more breaks are added to the previous selected hypothesis. Analytical studies (e.g. Mestre, 1999) show that this double step procedure gives better detection results than the single step procedure for up-and-down breaks (and without significant improvement for staircase configuration). Furthermore, a triple step procedure, much more greedy in terms of computation time, leads to small improvements (e.g. Mestre, 1999, 2000). The Causinus-Mestre method, with a double step procedure, is now the standard detection part of the homogenization method used in Météo-France (e.g. Moisselin and Mestre, 2002; Moisselin et al., 2002).

Correction of breaks and outliers

The knowledge of break positions can be a very interesting aspect for some users. For many applications (such as climate change studies) it is the first half-part of the problem. The other one, described below, is the break correction.

A two factors linear model is proposed for correction purposes (e.g., Mestre, 2000). The series within the same climatic area are considered to be affected by the same climatic signal factor at each time, while the station factor remains constant between two breaks. The model is applied after break detection. It provides the correction coefficient of a set of inhomogeneous series, through weighted least-squares estimation of the parameters. The weighted least squares allow correction of series with missing data. It also allows the data weighting, according to their supposed quality, which can be estimated, for example, with the correlation between the stations.

The above formulation is equivalent to an exact modelling of the relative homogeneity principle. Given a set of inhomogeneous instrumental series, it allows unbiased estimations of the breaks affecting these series. This method does not require computation of regional reference series, and is currently the standard correction part of the homogenization method used at Météo-France (e.g., Moisselin and Mestre, 2002; Moisselin et al., 2002)

Trend Calculation

The obtained homogenized time series of precipitation indices were smoothed by a 5-years running average as well as a linear trend. The linear trend is computed from the indices series using a Kendall's tau based slope estimator due to Sen (1968). This estimator is robust to the effect of

outliers in the series. It has been widely used to compute trends in hydrometeorological series (e.g., Wang and Swail, 2001; Zhang et al., 2000). The significance of the trend is determined using Kendall's test because this test does not assume an underlying probability distribution of the data series. Another non-parametric test was used in order to determine the possible existence of statistically significant trends of the precipitation indices assuming a 95% probability level – the Spearman and rank statistics (e.g., WMO, 1990).

Results

Precipitation homogenization - control, break detection and correction

The common conditions of detection and correction were the need of correlated series and the homogenization procedure concerned only monthly data. At a lower time scale, correlations are considered insignificant. The homogenization process was performed on sets of about 15 series merged with geographical criteria.

The first step was the performance of a quality control of the long-term monthly series used in the study (Fig. 6.2). The anomalies of monthly precipitation for each year and station were compared and analyzed in order to locate and remove possible data errors. The obvious crude errors as well as some suspicious values of precipitation were checked out and when necessary replaced by the respective value for missing data (i.e. -999.9). The control procedure was executed several times till appropriate data sets were obtained.

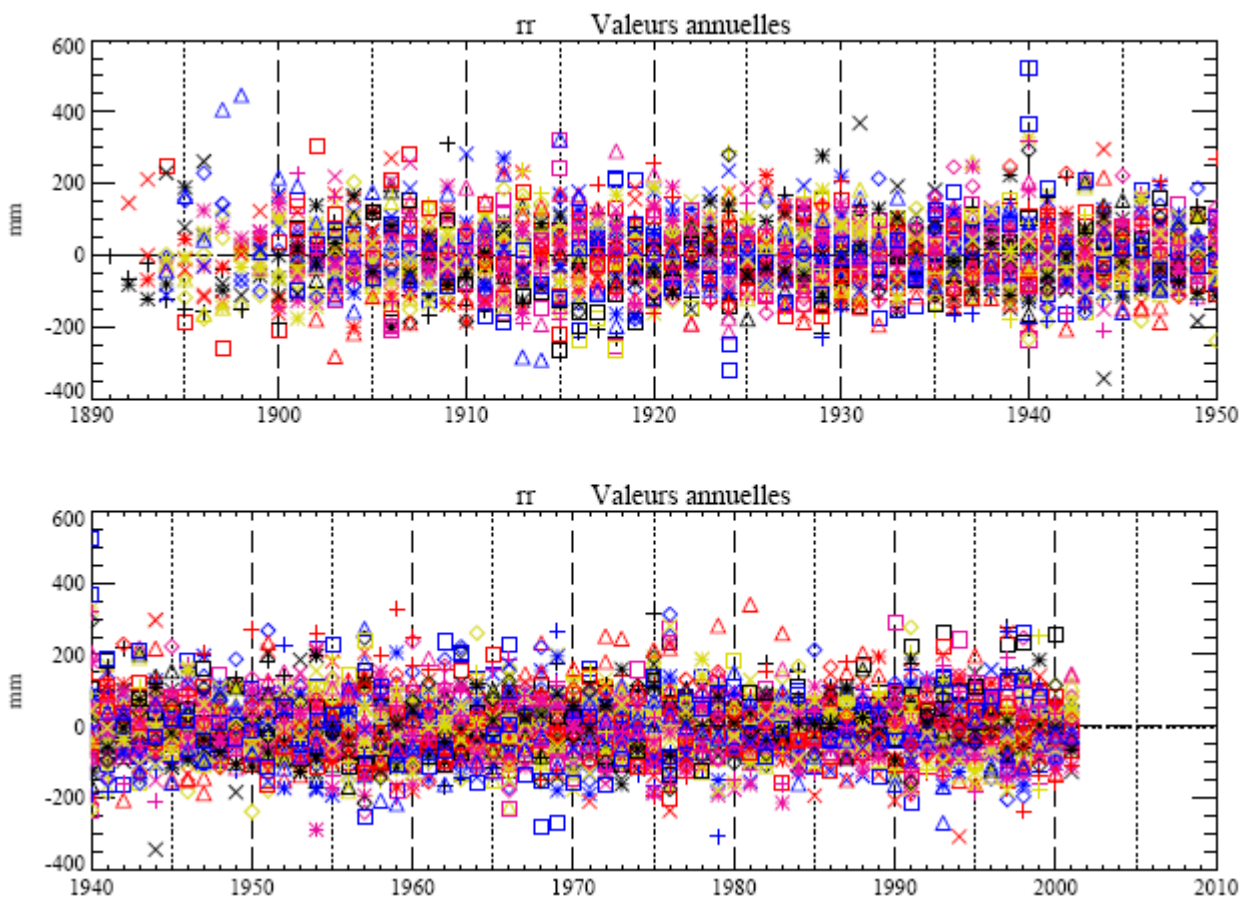


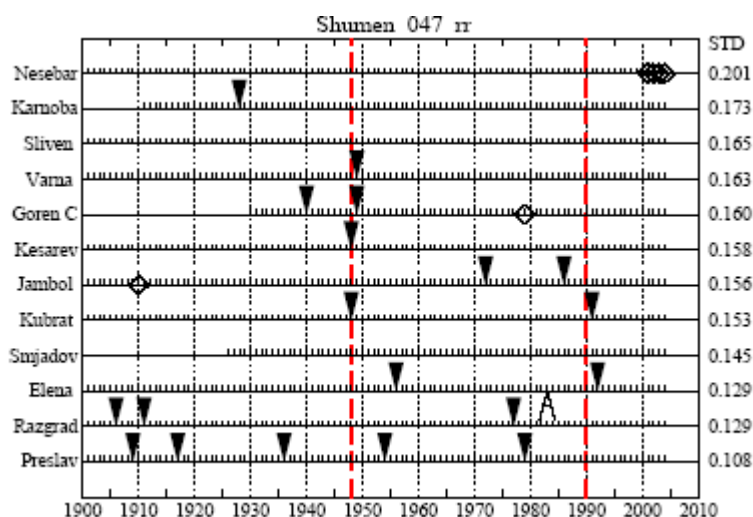
Figure 6.2. Anomalies of annual precipitation, used in the study, during application of data quality control

The next step was to calculate the respective ratios for precipitation. These ratios were then tested to put into evidence breaks or outliers. The typical homogenization techniques are based on the assumption that climatic variations affect in the same way a homogeneous regional reference series, whose reliability cannot be proved. The different methods (e.g., Alexandersson, 1986; Førland and Hanssen-Bauer, 1994; Peterson and Easterling, 1994) for creating such series do not guarantee their perfect homogeneity.

There is an easy way to get round the reference series. It is based on the simple statement that between two breaks a series is reliable (by definition), so these sections can be used as reference series (e.g. Mestre, 2000). Each single series is compared to others within the same climatic area by making a series of differences. These difference series are then tested for discontinuities.

At this stage, it is not known which individual series is the cause of a shift detected on a ratio series. However, it was already mentioned that according to the Caussinus-Mestre method, if a detected break remains constant throughout the set of comparisons of a candidate station in respect to its neighbours, it can be attributed to this candidate station. The detection of the outliers follows the same principle.

Ratio series were computed and constituted between all weather stations, used in the study, and their respective neighbour weather stations. The breaks and outliers were then put automatically into evidence by the double-step procedure applied within the Caussinus-Mestre method. Some detected breaks and outliers are shown in Figures 6.3 and 6.4. The black triangles indicate the position of the detected breaks in the ratio series of a station versus the other weather stations, while A points out the outliers and the empty rhombs are representing missing data. The weather stations are ordered from the top to the bottom with respect to increasing values of the estimated standard deviation STD. Hence, in practice, the reliability of the comparisons slightly increases from the bottom to the top.



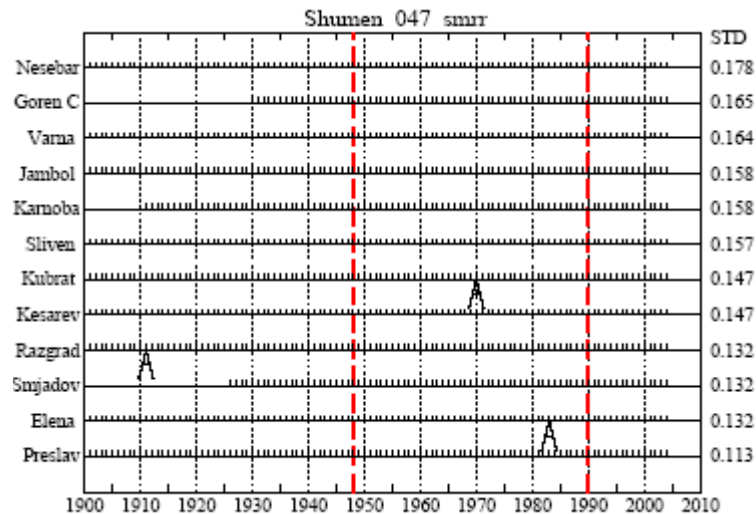


Figure. 6.3. Homogenization of precipitation data in Shumen: \square - break; A – outlier; red dash line – validated break and then corrected; \diamond – missing values; bottom – end of homogenization

Some breaks during the 20th century could be detected easily in Figures 6.3 (top) and 6.4 (top), considering the relatively good alignment of breaks in precipitation. The knowledge of break positions for many applications including climate variability and change studies is the first 50% of the final goal. The second part of the homogenization goal is the break correction. The two factors linear model was applied after break detection. It was assumed that the series within the same climatic area are considered as affected by the same climatic signal factor at each time, while the station factor remains constant between two breaks. The model computed the correction coefficients of a set of non-homogeneous series, through weighted least squares estimation of the parameters.

It was impossible to locate straightaway all possible breaks: the pronounced breaks hid smaller one's. Thus, the procedure of detection and correction of breaks and outliers was not automatic. It was iterative and the expert knowledge and strategy was essential. The whole procedure of break detection and corrected took a long time – it was run near 10 times in order to locate, validate and correct possible breaks and outliers. Every time the expert team validated the breaks keeping in mind some statistical and climatological issues. This iteration ended when all or most break risk was gone (Fig. 6.3 (bottom) and 6.4 (bottom)). Series were considered "homogeneous" (e.g., Moisselin and Mestre, 2002), a relative notion linked to the Amplitude of Residual Breaks (ARB), which was estimated by the method of homogenization. In this particular study ARB was assumed about 10% of the annual amount of precipitation.

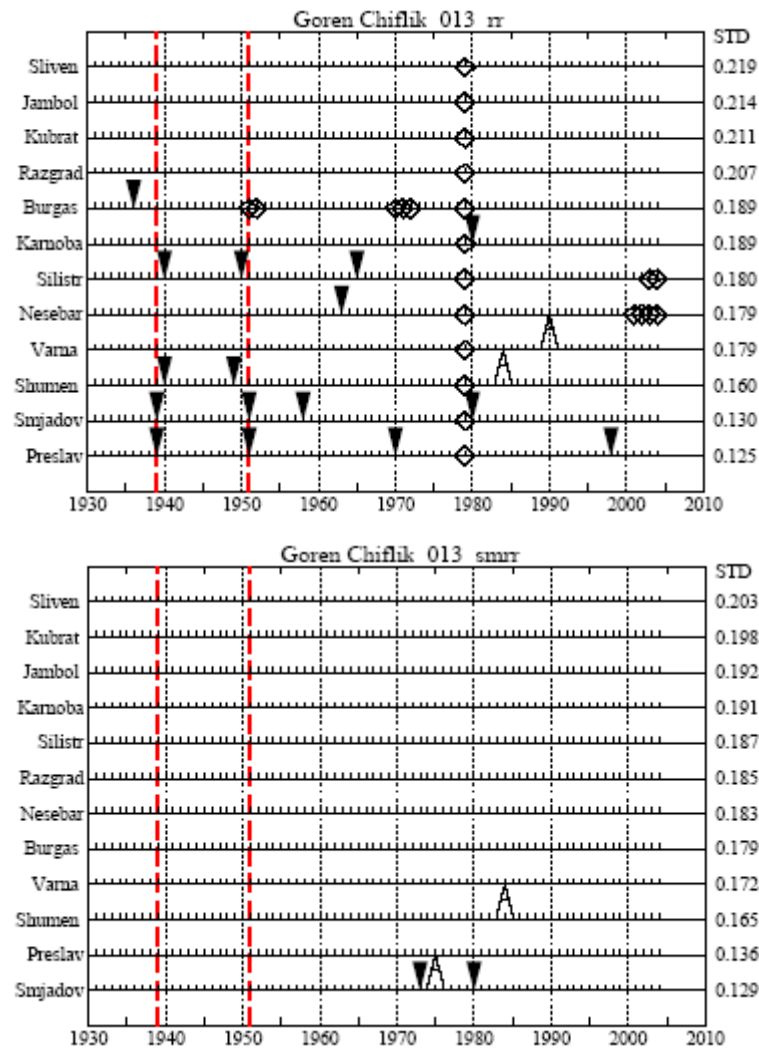


Figure. 6.4. Homogenization of precipitation data in Goren Chiflik: \square - break; A – outlier; red dash line – validated break and then corrected; \diamond – missing values; bottom – end of homogenization

The final step in the homogenization procedure was to replace missing monthly values. The two factors linear model by means of the computed weighted least squares allows correction of series with missing data. For this purpose, the linear model was run the last time with the option for correction of missing data (Fig. 6.3 (bottom) and 6.4 (bottom)).

Precipitation indices

It was assumed that when there is a break in a monthly weather series, the respective daily weather series is affected also by a break. That is why, one of the criterion applied within the study was to cut daily series before significant break occurrence in monthly precipitation in the same weather station. The accepted significant threshold was 10%. The other criteria for establishment of reference daily weather series was to have less than 20% of missing values for the periods between the last significant break and the end of the data records (usually 2002). The beginning of the final

constructed reference series of daily precipitation, covering the considered period 1951-2000, is presented in Table 6.2.

Table 6.2. Weather stations beginning (year) of reference series regarding daily precipitation

<i>Station</i>	year	<i>station</i>	year
Elhovo	1946	Pleven	1906
Haskovo	1906	Plovdiv	1946
Ivajlovgrad	1933	Russe	1928
Karnobat	1928	Sadovo	1933
Kjustendil	1919	Sliven	1900
Knesha	1926	Tran	1932
Kurdjali	1929	Vidin	1910
Lom	1931	Vratza	1929
Orjahovo	1948	-	-

All precipitation indices listed in Table 6.1 were calculated, however, the results below are based only on the following STARDEX core precipitation indices:

- prec90 90th percentile of rainday amounts
- R5d Greatest 5-day total rainfall
- SDII Simple daily intensity
- CDD Maximum number of consecutive dry days
- R90T % of total rainfall from events > long-term 90th percentile
- R90N Number of events > long-term 90th percentile

The precipitation indices provide a good mix of measures of intensity (prec90, R5d, SDII), frequency (R90N, CDD) and proportion of total (R90T). Some of the indices consider properties of just the rainday distribution (prec90, SDII) while the others use the entire distribution. All thresholds are percentile-based and so can be used for a wide variety of climates.

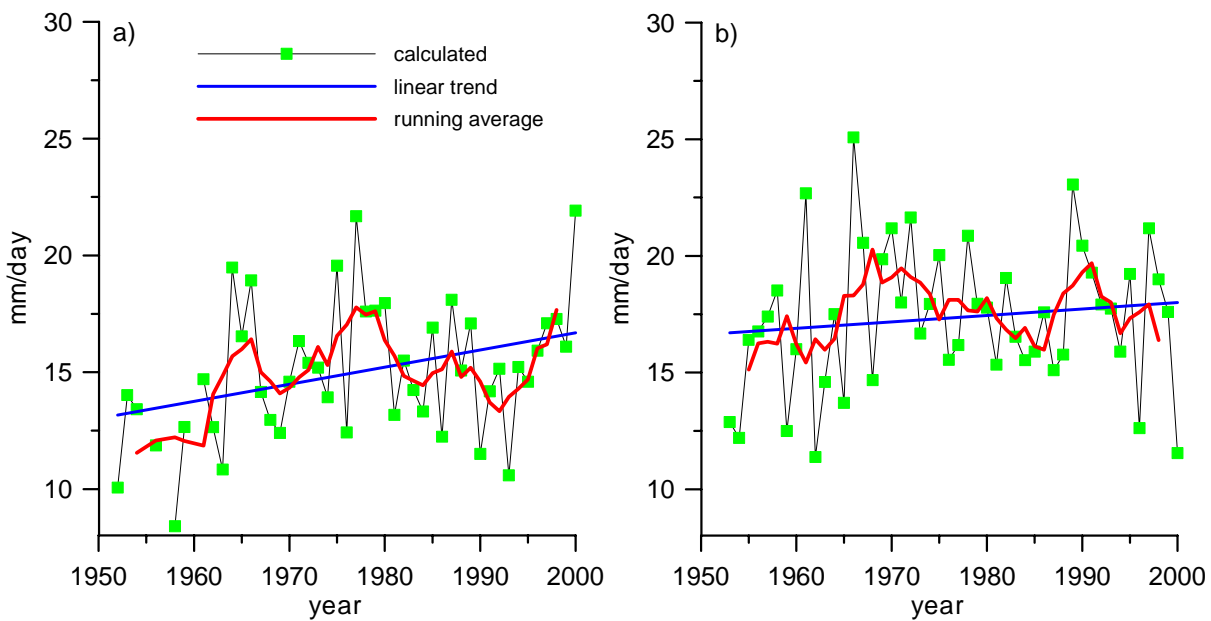
The annual index – the 90th percentile of the rainday amounts (prec90) - varied mainly from 10 to 20 mm/day during the second half of the previous century (Fig. 6.5). Opposite trends are observed in some regions of the country. For example, prec90 has a negative tendency in the weather stations in southern Bulgaria, while most of the other stations are faced with a positive (although insignificant) trend (Fig. 6.6). The other indices characterizing the precipitation intensity (R5d and SDII) showed also various trends depending on the weather station locations. From the first side, the index of the greatest 5-day total rainfall R5d has decreased significantly in the stations Plovdiv and Ivajlovgrad – both in southern Bulgaria (Fig. 6.7 and 6.8c). On the second side, however, two neighbor stations in the north-western part of the Danube Plain (Knesha and Orjahovo) are characterized by considerable increasing trend (Fig. 6.7). Regarding the simple daily intensity index SDII, the following picture was found: most of the considered weather stations located in South

Bulgaria have a negative trend for the period 1951-2000, but it is vice versa in North Bulgaria (Fig. 6.9).

The precipitation index CDD presenting the maximum number of the consecutive dry days shows one and the same signal across the country (Fig. 6.10 and 6.11). Although the registered increasing trend is not statistically significant one, the obtained trend is clear. It seems that frequency of drought events at the end of the 20th century have changed. It should be noted that the country was affected by drought periods of various intensity from 1982 to 1994. The year 2000 was the driest year during the second half of the last century.

The proportion of total, the precipitation index R90T, is slightly reducing in the considered region of southeastern Bulgaria (the weather stations located at the valley of the Maritza river and/or south of it) – Figure 6.12. But, most of the rest weather stations, applied within the study, demonstrated an insignificant increasing tendency.

As it was mentioned above, the precipitation index R90N gives a measure of precipitation frequency. All considered weather stations in southern Bulgaria are faced by a significant decreasing trend (Fig. 6.13 and 6.14). The same considerable trend of R90N reduction was also registered in Kustendil (western Bulgaria) and Vidin (northwestern Bulgaria) (Fig. 6.13).



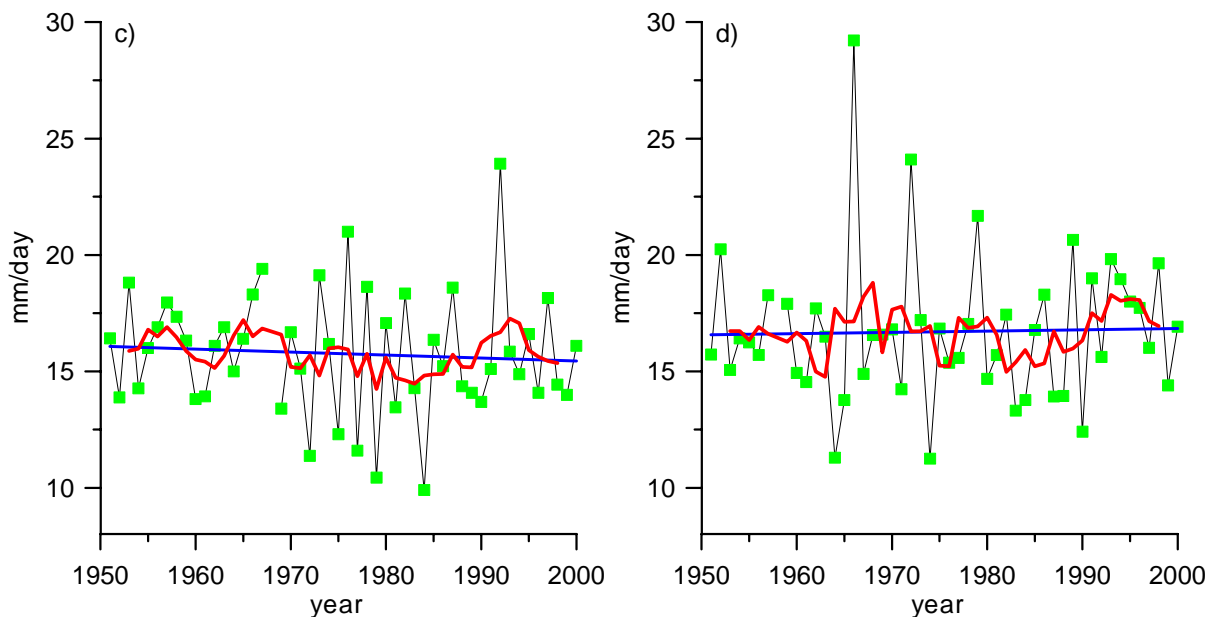


Figure 6.5. prec90 annual variability in Kneja (a), Ruse (b), Kustendil (c) and Elhovo (d)

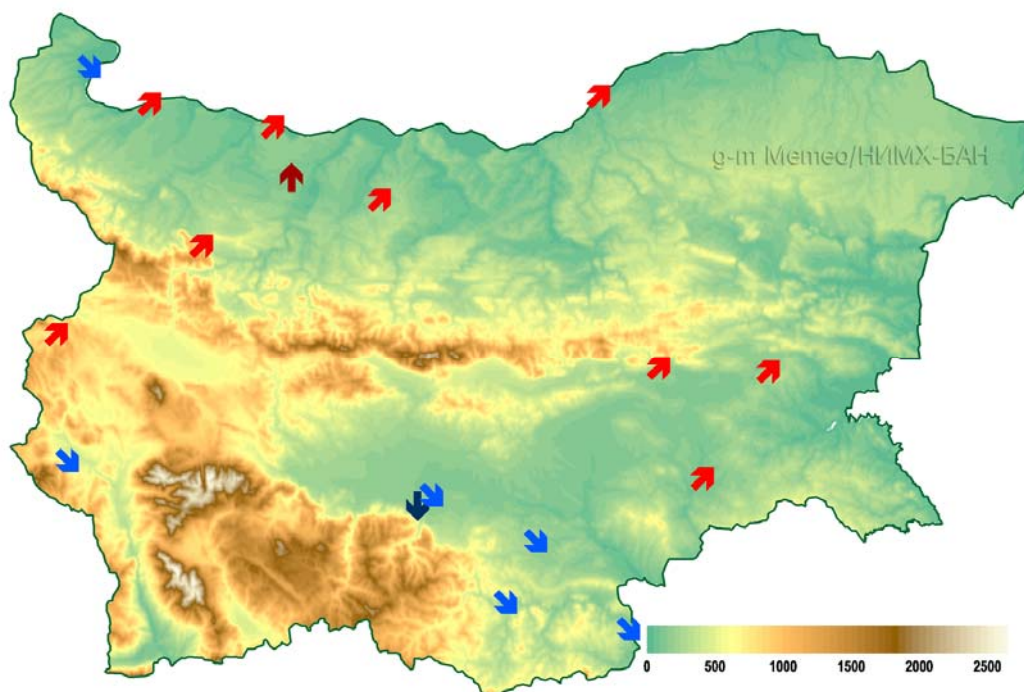


Figure 6.6. Spatial distribution of annual prec90 trends (1951-2000) by applying the Spearman test; dark red arrows – significant increasing trend; red arrows – increasing trend; blue arrows – decreasing trend; dark blue arrows – significant decreasing trend

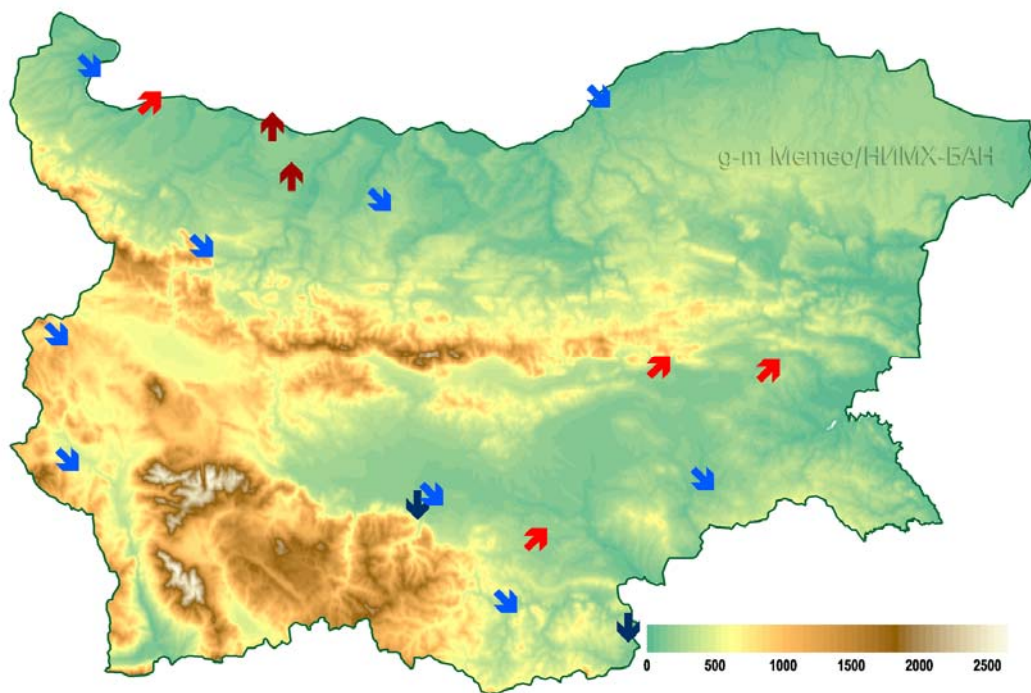
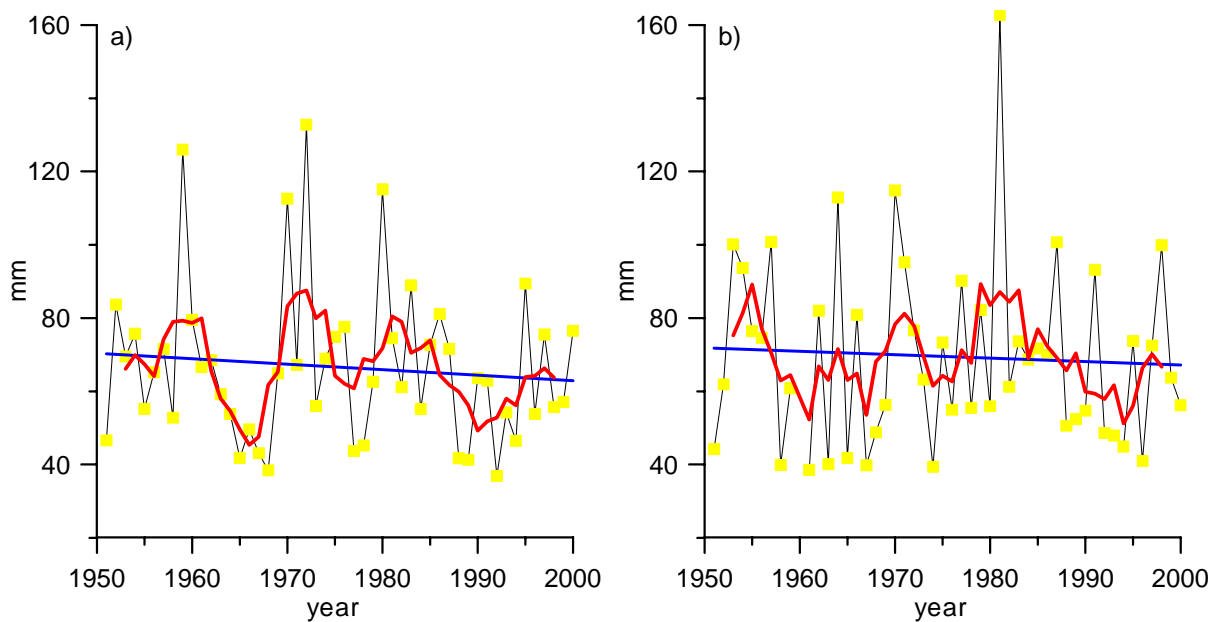


Figure 6.7. Spatial distribution of annual R5d trends (1951-2000) by applying the Spearman test; dark red arrows – significant increasing trend; red arrows – increasing trend; blue arrows – decreasing trend; dark blue arrows – significant decreasing trend



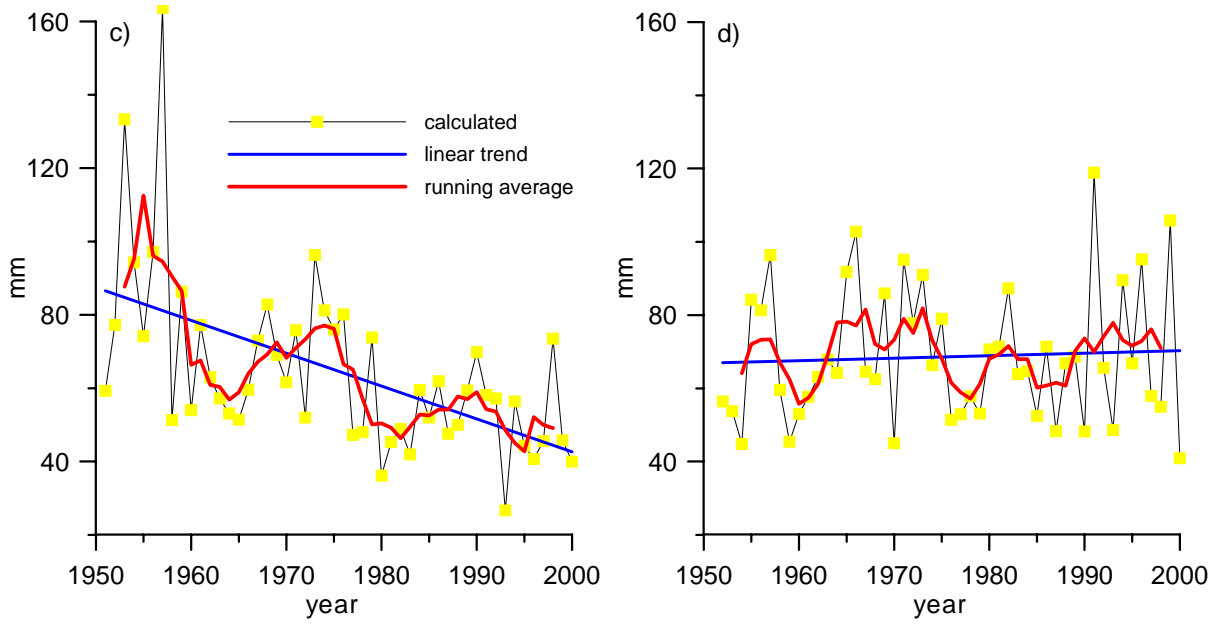


Figure 6.8. R5d annual variability in Vidin (a), Pleven (b), Ivajlovgrad (c) and Sliven (d)

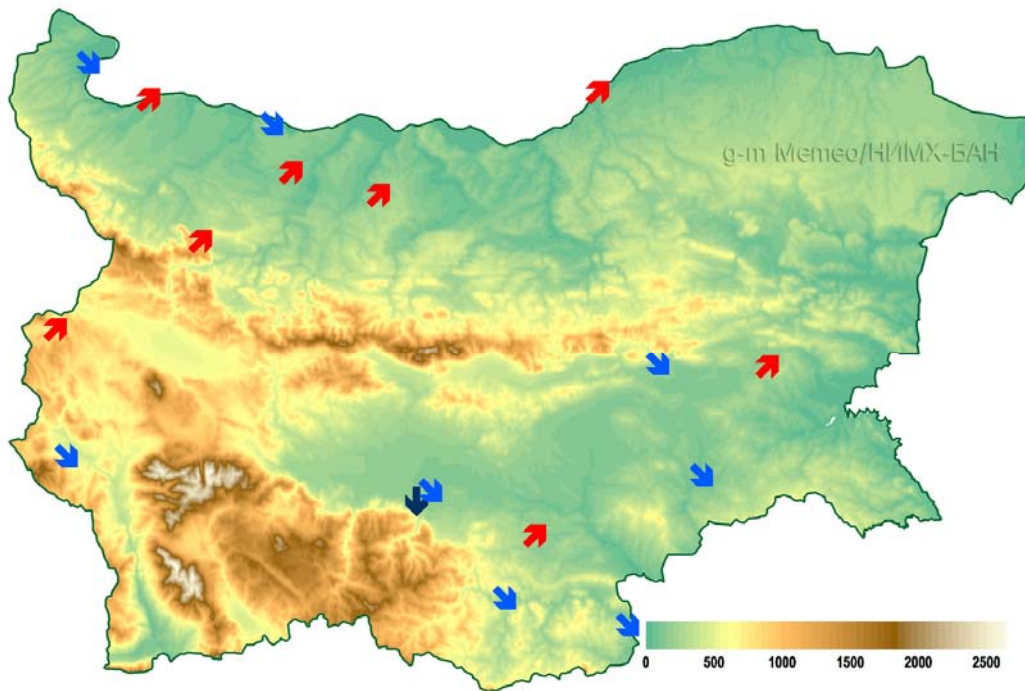


Figure 6.9. Spatial distribution of annual SDII trends (1951-2000) by applying the Spearman test; red arrows – increasing trend; blue arrows – decreasing trend; dark blue arrows – significant decreasing trend

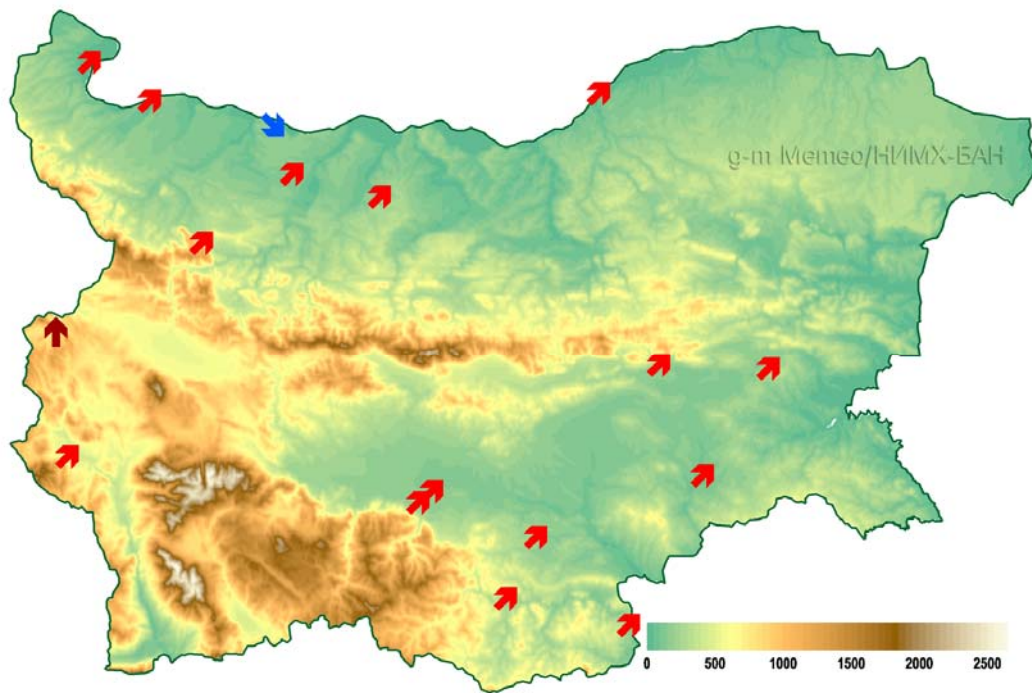
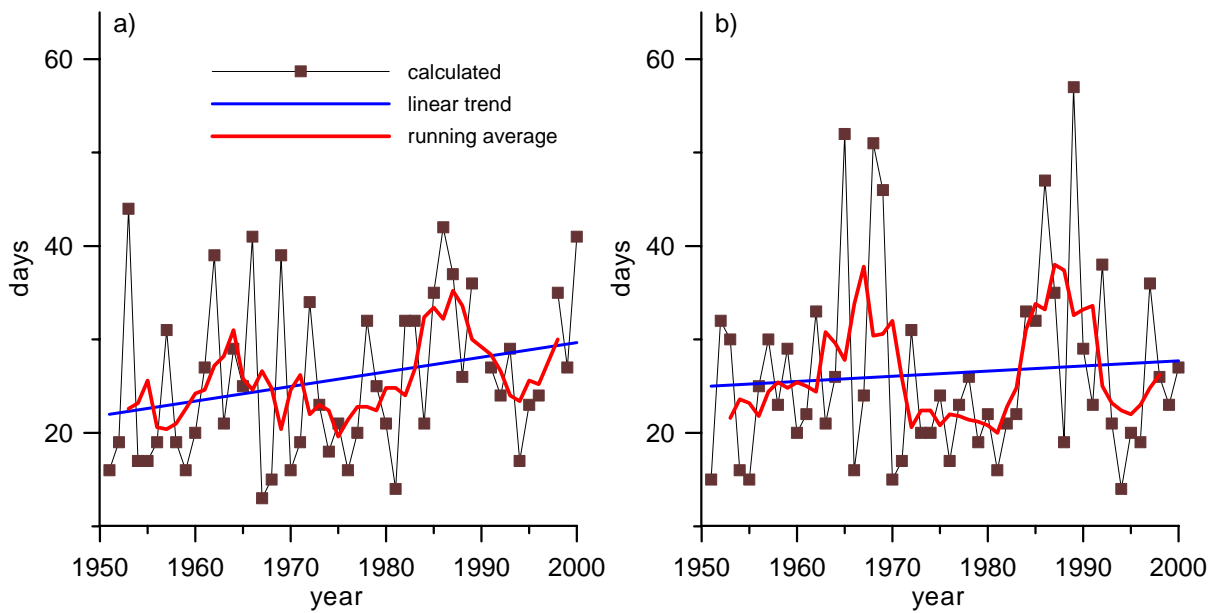


Figure 6.10. Spatial distribution of annual CDD trends (1951-2000) by applying the Spearman test; dark red arrows – significant increasing trend; red arrows – increasing trend; blue arrows – decreasing trend



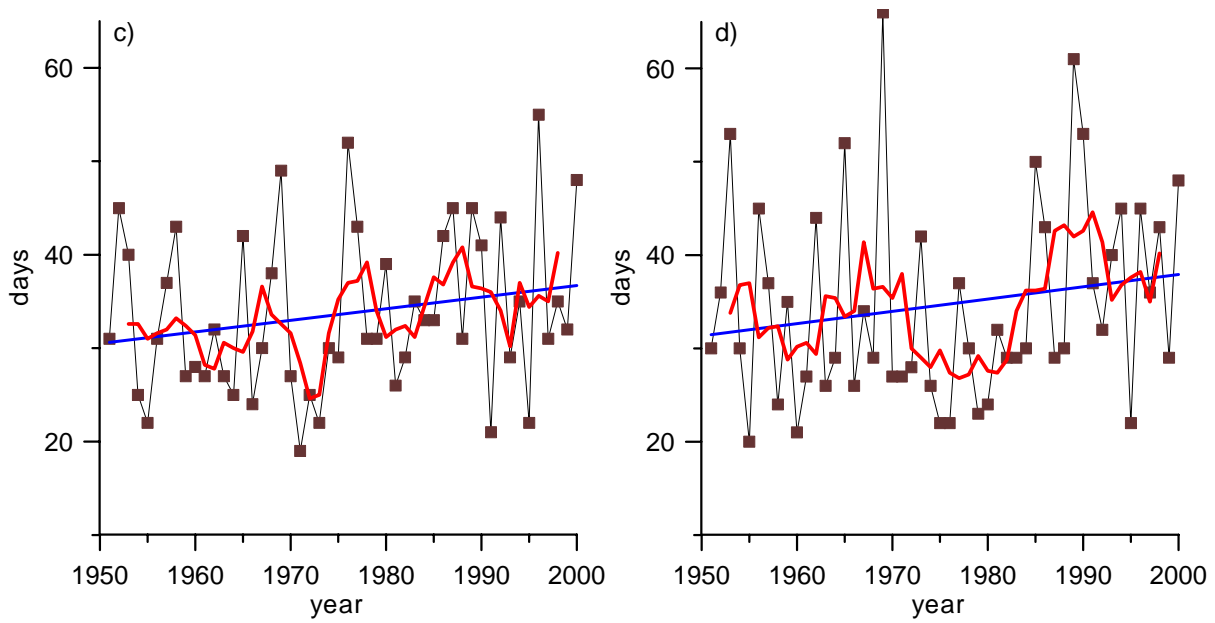


Figure 6.11. CDD annual variability in Tran (a), Vratza (b), Sadovo (c) and Karnobat (d)

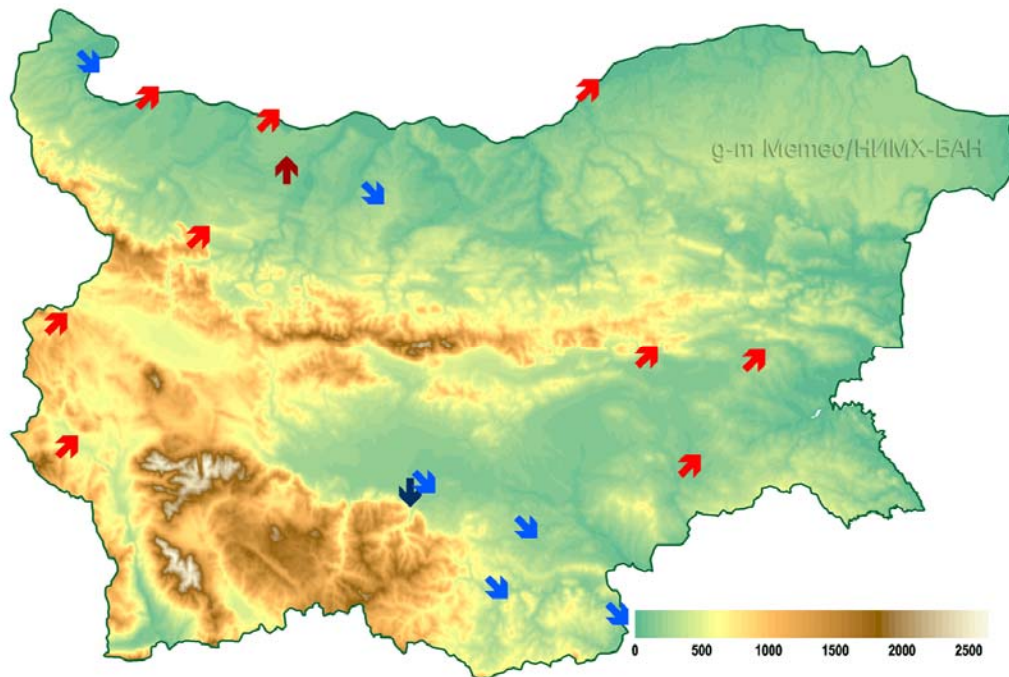


Figure 6.12. Spatial distribution of annual R90T trends (1951-2000) by applying the Spearman test; dark red arrows – significant increasing trend; red arrows – increasing trend; blue arrows – decreasing trend; dark blue arrows – significant decreasing trend

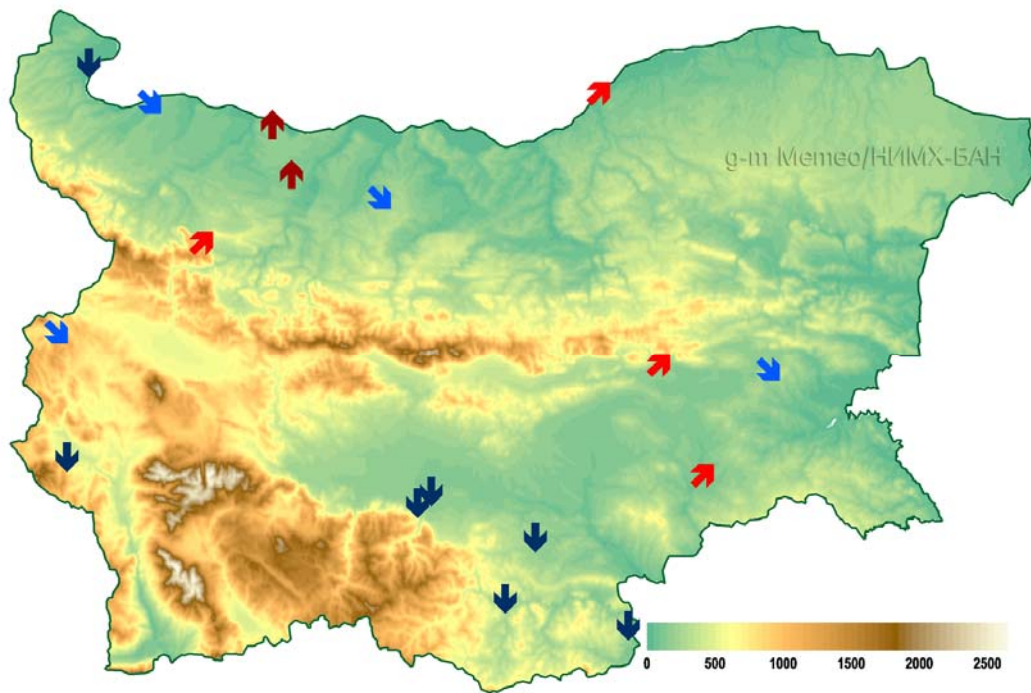


Figure 6.13. Spatial distribution of annual R90N trends (1951-2000) by applying the Spearman test; dark red arrows – significant increasing trend; red arrows – increasing trend; blue arrows – decreasing trend; dark blue arrows – significant decreasing trend

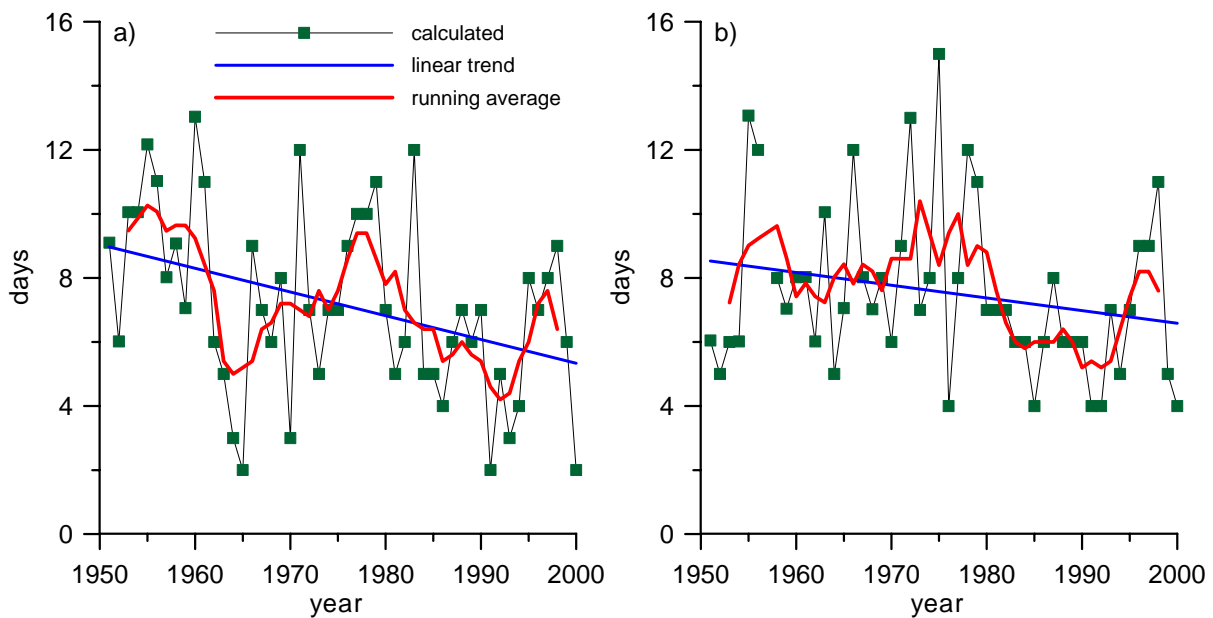


Figure 6.14. R90N annual variability in Plovdiv (a) and Haskovo (b)

Concluding remarks

Variability and trends in 42 indices, mainly highlighting changes in extreme precipitation in Bulgaria for the period 1951–2000, have been examined. It is considered this study makes an additional contribution to the climate variability and change research for Bulgaria.

Houghton et al. (2001) stated that it is likely that there has been a statistically significant increase in the amount of the extreme precipitation events when averaged across the mid and high latitudes. According to the hypothesis of Groisman et al. (1999), there should be an amplified response of the extreme precipitation events relative to the change in total amount. It is necessary to point out that annual precipitation in Bulgaria is characterized by strong interannual variability without any significant trend during the 20th century. The trends in the core STARDEX precipitation indices, including the 90th percentile of the rainday amounts, greatest 5-day total rainfall, simple daily intensity, maximum number of consecutive dry days, percentage of total rainfall from events higher than long-term 90th percentile, number of events higher than long-term 90th percentile are weak and are not very significant in general. The significant trends were observed in separate weather stations or areas only. It is necessary to mention that the calculated tendencies of the above indices in most cases are with low spatial coherence.

Additional work is planned to be done on precipitation indices in Bulgaria. A special attention will be paid in the future on the most extreme precipitation indices as the country was recently affected by severe drought and flood events. Further analysis of precipitation related indices is needed as well as comparison of the results with the ones obtained in different European regions.

Acknowledgements

Acknowledgements are addressed to the French Meteorological Society (SMF) and Météo-France for their support related to the study. Thanks are expressed to the Direction of Climatology at Météo-France as well as the National Institute of Meteorology and Hydrology in Sofia.

References

- Alexandersson, H., 1986: A homogeneity test applied to precipitation data. Int J Climatol, 6: 661-675*
- Bessemoulin, P. and J.M. Moisselin, 2005: French multidisciplinary IMFREX project, evolution of climate extremes. (personal communication)*
- Bonsal, B. R., X. Zhang, L. A. Vincent, and W. D. Hogg, 2001: Characteristics of daily and extreme temperatures over Canada, J. Clim., 14: 1959–1976*
- Caussinus, H. and F. Lyazrhi, 1997: Choosing a linear model with a random number of change-points and outliers. Ann Inst Statist Math, 49: 761-775*
- Caussinus, H. and O.Mestre, 1997: New mathematical tools and methodologies for relative homogeneity testing. Proceedings of the First Seminar for Homogenization of Surface Climatological Data, Budapest, Hungary, pp. 63-82*
- Easterling, D. R., L. V. Alexander, A. Mokssit, and V. Detemmerman, 2003: CI/CLIVAR workshop to develop priority climate indices, Bull. Am. Meteorol. Soc., 84: 403–407*
- Groisman, P.Y., T.R. Karl, D.R. Easterling, R.W. Knight, P.F. Jamason, K.J. Hennessy, R. Suppiah, C.M. Page, J. Wibig, K. Fortuniak, V.N. Razuvaev, A. Douglas, E. Forland, and P-M. Zhai, 1999: Changes in the probability of heavy precipitation: important indicators of climatic change. Climatic Change, 43: 243-283*

- Hawkins, D.M., 2001:** *Fitting multiple change-points to data. Comput Statist Data Anal, 37: 323-341*
- Houghton, J.T., Y. Ding, D.J. Griggs, M. Noguer, P.J van der Linden, and D. Xiaosu (eds.), 2001:** *Climate Change 2001: The Scientific Basis. Contribution of Working Group I to the Third Assessment Report of the Intergovernmental Panel on Climate Change (IPCC). Cambridge University Press, UK, 944 pp.*
- Førland, E.J. and I.Hanssen-Bauer, 1994:** *Homogenizing long Norwegian precipitation series. Journal of Climate, 7: 1001-1013*
- Frich, P., L. V. Alexander, P. Della-Marta, B. Gleason, M. Haylock, A. M. G. Klein Tank, and T. Peterson, 2002:** *Observed coherent changes in climatic extremes during the second half of the twentieth century, Clim. Res., 19: 193– 212*
- Karl, T. R., N. Nicholls, and A. Ghazi, 1999:** *CLIVAR/GCOS/WMO workshop on indices and indicators for climate extremes: Workshop summary, Clim. Change, 42: 3–7*
- Klein Tank, A., 2004:** *Changing Temperature and Precipitation Extremes in Europe's Climate of the 20th Century. PhD thesis, ISBN 90-369-2254-2, The Netherlands, 124 pp.*
- Koleva, E., N. Slavov and V. Alexandrov, 2004:** *Drought during the 20 Century. In: Knight, C. G., I. Raev and M. Staneva (eds.). 2004. Drought in Bulgaria: A Contemporary Analog for Climate Change. Aldershot, UK: Ashgate Publishing Limited, pp. 53-66.*
- Lavielle, M., 1998:** *Optimal segmentation of random processes. IEEE Transactions on Signal Processing 46(5): 365-1373*
- Mestre, O., 1999:** *Step-by-step procedures for choosing a model with change points. Proceedings of the Second Seminar for Homogenization of Surface Climatological Data, WMO-TD, No.962, WMO, Geneva, pp. 15-26*
- Mestre, O., 2000:** *Méthodes statistiques pour l'homogénéisation de longues séries climatiques. Thèse de doctorat de l'Université Paul Sabatier. Toulouse: Université Paul Sabatier*
- Moisselin, J.M. and O.Mestre, 2002:** *Research, Digitisation and Homogenization of Long-Term Data Series. Actes du Colloque "La Pérennisation et la Valorisation des données scientifiques et techniques" (Ensuring Long-Term Preservation and adding Value to scientific and technical data) organisé par le CNES du 5 au 7/11/2002, Toulouse*
- Moisselin, J-M, M. Schneider, C. Canellas and O. Mestre, 2002:** *Les changements climatiques en France au XXe siècle. Etude des longues séries homogénéisées de données de température et de précipitations. La Météorologie 38: 45-56*
- Peterson, D.C. and D.R.Easterling, 1994:** *Creation of homogeneous composite climatological reference series. Int J Climatol, 14: 671-679*
- Peterson, T.C. et al., 1998:** *Homogeneity adjustments of In Situ atmospheric climate data: a review. Int J Climatol, 18:1493-1517*
- Peterson, T. C., et al., 2002:** *Recent changes in climate extremes in the Caribbean region, J. Geophys. Res., 107(D21)*
- Peterson, T.C., C. Folland, G. Gruza, W. Hogg, A. Mokssit, and N. Plummer, 2001:** *Report on the Activities of the Working Group on Climate Change Detection and Related Rapporteurs 1998-2001. Report WCDMP-47, WMO-TD 1071, World Meteorological Organisation, Geneva, Switzerland*
- Sen, P. K., 1968:** *Estimates of the regression coefficient based on Kendall's Tau, J. Am. Stat. Assoc., 63: 1379–1389*
- Wang, X. L., and V. R. Swail, 2001:** *Changes of extreme wave heights in Northern Hemisphere oceans and related atmospheric circulation regimes, J. Clim., 14: 2204–2220*
- World Meteorological Organization (WMO), 1990:** *On the statistical analysis of series of observations. Technical Note 143/WMO 415. Geneva: WMO*

Zhang, X. et al., 2005: Trends in Middle East climate extreme indices from 1950 to 2003. Journal of Geophysical Research, 110

Zhang, X., L. A. Vincent, W. D. Hogg, and A. Niitsoo, 2000: Temperature and precipitation trends in Canada during the 20th century, Atmos. Ocean, 38: 395–429

D4.2.7 Aristotle University of Thessaloniki, Greece (AUTH)

Large-scale circulation patterns, such as the ones connected to the North Atlantic Oscillation (NAO) or northern hemisphere atmospheric blocking, are known to control westerly flow of air into the European continent, thus affecting local weather and climate. Our aim is to investigate their effects in detail over Europe, and specifically their relation to temperature and precipitation changes using high resolution data. To achieve this, we use existing data from simulations performed with Regional Climate Models (RCMs) in the framework of the European project ENSEMBLES, and compare the results with observations when applicable.

Past changes (1961-2000)

As a first step, we have analysed output data from a number of RCM simulations driven with the ERA40 reanalysis dataset, over the period 1961-2000. The results are compared to analyses performed with either local station data, or gridded large data sets.

i) NAO related effects

In order to examine in the effect of NAO as depicted by the detailed output of RCMs we have used temperature (mean, maximum and minimum) and precipitation data as monthly means. Seasonal mean averages were calculated, and regression analysis was performed in order to assess the effect of the NAO, which is described using as a proxy the normalized seasonal mean indices calculated by J. Hurrell. Although the analysis is performed for all seasons, the main focus is in northern winter (December through February), when the effects are more pronounced.

Results from the models analysed showed good agreements to each other. The main results were similar to the observed NAO effects over Europe, i.e. warm and wet over North-Eastern Europe and dry over the Mediterranean when NAO is in the positive phase (positive NAO Index).

In our preliminary analysis, we were able to deduce in detail the effect of a positive change (of the magnitude of 1 sigma of the normalized Index) in temperature and precipitation. The largest changes in average temperature were found over Scandinavia and around the Baltic Sea, reaching 2 degrees for a 1 sigma change in NAOI. Central Europe, and in particular the target area in CECILIA does not present large significant anomalies. However, a detailed analysis (which is under way) for all seasons and monthly or daily values may reveal significant effects over more areas.

The above results are seen not only in average daily mean temperature, but in daily maximum and minimum temperatures as well. It should be noted that the effect is large in daily minimum temperatures over greater areas. In the case of precipitation, Mediterranean (and its northern surrounding area) is found to become drier for positive changes of NAO Index, while central and northern Europe experience more wet weather. This analysis is continuing as more data from the ENSEMBLES database become available.

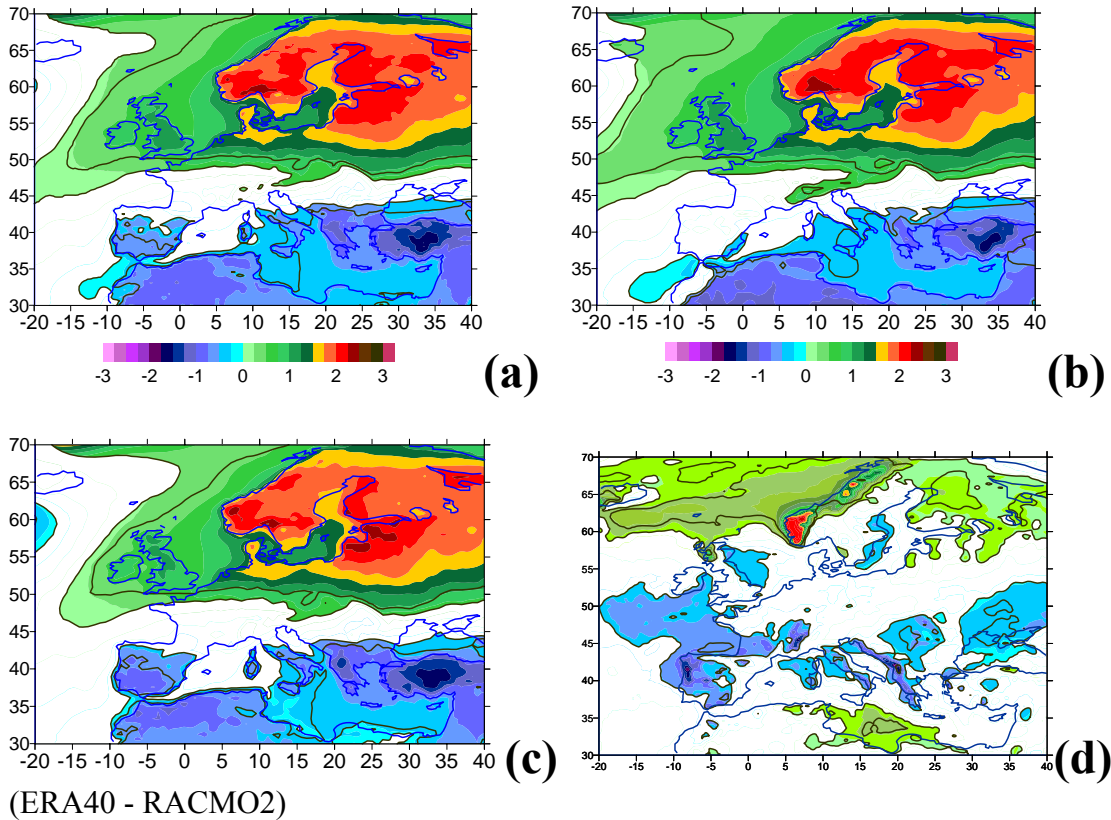
Atmospheric blocking in the Euro-Atlantic region.

This circulation feature is known to affect the weather locally over Europe, persisting over a number of days and causing large changes in precipitation and temperature. A number of indices are proposed in order to define a blocking situation in the northern hemisphere, the most widely used being the one by Tibaldi and Molteni (1982) (TM). We use this index to define whether a particular longitude is blocked, with some slight modifications regarding the higher latitude limit, which we have set at 70N, as this is the limit in the ENSEMBLES model runs. As the various model outputs were given on different grids (also rotated latitude and longitude), and due to the index definition, the daily 500hPa geopotential heights from the various models were interpolated in 2.5x2.5 degree grids, and the TM criteria for the definition of blockings were applied. Blocking activity is found in all seasons, more pronounced over Europe in winter (December through February) and spring (March through May). In this present analysis we have focused in the winter season (December through February).

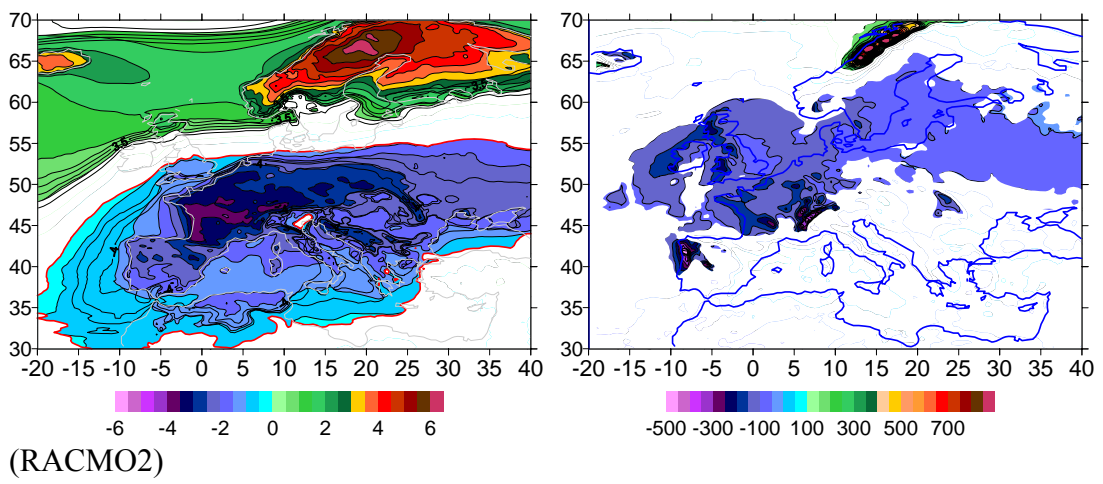
Even though the RCM output grids are given only over Europe, the results were in good agreement with the analysis performed on the daily mean 500hPa geopotential height data from the ERA40 reanalysis. The peak longitudes of highest blocking activity, as well as the frequency of blocked days were in very good agreement with the observations. The duration of the blockings did not appear to be as long in some of the RCMs as in the reanalysis data, this being a known feature of the blocking activity simulation in General Circulation Models (GCMs) as well. The effect of the blocking activity was examined in a number of RCMs during winter by calculating daily composites of departures of temperature and precipitation from the long-term mean for the days central to blocking episodes with duration more than 5 days. Our preliminary results show significantly lower temperatures and precipitation over central Europe during blockings, while Scandinavia and the Baltic Sea is warmer and drier.

Changes in a future climate (2001-2100)

- i) NAO: For the models driven by the General Circulation Model ECHAM5, a NAO Index is now being constructed from the means sea level pressure data of the runs that were used to drive the RCMs in ENSEMBLES. The NAO/temperature and precipitation relations are going to be examined in the future climate, as simulated by the RCMs.
- ii) Atmospheric blocking: Preliminary calculations using the 500hPa geopotential heights at 12:00UTC as given by available RCM output, and as described above, shows a possible change in the frequency of the atmospheric blocking in the future. As this needs to be further looked into, the daily 500hPa geopotential heights at 12:00UTC from ECHAM5 are now being analysed so that detailed comparisons can be made.



Winter (DJF) changes in temperature and precipitation related to a positive change (of 1 sigma) of the normalized NAO Index. From top left to bottom right (a) daily average, (b) daily maximum and (c) daily minimum temperature. Precipitation flux changes are given in (d). Blue color scale denotes drier and colder areas. No coloring indicates areas with insignificant response.



Temperature and precipitation composites for days central to blocking episodes in winter (DJF). Only areas with significant effects are plotted (>95% as deduced with Student's t-test).

D4.2.8 NMA Climate indices calculation for station data in Romania

For the calculation of observation-based WP4 indices, the NMA used the software ProClimDB developed by Petr Štěpánek.

Data quality control (QC)

Prior to calculation of the extreme indices (EI) the daily data from 162 stations in Romania were quality controlled with the ProClimDB software. This procedure allowed detection the outliers at each station against neighbors selected according to distance and altitude.

The results of QC for the elements Tmean, Tmax and Tmin are presented in Table 8.1.

The big amount of outliers detected by the software were checked individually in the written climatological archived. As Table 8.1 shows not all the detected outliers were real but the QC helped a lot to correct the daily data in the climatological data base.

Table 8.1 Results of the quality control test with ProClimDB software for daily temperature data at 162 stations in Romania

Element	No. stations with outliers	Total no. of outliers	Total no of corrected outliers
Tmean	27	176	14
Tmax	96	327	125
Tmin	127	766	223

Extreme indices (EI)

The NMA calculated the extreme indices (EI) with ProClimDB software for Romanian stations available for the period 1961-1990 and, in agreement with all the CECILIA partners contributing to D4.2 exemplification with the same indices for two selected seasons, winter (DJF) and summer (JJA), and annual (ANN) follows.

The maps were produced using the regression-kriging gstat package of R and then the results were visualized in ARGGIS and exported as jpg files.

The stations where the indices were calculated are represented with circles on the map.

Ind 001 DJF – Figure 8.1a)

- < - 4.0 to - 2.0° C - at high altitudes of the Carpathian mountains
- 0.0 to 2.0°C - in the central and eastern part of the country
- 2.0 to 4.0 °C – in south and west
- > 4.0 °C - in the south west and Black Sea coast

Ind 001 JJA – Figure 8.1b)

- < 12 °C - at very high altitudes (> 1500 m)
- 16.0 to 20.0 °C at the mountains and adjacent areas
- 20.0 to 24.0°C at lower altitudes, intra Carpathians, NE of the country and Black Sea coast

Ind 002 DJF – Figure 8.2a)

- < -10°C - at very high altitudes (> 1500 m)
- 10.0°C to -6.0 °C - at the mountains
- 6.0°C to -4.0 °C - intra and extra Carpathian region, adjacent to mountains
- 3.0°C to -2.0 °C - West of the country and adjacent areas to Black Sea
- > - 2.0 °C - in SW and Black Sea coast

Ind 002 JJA – Figure 8.2b)

- 4.0°C- to 10.0 °C - at very high altitudes (> 1500 m)
- 10.0°C to 12.0 °C – central part of the country and mountain adjacent areas
- 12.0°C to 14.0 °C extra Carpathian and western part of Romania
- > 14.0°C Southern, easternmost and local spots in W-SW

Ind 003 DJF – Figure 8.3a)

- > 7.0°C to -3.0°C - at high altitudes of the Carpathian mountains
- 3.0°C to -1.0°C - intra and extra Carpathians and local spots in the South
- 1.0°C to 1.0°C - South, West and SE of Romania
- > 1.0°C - Black Sea coast and local spot in SW

Ind 003 JJA – Figure 8.3b)

- > 6.0°C to 14.0°C - at high altitudes of the Carpathian mountains
- 14.0°C to 18.0°C - intra and extra Carpathians and adjacent to mountains
- 18.0°C to 20.0°C - intra and extra Carpathians at lower altitudes
- 20.0°C to 22.0°C - South, West of the country
- > 22.0° C - Southern most of Romania

Ind 058 ANN – Figure 8.4a)

- < 3.0% to 15.0% - at high altitudes of the Carpathian mountains
- 15.0% to 21 % - intra and extra Carpathians adjacent to mountains
- 21.0% to 27.0% - Western and Southern parts of Romania
- > 27.0% - Southern part of Romania

Ind 059 ANN – Figure 8.4b)

- < 0.5% - most of the country
- 0.5% to 2.0% - South of the country
- 2.0% to 3.0% - SE , close to the Black Sea coast
- > 3% - Black Sea coast

Ind 066 ANN – Figure 8.5a)

- < 1.0% to 2.0% - High altitudes of Carpathian
- 2.0% to 5.0% - intra and extra Carpathian
- 5.0% to 7.0% - Western, Southern parts of the country adjacent to mountains
- 7.0% to 9.0% - South and Western part of the country
- > 9.0% - Southern most of Romania

Ind 067 ANN – Figure 8.5b)

- < 0.14% - Northern half of Romania including Carpathians, intra and extra Carpathian regions
- 0.14% to 0.85% - Southern Romania
- 0.85% to 1.25% - Southern Romania

Ind 068 ANN – Figure 8.6

- < 1.8% to 7.0% - High altitudes of Carpathians
- 7.0% to 12.0% - intra and extra Carpathian areas adjacent to mountains
- 12.0% to 16.0% - Western and Southern parts of Romania
- > 16.0% - Black Sea coast

Concluding remarks

- The spatial distribution of EIs for the period 1961-1990 both at seasonal and annual time resolution reflects the climate characteristics of Romania that is influenced by its orography.
- Both mean Tmax (I001) and mean Tmin (I002) show highest values in the southern part of Romania, mostly enhanced during summer, being in agreement with spatial distribution of Tmean (I003)
- The highest percentage of summer days (I058) and tropical nights (I059) are shown also in the southern part of the country as well as for hot days (I066) and extremely hot days (I067)
- The highest percentage of severe cold days (I068) appears in the Carpathians and adjacent areas
- The trend analysis of these indices based on observation will complete the information on climate extremes in Romania for the reference period against which the high resolution runs will be compared.

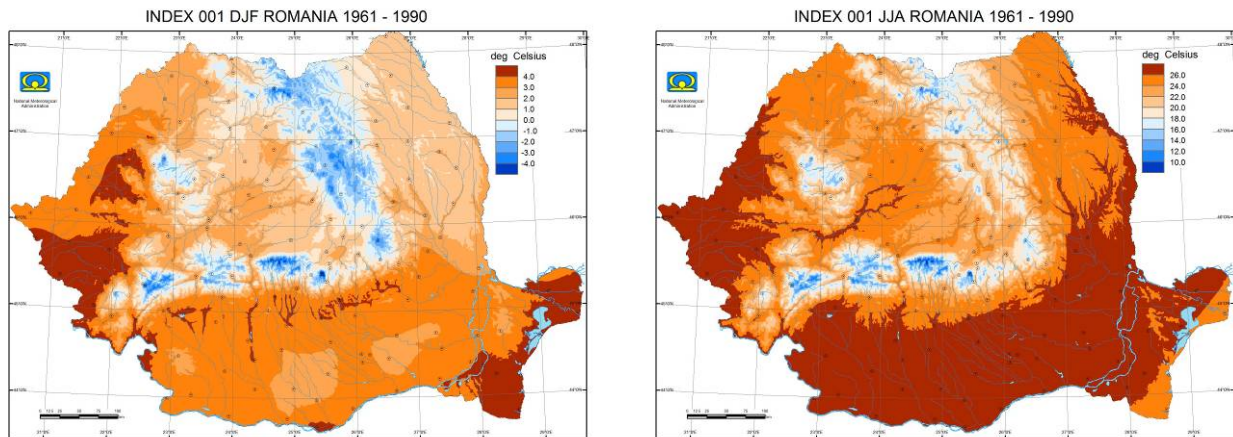


Figure 8.1 Index 001 - Mean Tmax – daily max averaged over 1961-1990

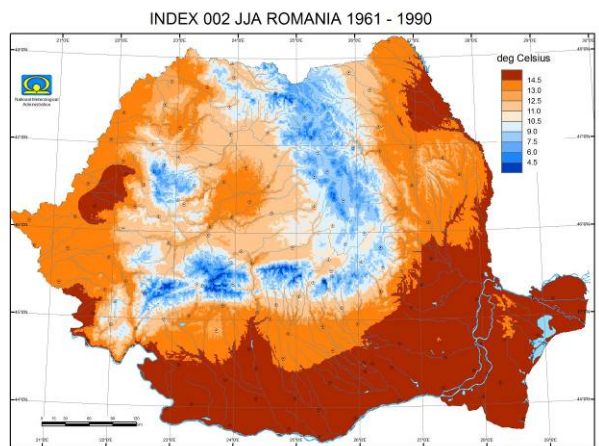
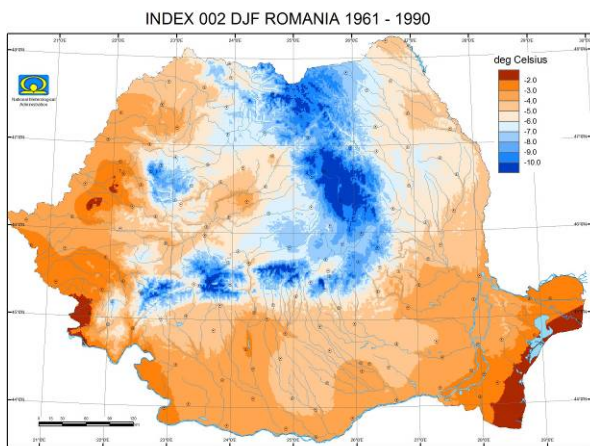


Figure 8.2 Index 002 - Mean Tmin - daily min averaged over 1961-1990

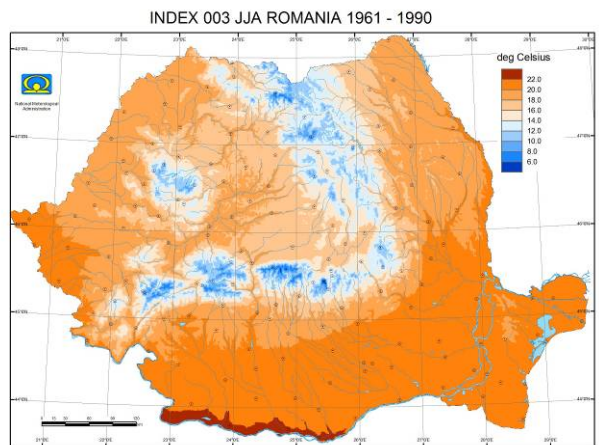
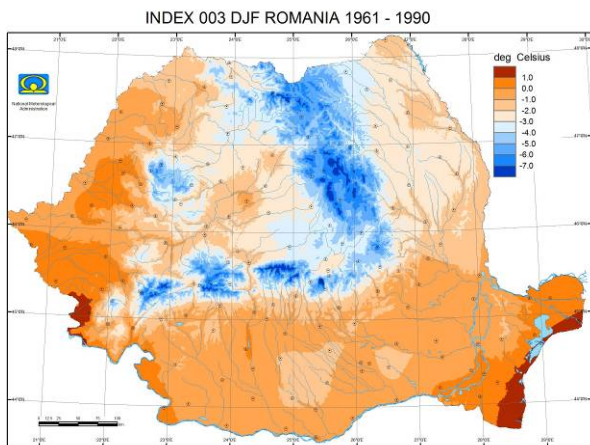


Figure 8.3 Index 003 - Mean Tmean - daily mean averaged over 1961-1990

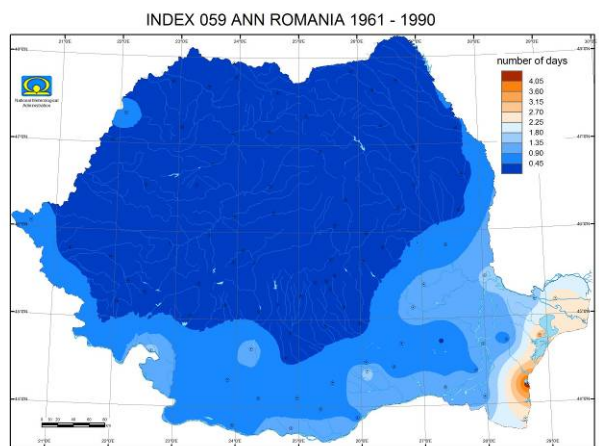
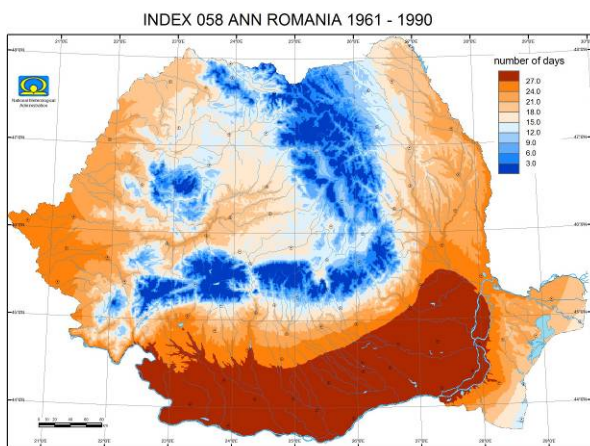


Figure 8.4

a) Index 058 - Percentage of “summer days” - %age of days where Tmax \geq 25C and

b) Index 059 - Percentage of “tropical nights” - %age of days where $T_{min} \geq 20C$

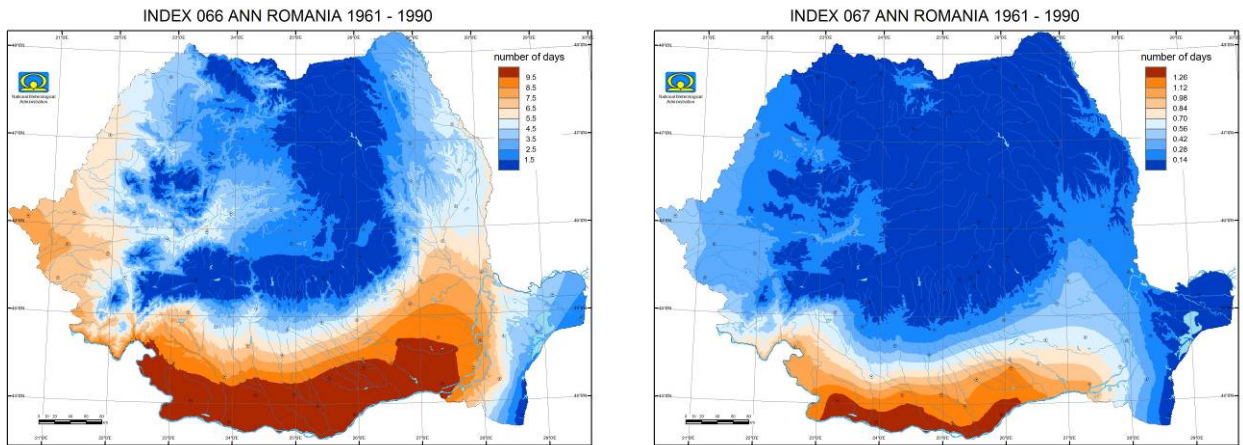


Figure 8.5

- a) Index 066 - Percentage of hot days - %age of days with $T_{max} \geq 30C$
- b) Index 067 - Percentage of extremely hot days - %age of days with $T_{max} \geq 35C$

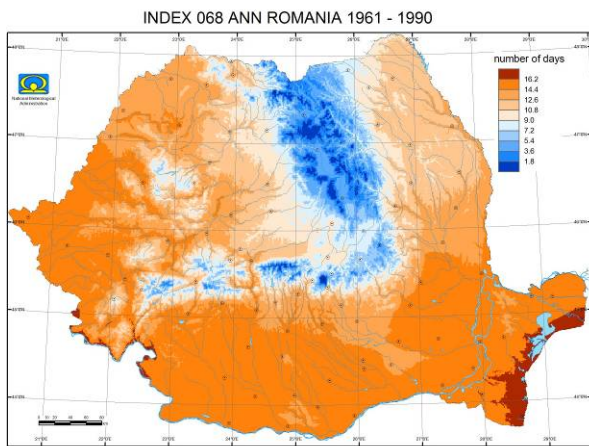


Figure 8.6 Index 068 - Percentage of severe cold days - %age of days with $T_{min} = < -10C$

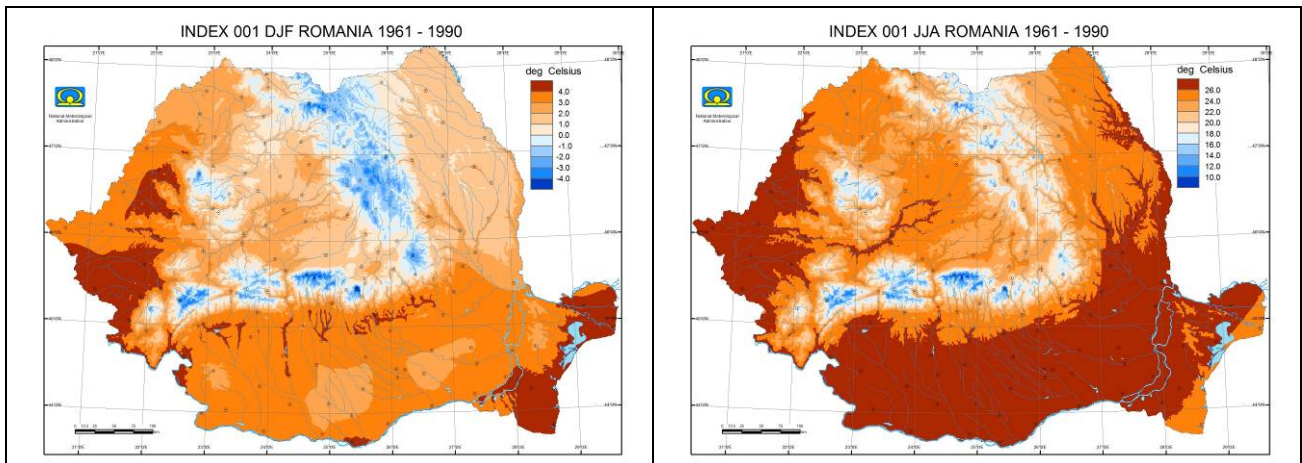


Figure 8.7 Index 067 - Percentage of extremely hot days - %age of days with $T_{max} \geq 35C$

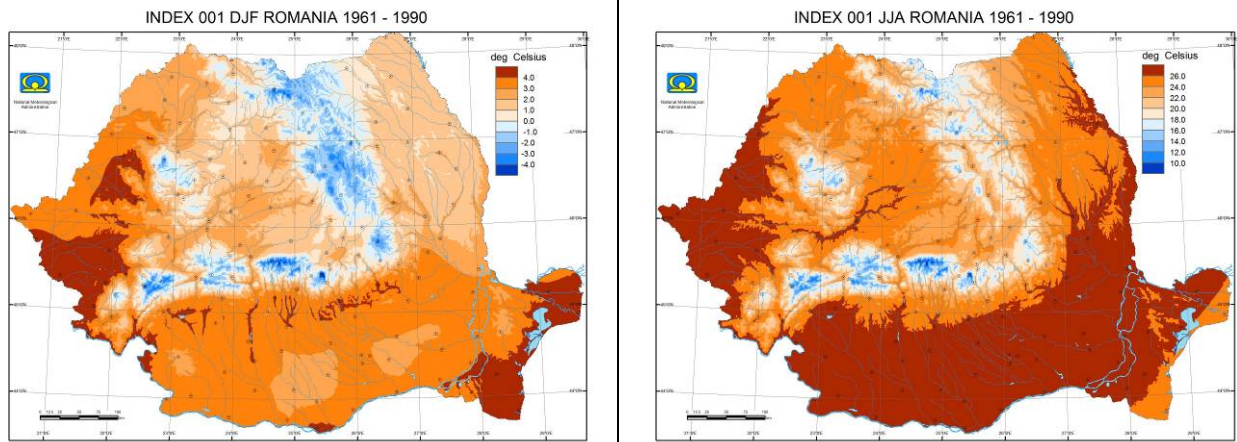


Figure 8.8 Index 068 - Percentage of severe cold days - %age of days with $T_{min} \leq -10C$

Appendix A:

CECILIA WP4 DELIVERABLE D4.1, revision 1

Lead partner for deliverable: ETH

Contributing partners: DMI, CUNI, NMA, CHMI, ELU, IAP, OMSZ, ICTP, AUTH, NIMH

First revision December 1, 2006

Revised March 12, 2008

1. Introduction

The purpose of this deliverable is to provide a concerted research plan between the WP4 partners. In particular, this report entails following information:

- Definition of which measures and indices are to be validated within WP4 (based on indices of extremes as defined by the WMO and the STARDEX project)
- Identification of the observational datasets to be used for the validation of extremes.
- Detailed implementation plan concerning the analyses to be performed under D4.2, D4.3, D4.4, and D4.5.

2. List of indices to be analyzed within CECILIA WP4

This section presents a first-stage list of 131 indices chosen by the WP4 partners for the analysis of extremes in WP4. This list is primarily based on STARDEX and WMO indices, but also includes additional indices considered useful for the analyses to be conducted within WP4. The final list of indices will be defined at the CECILIA January 2007 meeting in Semmering. A software will be developed by CHMI based on the existing software by Štěpánek (2006) for computing the final list of indices from daily data as part of D4.2. This software will be available to all WP4 partners. This will guarantee that the indices are computed in a consistent way for all considered observational (and modeling) datasets. From the total list of 131 indices, 41 "core indices" are highlighted in bold face. The list of core indices is based on the ECA&D indices and inputs from WP4 partners.

Whenever possible, the indices will be computed for annual, seasonal (MAM, JJA, SON, DJF) **and** monthly time frames. This will allow us to identify changes in the seasonality of extreme events, which can also better be linked with responsible physical processes. In order to identify trends in extreme indices, these will be computed as climatological estimates over the following time periods: 1961-1990, 1961-1970, 1966-1975, 1971-1980, 1976-1985, 1981-1990, 1986-1995, 1991-2000, 1996-2005. **The core indices will be provided as yearly output (indicated in bold in Tables A.1-3).**

Years and decades go from January to December. Winter seasons are consecutive, e.g. DJF 1962 goes from the first day of December 1961 to the last day of February 1962. The first winter, DJF 1961, will be based on only two months, first day of January 1961 till the end of February 1961.

For indices related to hot/cold/dry/wet spells, we do “day weighting” as opposed to “spell weighting”. If the sequence of days in the relevant period which belong to a spell of length at least 2 (or 6) is $n=1, \dots, N$, and each day belongs to a period of length j_n , then the average spell length is $\frac{1}{N} \sum_{n=1}^N j_n$. For medians we calculate the median spell length.

Spell lengths are calculated in two versions for indices 48, 52, 52a, 53, 53a, 55-57, 103, 104 and 107-112. One (e.g. 52) where only the spell length *within* the time frame is counted, and one (e.g. 52f) where the *full* length is counted.

For medians and maxima of spell lengths, any spell crossing a frame boundary is allocated to the mid day with rounding towards the later time frame.

2.a. Reference time period

The period 1961-1990 will be used as base period for the computation of the reference percentiles whenever required.

In the second revision of this report, the identification of some definition ambiguities has caused some indices (48, 52, 52a, 53, 53a, 55-57, 103, 104 and 107-112) to be defined in two alternate ways, and a few new indices (46a, 52a, 53a, 55a and 56a) have been introduced. Finally, to avoid conflicts with the actual definition, indices 52, 53, 55 and 56 have been renamed.

2.b. Temperature indices

The first-stage list of temperature indices is given in Tables A.1 (indices over all time frames) and A.2 (annual indices). For each index, the tables indicate whether the given index has been used in previous projects and softwares. The letters A-E correspond respectively to:

- A: index from STARDEX 57-indices list
(http://www.cru.uea.ac.uk/projects/stardex/deis/Diagnostic_tool.pdf)
- B: index from STARDEX core 10 indices list
(http://www.cru.uea.ac.uk/projects/stardex/deis/Core_Indices.pdf)
- C: index from ClimDex list
(<http://cccma.seos.uvic.ca/ETCCDMI/software.html>;
http://cccma.seos.uvic.ca/ETCCDMI/list_27_indices.html)
- D: index from RCLimDex list
(<http://cccma.seos.uvic.ca/ETCCDMI/software.html>;
<http://cccma.seos.uvic.ca/ETCCDMI/ClimDex/climindex-v1-3-users-guide.pdf>)
- E: index from ECA&D list
(<http://eca.knmi.nl/indicesextremes/indicesdictionary.php>)

If a modified version of the proposed index has been used in these previous projects or softwares, the corresponding cross is set between parentheses (“(x)”).

Comments on content of Tables A.1&A.2

NB: “time frame” refers to annual, seasonal, and monthly time frames

in blue: this index is computed from the total number of available days over all years (i.e. for a monthly time frame and a 10-year time period, from 300 values)

in green: this index is computed separately for each year and averaged over all years (i.e. for a monthly time frame and a 10-year time period, mean of 10 values, each one of which is computed from 30 values)

in gray: indices with special definition

The indices denoted in bold face will be provided as yearly output for the observational datasets analyzed in WP4 (“core indices”)

Table A.1: Temperature indices to be computed over all time frames

	Index	A	B	C	D	E	Definition
1	Mean Tmax	x				x	daily max T° averaged over time frame
2	Mean Tmin	x				x	daily min T° averaged over time frame
3	Mean Tmean	x				x	daily mean T° averaged over time frame
4	Mean diurnal temperature range	x			(x)	x	daily values of (Tmax-Tmin) averaged over time frame
5	10 th percentile diurnal temperature range	x					10 th percentile of daily values of (Tmax-Tmin) within given time frame
6	90 th percentile diurnal temperature range	x					90 th percentile of daily values of (Tmax-Tmin) within given time frame
7	Tmax 1 st percentile						1 st percentile of daily values of Tmax within given time frame
8	Tmax 5 th percentile						5 th percentile of daily values of Tmax within given time frame
9	Tmax 10 th percentile	x					10 th percentile of daily values of Tmax within given time frame
10	Tmax 20 th percentile						20 th percentile of daily values of Tmax within given time frame
11	Tmax 30 th percentile						30 th percentile of daily values of Tmax within given time frame
12	Tmax 40 th percentile						40 th percentile of daily values of Tmax within given time frame
13	Tmax 50 th percentile						50 th percentile of daily values of Tmax within given time frame
14	Tmax 60 th percentile						60 th percentile of daily values of Tmax within given time frame
15	Tmax 70 th percentile						70 th percentile of daily values of Tmax within given time frame
16	Tmax 80 th percentile						80 th percentile of daily values of Tmax within given time frame
17	Tmax 90 th percentile	x	x				90 th percentile of daily values of Tmax within given time frame
18	Tmax 95 th percentile						95 th percentile of daily values of Tmax within given time frame
19	Tmax 99 th percentile						99 th percentile of daily values of Tmax within given time frame
20	Tmean 1 st percentile						1 st percentile of daily values of Tmean within given time frame
21	Tmean 5 th percentile						5 th percentile of daily values of Tmean within given time frame
22	Tmean 10 th percentile						10 th percentile of daily values of Tmean within given time frame
23	Tmean 20 th percentile						20 th percentile of daily values of Tmean within given time frame
24	Tmean 30 th percentile						30 th percentile of daily values of Tmean within given time frame
25	Tmean 40 th percentile						40 th percentile of daily values of Tmean within given time frame
26	Tmean 50 th percentile						50 th percentile of daily values of Tmean within given time frame
	Index	A	B	C	D	E	Definition
27	Tmean 60 th percentile						60 th percentile of daily values of Tmean

							within given time frame
28	Tmean 70 th percentile						70 th percentile of daily values of Tmean within given time frame
29	Tmean 80 th percentile						80 th percentile of daily values of Tmean within given time frame
30	Tmean 90 th percentile						90 th percentile of daily values of Tmean within given time frame
31	Tmean 95 th percentile						95 th percentile of daily values of Tmean within given time frame
32	Tmean 99 th percentile						99 th percentile of daily values of Tmean within given time frame
33	Tmin 1 st percentile						1 st percentile of daily values of Tmin within given time frame
34	Tmin 5 th percentile						5 th percentile of daily values of Tmin within given time frame
35	Tmin 10 th percentile	x	x				10 th percentile of daily values of Tmin within given time frame
36	Tmin 20 th percentile						20 th percentile of daily values of Tmin within given time frame
37	Tmin 30 th percentile						30 th percentile of daily values of Tmin within given time frame
38	Tmin 40 th percentile						40 th percentile of daily values of Tmin within given time frame
39	Tmin 50 th percentile						50 th percentile of daily values of Tmin within given time frame
40	Tmin 60 th percentile						60 th percentile of daily values of Tmin within given time frame
41	Tmin 70 th percentile						70 th percentile of daily values of Tmin within given time frame
42	Tmin 80 th percentile						80 th percentile of daily values of Tmin within given time frame
43	Tmin 90 th percentile	x					90 th percentile of daily values of Tmin within given time frame
44	Tmin 95 th percentile						95 th percentile of daily values of Tmin within given time frame
45	Tmin 99 th percentile						99 th percentile of daily values of Tmin within given time frame
46	Percentage of frost days	(x)	(x)	(x)	(x)	(x)	%age of days within time frame with Tmin < 0C (ECA&D Number of frost days)
46a	Days with freezing-point passage						Percentage of days within time frame with Tmin<0C and Tmax>0C
47	Percentage of days without defrost (ice days)	(x)			(x)	(x)	%age of days within time frame with Tmax < 0C (ECA&D: Number of ice days)
48	Consecutive frost days					x	Max. nb of consecutive frost days with Tmin < 0C. Lengths limited to the relevant time frame
48f	Consecutive frost days (full spell lengths)					x	Max. Nb of consecutive frost days with Tmin < 0C. Full lengths considered
49	Growing degree days (def1)	x				x	Sum of (Tmean-4C) for all days with Tmean>4C within time frame (ECA definition)
50	Growing degree days (def2)						Sum of (((Tmax+Tmin)/2)-10C) for all days with Tmax≥10C within time frame using the following rules: if Tmin<10C,

							then use 10C for Tmin; if Tmax>30C then use 30C for Tmax
	Index	A	B	C	D	E	Definition
51	Extreme temperature range within time frame	(x)		(x)		(x)	Range between max. Tmax and min. Tmin within time frame (for annual time frame equivalent to intra-annual extreme temperature range)
52	Mean heat wave occurrence	X		x		x	Let Tx_{ij} be the daily maximum temperature at day i of period j and let Tx_{inorm} be the calendar day mean calculated for a 5 day window centred on each calendar day during a specified period. Then counted is the percentage of days per period where, in intervals of at least 6 consecutive days: $Tx_{ij} > Tx_{inorm} + 5$ (adapted from STARDEX definition). Lengths limited to the relevant time frame (spells considered need to have a minimum of 6 days within the given time frame).
52f	Mean heat wave occurrence (full spell lengths)	X		x		x	Let Tx_{ij} be the daily maximum temperature at day i of period j and let Tx_{inorm} be the calendar day mean calculated for a 5 day window centred on each calendar day during a specified period. Then counted is the percentage of days per period where, in intervals of at least 6 consecutive days: $Tx_{ij} > Tx_{inorm} + 5$ (adapted from STARDEX definition). Full lengths considered (spells considered may be only partially within time frame; but only days within time frame are summed)
52a	Mean heat wave length						Day-weighted average of spell lengths of at least 6 days as defined in 52. Lengths limited to the relevant time frame .
52af	Mean heat wave length (full spell lengths)						Day-weighted average of spell lengths of at least 6 days as defined in 52. Full lengths considered.
53	90 th percentile-based maximum heat wave duration	x	x				Let Tx_{ij} be the daily maximum temperature at day i of period j and let $Txq90_{inorm}$ be the calendar day 90th percentile calculated for a 5 day window centred on each calendar day during a specified period. Then counted is the maximum number of consecutive days per period where: $T_{ij} > Txq90_{inorm}$ (adapted from STARDEX definition). Lengths limited to the relevant time frame .
	Index	A	B	C	D	E	Definition
53f	90 th percentile-based maximum heat wave	x	x				Let Tx_{ij} be the daily maximum temperature at day i of period j and

	duration (full spell lengths)						let $Txq90_{inorm}$ be the calendar day 90th percentile calculated for a 5 day window centred on each calendar day during a specified period. Then counted is the maximum number of consecutive days per period where: $T_{ij} > Txq90_{inorm}$ (adapted from STARDEX definition). Full length considered.
53a	90 th percentile-based mean heat wave length						Day-weighted average of spells lengths of at least 2 days as defined in 53. Lengths limited to the relevant time frame .
53af	90 th percentile-based mean heat wave length (full spell lengths)						Day-weighted average of spells of at least 2 days as defined in 53. Full lengths considered.
54	Heating degree days					x	Sum of 17C-Tmean for days with Tmean<17C
55	Mean cold wave occurrence	x				x	Let Tn_{ij} be the daily minimum temperature at day i of period j and let Tn_{inorm} be the calendar day mean calculated for a 5 day window centred on each calendar day during a specified period. Then counted is the percentage of days per period where, in intervals of at least 6 consecutive days: $Tn_{ij} < Tn_{inorm} - 5$ (adapted from STARDEX definition). Lengths limited to the relevant time frame .
55f	Mean cold wave occurrence (full spell lengths)	x				x	Let Tn_{ij} be the daily minimum temperature at day i of period j and let Tn_{inorm} be the calendar day mean calculated for a 5 day window centred on each calendar day during a specified period. Then counted is the percentage of days per period where, in intervals of at least 6 consecutive days: $Tn_{ij} < Tn_{inorm} - 5$ (adapted from STARDEX definition). Full length considered
55a	Mean cold wave length						Day-weighted average of spells of at least 6 days as defined in 55. Lengths limited to the relevant time frame .
	Index	A	B	C	D	E	Definition
55af	Mean cold wave length (full spell lengths)						Day-weighted average of spells of at least 6 days as defined in 55. Full lengths considered.
56	10 th percentile-based maximum cold wave duration	x					Let Tn_{ij} be the daily minimum temperature at day i of period j and let $Tnq10_{inorm}$ be the calendar day 10th percentile calculated for a 5 day window centred on each calendar day during a specified period. Then counted is the maximum number of consecutive days per period where: $Tn_{ij} < Tnq10_{inorm}$ (adapted from

							STARDEX def.). Lengths limited to the relevant time frame .
56f	10 th percentile-based maximum cold wave duration (full spell lengths)	x					Let Tn_{ij} be the daily minimum temperature at day i of period j and let $Tnq10_{inorm}$ be the calendar day 10th percentile calculated for a 5 day window centred on each calendar day during a specified period. Then counted is the maximum number of consecutive days per period where: $Tn_{ij} < Tnq10_{inorm}$ (adapted from STARDEX def.). Full length considered
56a	10 th percentile-based cold wave length						Day-weighted average of spells of at least 2 days as defined in 56. Lengths limited to the relevant time frame.
56af	10 th percentile-based mean cold wave length (full spell lengths)						Day-weighted average of spells of at least 2 days as defined in 56. Full lengths considered.
57	Frost season length	(x)					Mean duration within time frame of time spans of minimum 5 consecutive days where $T_{min} < 0$ (adapted from STARDEX definition). Day-weighted. Length limited to the relevant time frame .
57f	Frost season length (full spell lengths)	(x)					Mean duration within time frame of time spans of minimum 5 consecutive days where $T_{min} < 0$ (adapted from STARDEX definition). Day-weighted. Full length of spell considered.
58	Percentage of “summer days”				(x)	(x)	%age of days where $T_{max} \geq 25C$
59	Percentage of “tropical nights”				(x)	(x)	%age of days where $T_{min} \geq 20C$
60	Percentage of days with $T_{max} < 10^{th}$ percentile	x		x	x	x	%age of days with $T_{max} < 10^{th}$ percentile, where 10 th percentile is taken from all values for 5-day window around calendar day within base period (ECA&D def.)
	Index	A	B	C	D	E	Definition
61	Percentage of days with $T_{max} > 90^{th}$ percentile	x		x	x	x	%age of days with $T_{max} > 90^{th}$ percentile, where 90 th percentile is taken from all values for 5-day window around calendar day within base period (ECA&D def.)
62	Percentage of days with $T_{mean} < 10^{th}$ percentile					x	%age of days with $T_{mean} < 10^{th}$ percentile, where 10 th percentile is taken from all values for 5-day window around calendar day within base period (ECA&D def)
63	Percentage of days with $T_{mean} > 90^{th}$ percentile					x	%age of days with $T_{mean} > 90^{th}$ percentile, where 90 th percentile is taken from all values for 5-day window around calendar day within base period (ECA&D def.)
64	Percentage of days with $T_{min} < 10^{th}$ percentile	x		x	x	x	%age of days with $T_{min} < 10^{th}$ percentile, where 10 th percentile is

							taken from all values for 5-day window around calendar day within base period (ECA&D def.)
65	Percentage of days with Tmin > 90 th percentile	x		x	x	x	%age of days with Tmin > 90 th percentile, where 90 th percentile is taken from all values for 5-day window around calendar day within base period (ECA&D def.)
66	Percentage of hot days						%age of days with Tmax ≥ 30C (adapted from ELU definition)
67	Percentage of extremely hot days						%age of days with Tmax ≥ 35C (adapted from ELU definition)
68	Percentage of severe cold days						%age of days with Tmin < -10C (adapted from ELU definition)
69	Interannual variability of Tmean						Standard deviation of mean yearly values of Tmean averaged over given time frame (e.g. month)
70	Interannual variability of Tmax						Standard deviation of mean yearly values of Tmax averaged over given time frame (e.g. month)
71	Interannual variability of Tmin						Standard deviation of mean yearly values of Tmin averaged over given time frame (e.g. month)
72	Intra-annual variability of Tmean						Mean over whole time period (e.g. 10-yr period) of yearly standard deviation of Tmean within given time frame
73	Intra-annual variability of Tmax						Mean over whole time period (e.g. 10-yr period) of yearly standard deviation of Tmean within given time frame
74	Intra-annual variability of Tmin						Mean over whole time period (e.g. 10-yr period) of yearly standard deviation of Tmean within given time frame

Table A.2: Temperature indices to be computed only over annual time frames

	Index	A	B	C	D	E	Definition
75	Growing season length	x		x	x	x	Annual count between first span of at least 6 days with daily mean temperature Tmean>5C (counting starts on the first day of this span) and first span after July 1st of 6 days with Tmean<5C (counting stops on the last day before this span) (RClimDex definition).

2.c. Precipitation indices

The first-stage list of precipitation indices is given in Table A.3 (indices over all time frames). For each index, the table indicates whether the given index has been used in previous projects and softwares (see corresponding comments under 2.b. for temperature indices).

For precipitation indices, “wet days” and “dry days” are distinguished, where the wet-day precipitation ≥ 1 mm/d, and the dry-day precipitation is < 1 mm/d.

Comments on content of Table A.3

NB: “time frame” refers to annual, seasonal, and monthly time frames

in blue: this index is computed from the total number of available days over all years (i.e. for a monthly time frame and a 10-year time period, from 300 values)

in green: this index is computed separately for each year and averaged over all years (i.e. for a monthly time frame and a 10-year time period, mean of 10 values, each one of which is computed from 30 values)

in gray: indices with special definition

The indices denoted in bold face will be provided as yearly output for the observational datasets analyzed in WP4 (“core indices”)

Table A.3: Precipitation indices to be computed over all time frames

	Index	A	B	C	D	E	Definition
76	Mean climatological precipitation	x				x	Mean precipitation (including both wet and dry days)
77	Mean wet-day precipitation	x	x	x	x	x	Mean wet-day precipitation (equivalent to “simple daily intensity”)
78	Percentage of wet days					x	Nb wet days/ total nb of days [%]
	Index	A	B	C	D	E	Definition
79	10 th percentile of wet-day amounts						10 th percentile of wet-day amounts [mm/d]
80	20 th percentile of wet-day amounts	x					20 th percentile of wet-day amounts [mm/d]
81	30 th percentile of wet-day amounts						30 th percentile of wet-day amounts [mm/d]
82	40 th percentile of wet-day amounts	x					40 th percentile of wet-day amounts [mm/d]
83	50 th percentile of wet-day amounts	x					50 th percentile of wet-day amounts [mm/d]
84	60 th percentile of wet-day amounts	x					60 th percentile of wet-day amounts [mm/d]
85	70 th percentile of wet-day amounts						70 th percentile of wet-day amounts [mm/d]
86	80 th percentile of wet-day amounts	x					80 th percentile of wet-day amounts [mm/d]
87	90 th percentile of wet-day amounts	x	x				90 th percentile of wet-day amounts [mm/d]
88	95 th percentile of wet-day amounts	x					95 th percentile of wet-day amounts [mm/d]
89	99 th percentile of wet-day amounts						99 th percentile of wet-day amounts [mm/d]
90	Fraction of total precipitation above annual 10 th percentile						Fraction of total precipitation above annual 10 th percentile (sum and percentile based on wet-day amounts)
91	Fraction of total precipitation above	x					Fraction of total precipitation above annual 20 th percentile (sum and

	annual 20 th percentile						percentile based on wet-day amounts)
92	Fraction of total precipitation above annual 30 th percentile						Fraction of total precipitation above annual 30 th percentile (sum and percentile based on wet-day amounts)
93	Fraction of total precipitation above annual 40 th percentile	x					Fraction of total precipitation above annual 40 th percentile (sum and percentile based on wet-day amounts)
94	Fraction of total precipitation above annual 50 th percentile	x					Fraction of total precipitation above annual 50 th percentile (sum and percentile based on wet-day amounts)
95	Fraction of total precipitation above annual 60 th percentile	x					Fraction of total precipitation above annual 60 th percentile (sum and percentile based on wet-day amounts)
96	Fraction of total precipitation above annual 70 th percentile						Fraction of total precipitation above annual 70 th percentile (sum and percentile based on wet-day amounts)
97	Fraction of total precipitation above annual 80 th percentile	x					Fraction of total precipitation above annual 80 th percentile (sum and percentile based on wet-day amounts)
	Index	A	B	C	D	E	Definition
98	Fraction of total precipitation above annual 90 th percentile	x					Fraction of total precipitation above annual 90 th percentile (sum and percentile based on wet-day amounts)
99	Fraction of total precipitation above annual 95 th percentile	x					Fraction of total precipitation above annual 95 th percentile (sum and percentile based on wet-day amounts)
100	Fraction of total precipitation above annual 99 th percentile						Fraction of total precipitation above annual 99 th percentile (sum and percentile based on wet-day amounts)
101	Percentage of wet days above 10 mm/d	(x)		(x)	(x)	(x)	%age of wet days above 10 mm/d (ECA&D: number of days)
102	Percentage of wet days above 20 mm/d				(x)	(x)	%age of wet days above 20 mm/d (ECA&D: number of days)
103	Max. nb of consecutive dry days	x	x	x	x	x	Max. nb of consecutive dry days. Length limited to relevant time frame.
103f	Max. nb of consecutive dry days (full spell lengths)	x	x	x	x	x	Max. nb of consecutive dry days. Full length considered.
104	Max. nb of consecutive wet days	x			x	x	Max. nb of consecutive wet days. Length limited to relevant time frame .
104f	Max. nb of consecutive wet days (full spell lengths)	x			x	x	Max. nb of consecutive wet days. Full length considered.
105	Mean wet-day persistence	x					Total number of consecutive (at least 2) wet days/Total number of wet days (STARDEX definition)
106	Mean dry-day persistence	x					Total number of consecutive (at least 2) dry days/Total number of dry days
107	Mean wet spell length (days)	x					Mean wet spell length (days) Length limited to relevant time frame . Day-weighted
107f	Mean wet spell length	x					Mean wet spell length (days). Full

	(days) Full spell lengths						length considered. Day-weighted
108	Median wet spell length (days)	x					Median wet spell length (days) Length limited to relevant time frame .
108f	Median wet spell length (days) Full spell lengths	x					Median wet spell length (days). Full length considered.
109	Standard deviation of wet spell length (days)	x					Standard deviation of wet spell length (days) Length limited to relevant time frame . Day-weighted.
109f	Standard deviation of wet spell length (days) Full spell lengths	x					Standard deviation of wet spell length (days) Full length considered. Day-weighted.
	Index	A	B	C	D	E	Definition
110	Mean dry spell length (days)	x					Mean dry spell length (days) Length limited to relevant time frame . Day-weighted.
110f	Mean dry spell length (days) Full spell lengths	x					Mean dry spell length (days). Full length considered. Day-weighted.
111	Median dry spell length (days)	x					Median dry spell length (days) Length limited to relevant time frame .
111f	Median dry spell length (days) Full spell lengths	x					Median dry spell length (days). Full length considered.
112	Standard deviation of dry spell length (days)	x					Standard deviation of dry spell length (days) Length limited to relevant time frame . Day-weighted.
112f	Standard deviation of dry spell length (days) Full spell lengths	x					Standard deviation of dry spell length (days). Full length considered.
113	Greatest 1-day total rainfall					x	Greatest 1-day total rainfall (ECA&D: max. daily precipitation)
114	Greatest 3-day total rainfall	x					Greatest 3-day total rainfall
115	Greatest 5-day total rainfall	x	x	x		x	Greatest 5-day total rainfall
116	Greatest 10-day total rainfall	x					Greatest 10-day total rainfall
117	Percentage of rainfall from events > base-period 90 th percentile	x	x				%age of rainfall from events > base-period 90 th percentile (for given time frame) (based on wet-day amounts)
118	Percentage of rainfall from events > base-period 95 th percentile			(x)	(x)		%age of rainfall from events > base-period 95 th percentile (for given time frame) (based on wet-day amounts)
119	Percentage of rainfall from events > base-period 99 th percentile						%age of rainfall from events > base-period 99 th percentile (for given time frame) (based on wet-day amounts)
120	Percentage of wet days > base-period 75 th percentile					x	(Nb of wet days > base-period 75 th percentile)/Nb of wet days [%] (percentile for given time frame, based on wet-day amounts)
121	Percentage of wet days > base-period 90th percentile	(x)	(x)				(Nb of wet days > base-period 90th percentile)/Nb of wet days [%] (percentile for given time frame, based on wet-day amounts)
122	Percentage of wet days > base-period 95th percentile					x	(Nb of wet days > base-period 95th percentile)/Nb of wet days [%] (percentile for given time frame, based on wet-day amounts)

123	Percentage of wet days > base-period 99 th percentile					x	(Nb of wet days > base-period 99 th percentile)/Nb of wet days [%] (percentile for given time frame, based on wet-day amounts)
	Index	A	B	C	D	E	Definition
124	Percentage of wet days > 20mm						(Nb of wet days > 20mm)/Nb of wet days [%]
125	Percentage of wet days > 10mm						(Nb of wet days > 10mm)/Nb of wet days [%]
126	Percentage of wet days > 5mm						(Nb of wet days > 5mm)/Nb of wet days [%]
127	Interannual variability of mean precipitation						Standard deviation of mean yearly values of precipitation averaged over given time frame (e.g. month)
128	Interannual variability of wet-day precipitation						Standard deviation of mean yearly values of wet-day precipitation averaged over given time frame (e.g. month)
129	Intra-annual variability of mean precipitation						Mean over whole time period (e.g. 10-yr period) of yearly standard deviation of mean precipitation within given time frame
130	Intra-annual variability of wet-day precipitation						Mean over whole time period (e.g. 10-yr period) of yearly standard deviation of wet-day precipitation within given time frame
131	Correlation of (T _{mean} , P _{mean})						Correlation over whole time period (e.g. 10-yr period) between mean temperature and mean precipitation within given time frame

Appendix B

Preliminary analysis of observational datasets and climate simulations

For the calculation of observation-based WP4 indices, the software ProClimDB developed by Petr Štěpánek has been used. For the ECA&D observational database, similar programs in the language “R” has been used, and for gridded model data routines in MATLAB have been employed. A very thorough intercomparison work has been conducted in order to ensure that the software produced identical results on identical input.

The many plots in the present section have been prepared with similar colour scales, but not with the same absolute contour levels, and they have been prepared by the individual institutions delivering the data. It has been deemed useful to deliver these plots now instead of waiting for a more homogeneous analysis in order to enable a first inspection of this comprehensive and new data set.

In the area of interest, the new country-based observation data sets add a large amount of information, where the ECA&D data set is very sparse.

Comparing the temperature plots it is seen that the various observational sets agree well, and that the numerical simulation performs better in winter than in summer, where it is too warm.

Winter precipitation in the simulation lacks regional features and the absolute values seem high. In summer the values seem realistic as well. The percentages of wet days are realistic, but extreme rainfall is underestimated significantly in the current intermediate-resolution regional simulation.

Calculation of indices for the Czech Republic by CHMI

Before indices calculation, station data were subject of thorough quality control and homogenization using the ProClimDB and AnClim software (Štěpánek, 2007, Štěpánek, 2006). Details about the process can be found e.g. in Štěpánek *et al.* (2008). After detecting and correction of outliers in the series and time series homogenization, the gaps in the station data were filled using neighboring stations.

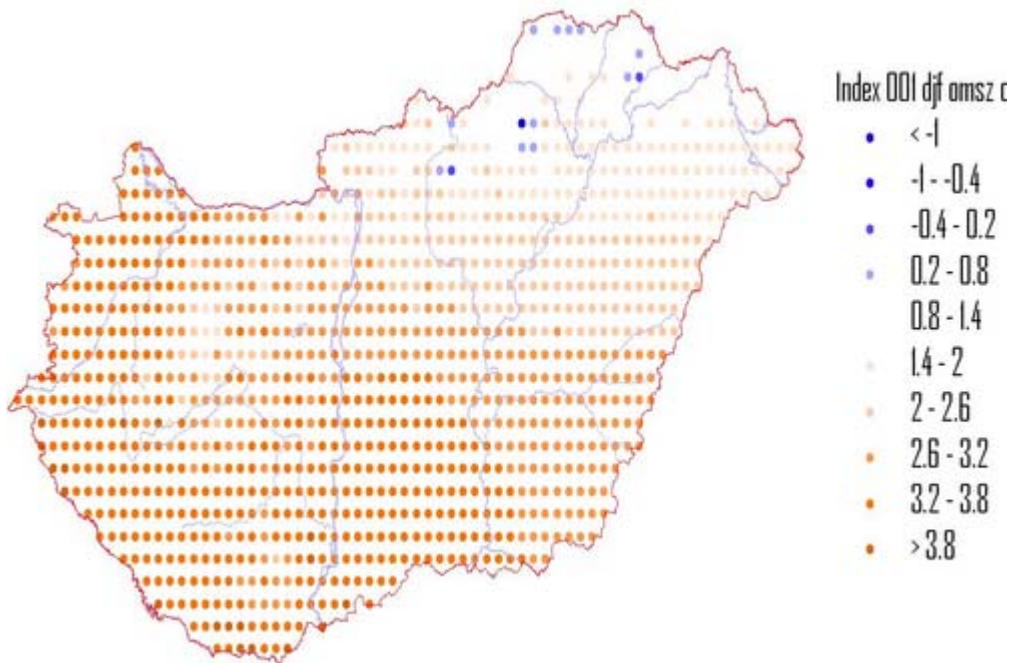
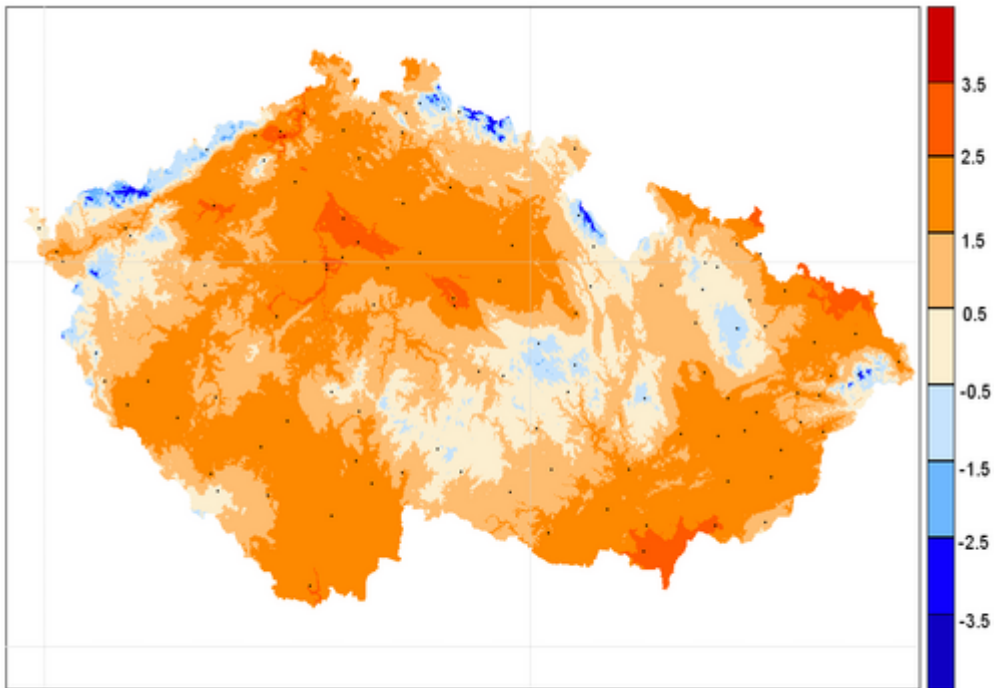
For the indices calculation, 109 climatological and 501 precipitation stations were available. Positions of the used stations are marked on the following maps by black dots. Calculated indices in locations of the stations were interpolated into the area of the Czech Republic using kriging and regional regression (dependence on altitude) by method of Šercl and Lett (2002).

Štěpánek, P. (2006): AnClim - software for time series analysis. Dept. of Geography, Fac. of Natural Sciences, MU, Brno, 1.47 MB. <http://www.climahom.eu/AnClim.html>

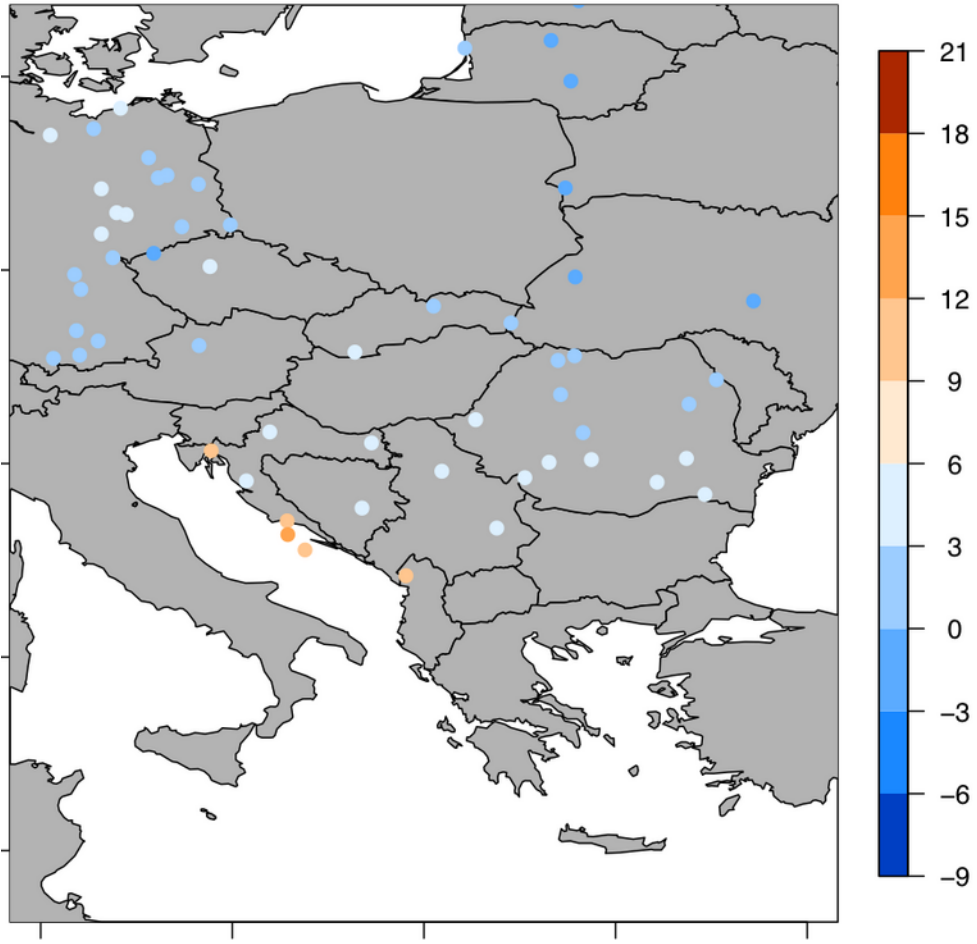
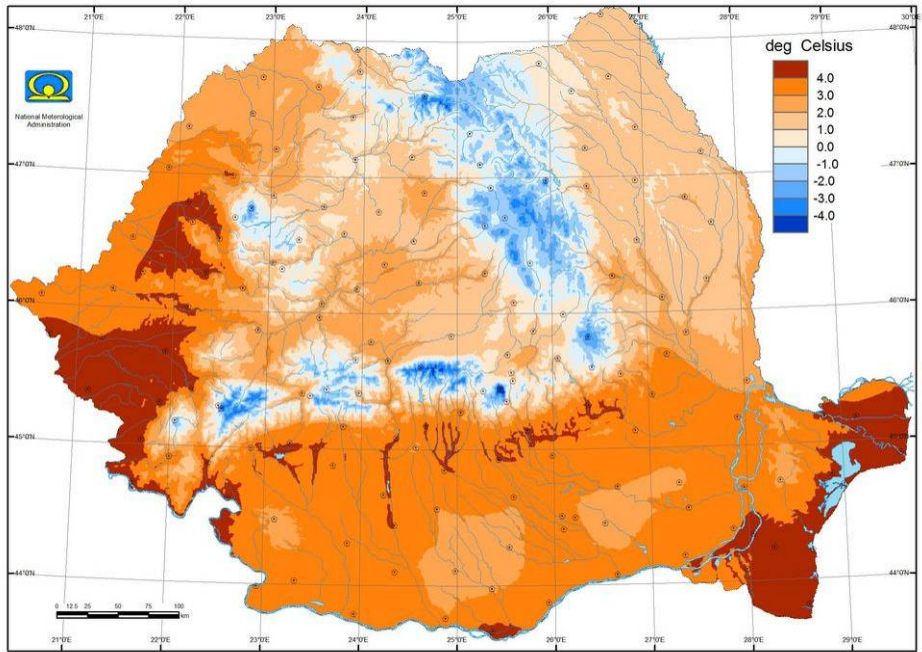
Štěpánek, P. (2007): ProClimDB – software for processing climatological datasets. CHMI, regional office Brno. <http://www.climahom.eu/ProcData.html>

Štěpánek, P., Rezníčková, L., Brázdil, R. (2008): Homogenization of daily air pressure and temperature series for Brno (Czech Republic) in the period 1848–2005. In: Fifth seminar for homogenization and quality control in climatological databases (29 May – 2 June 2006), WCDMP WMO, Genova. (in print)

Šercl, P., Lett, P. (2002): Výpočet rastru srážek v prostředí GIS (s využitím ArcView Spatial Analyst). Uživatelská příručka verze 2.0.1, ČHMÚ, OPV, Praha.



INDEX 001 DJF ROMANIA 1961 - 1990



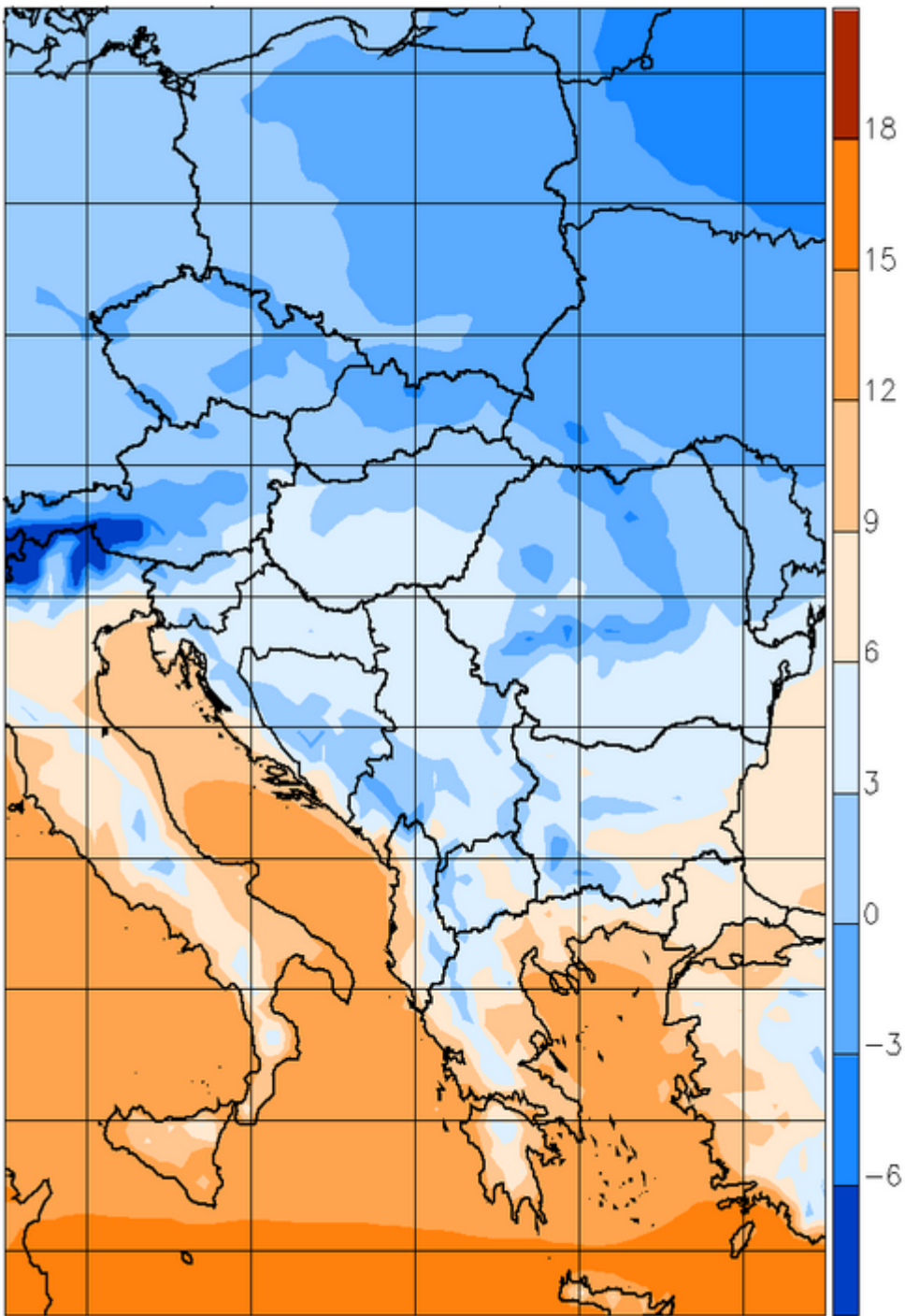
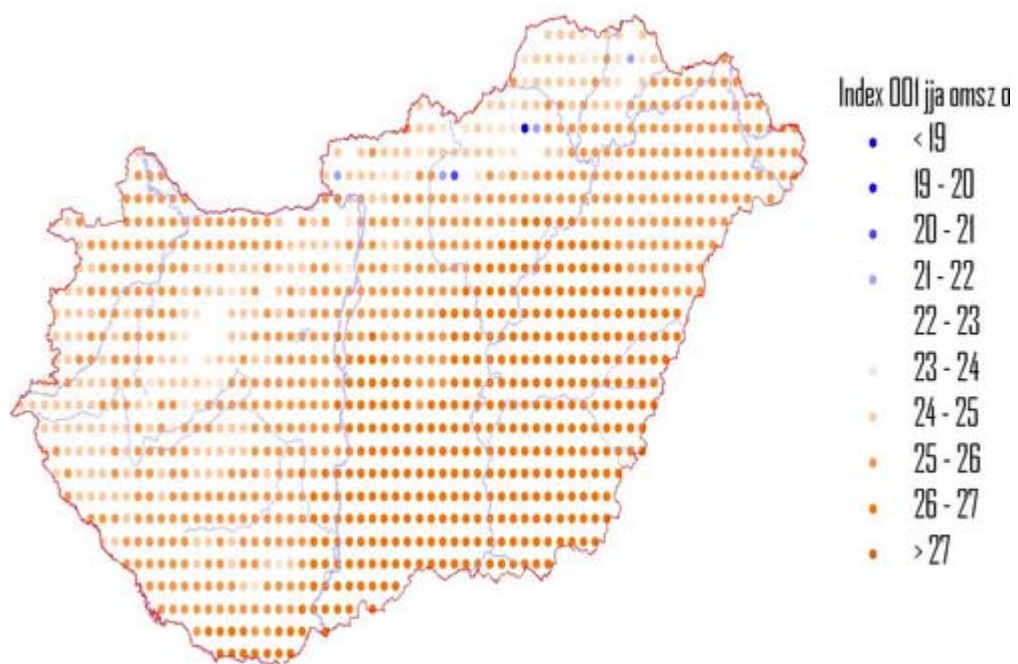
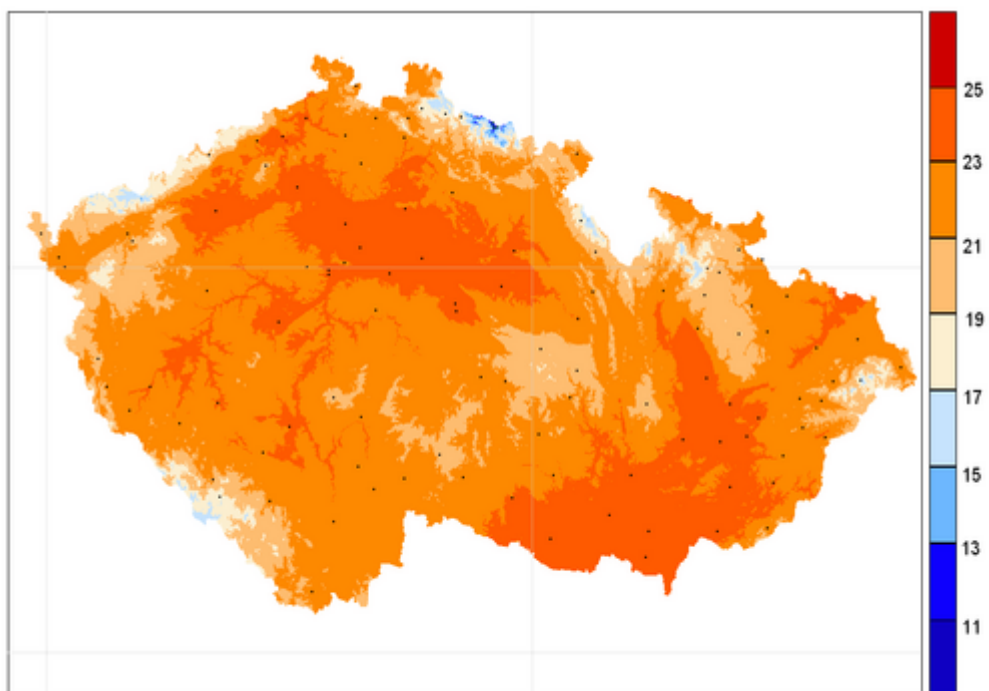
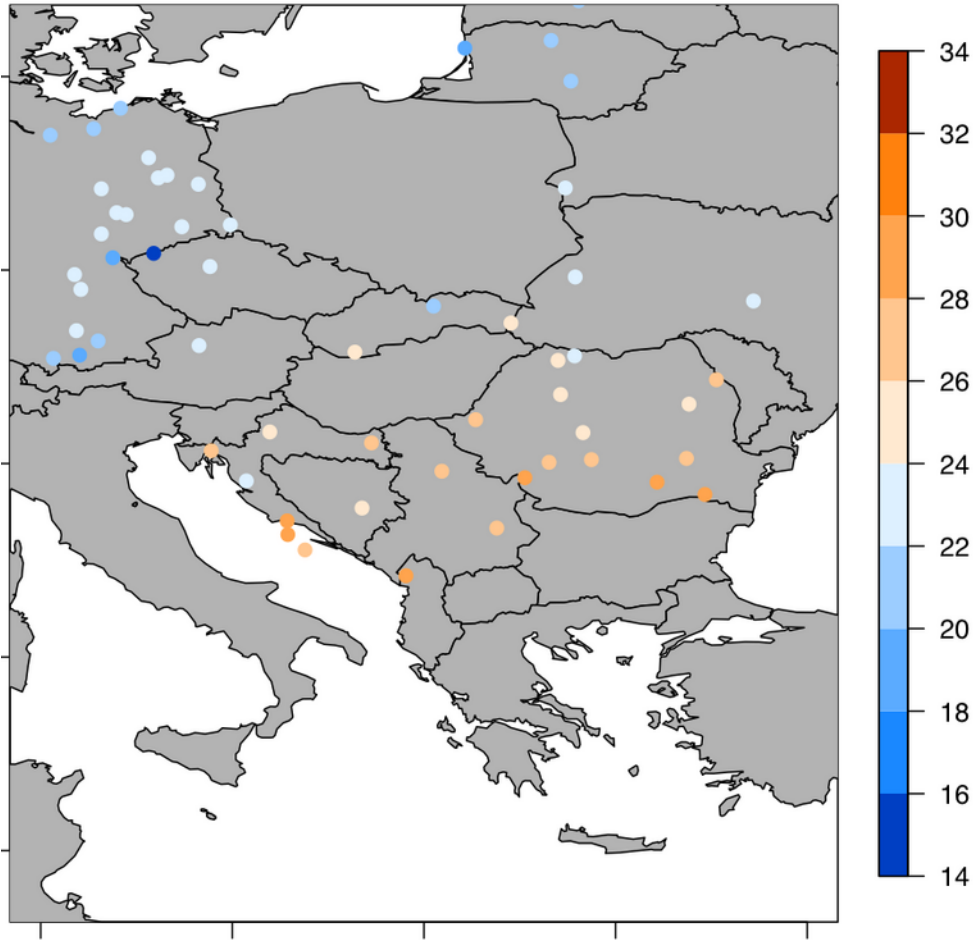
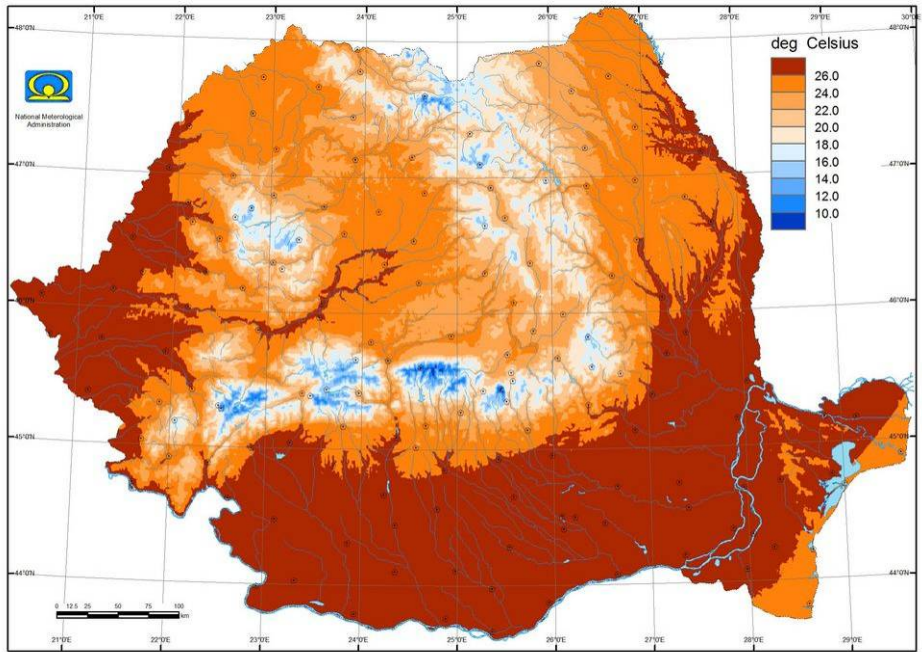


Figure B1 Mean daily-maximum temperature for winter (DJF) for the period 1961-1990. From top to bottom: observations from the Czech Republic; observations from Hungary; observations from Romania; observations from the ECA&D dataset; regional model output from the ENSEMBLES reanalysis-based HIRHAM5-experiment performed at the DMI.



INDEX 001 JJA ROMANIA 1961 - 1990



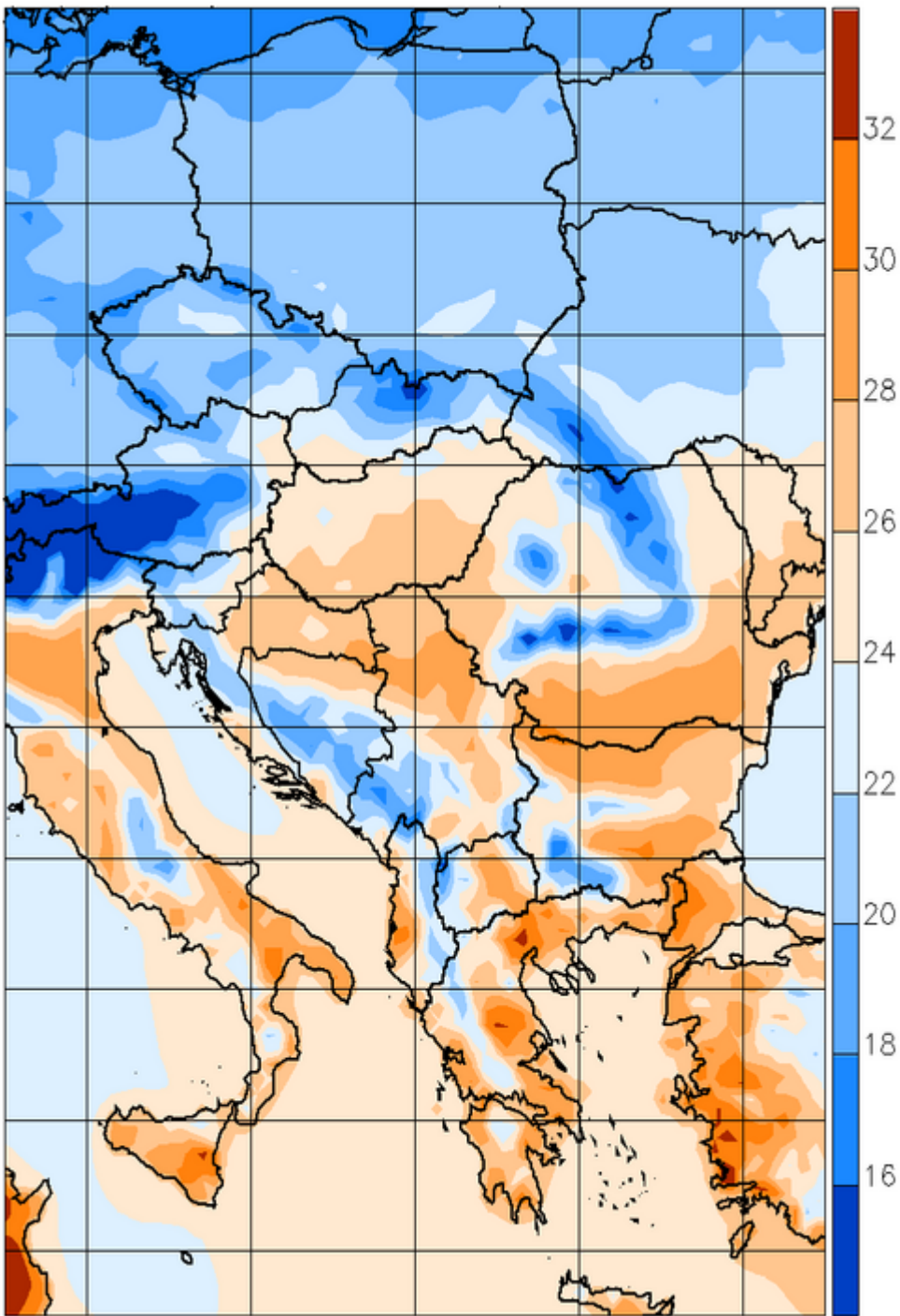
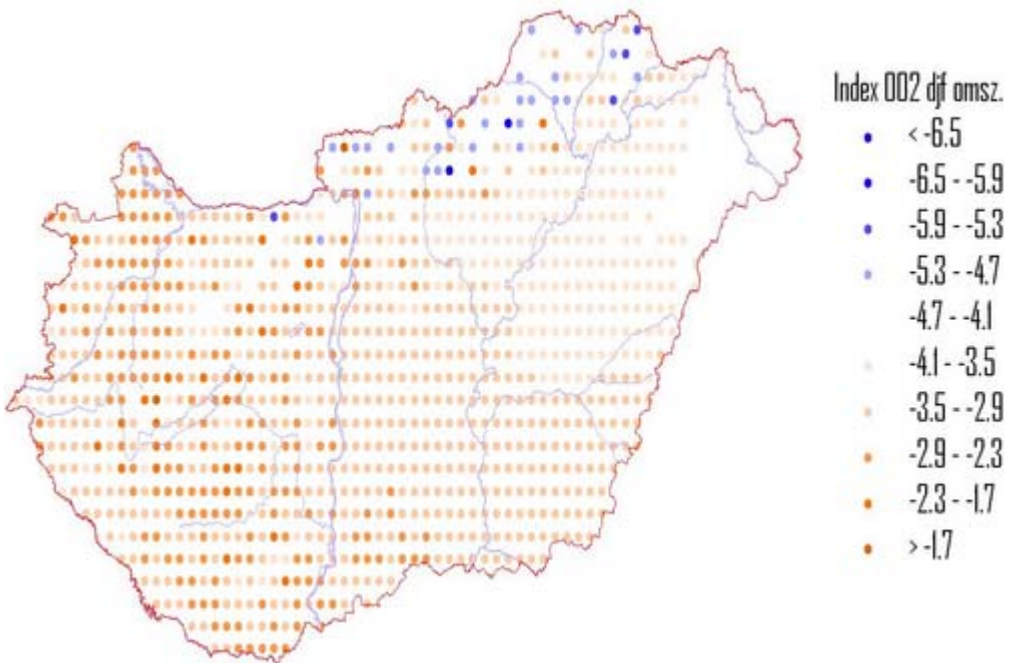
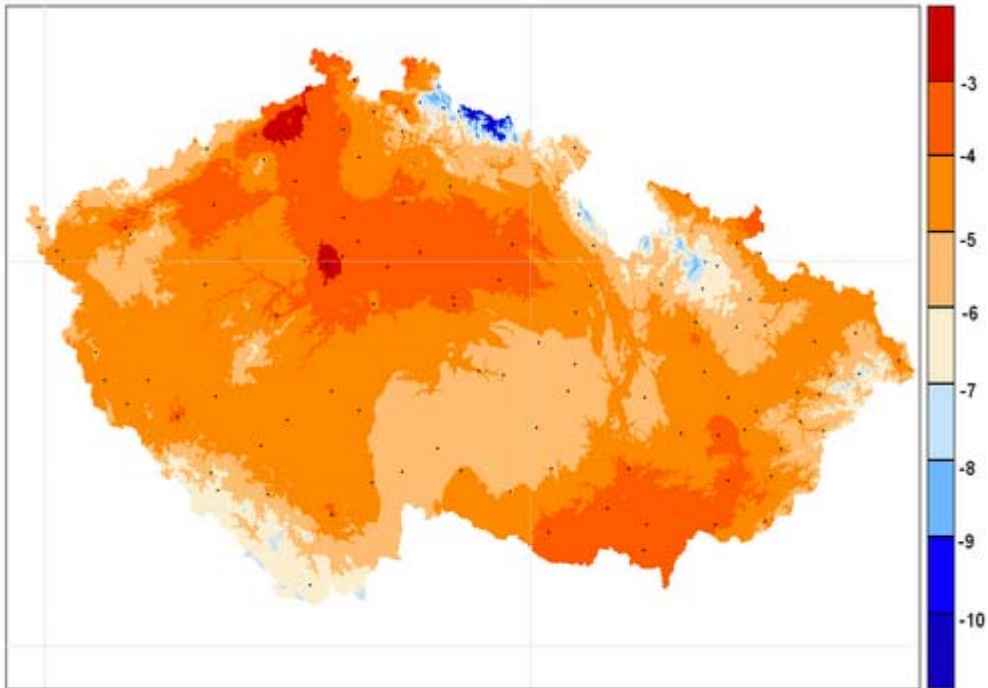
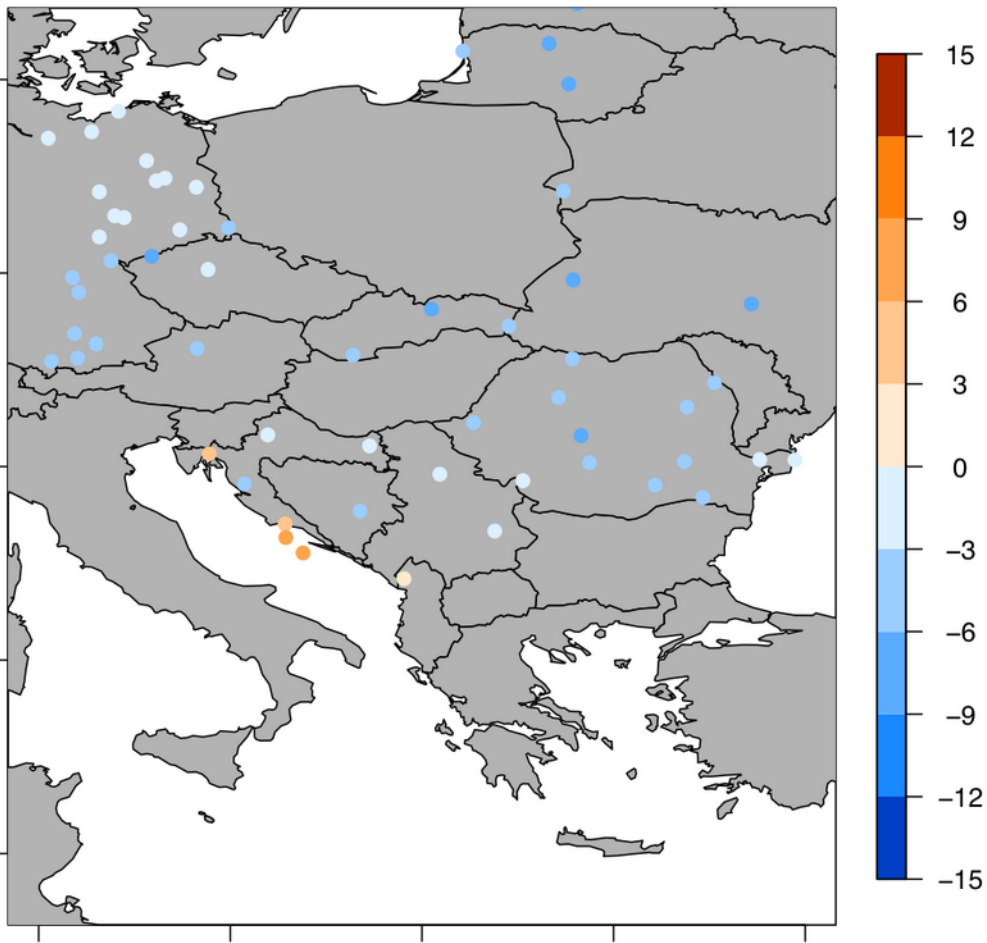
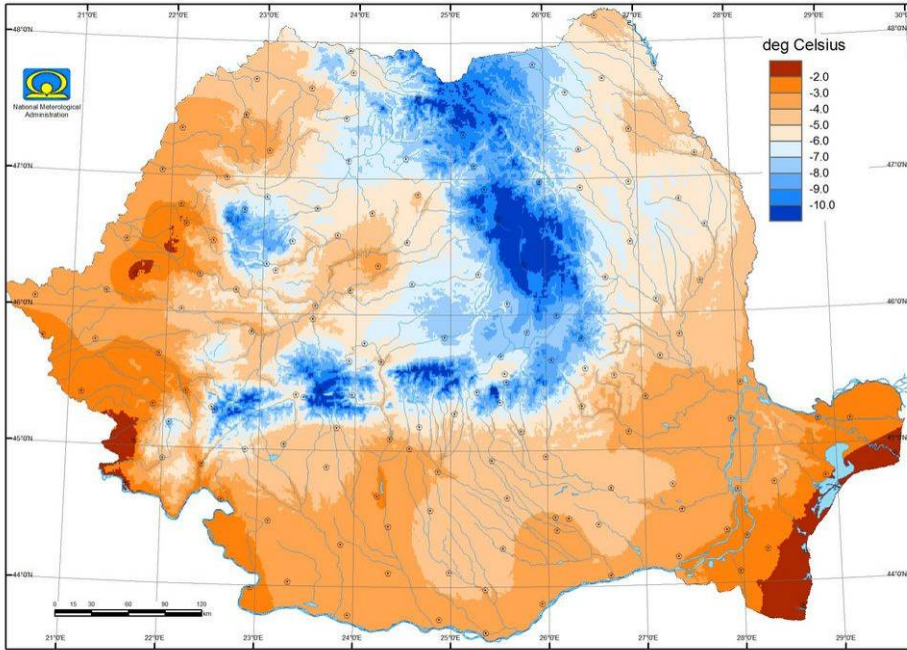


Figure B2 Mean daily-maximum temperature for summer (JJA) for the period 1961-1990. Panels like the previous figure.



INDEX 002 DJF ROMANIA 1961 - 1990



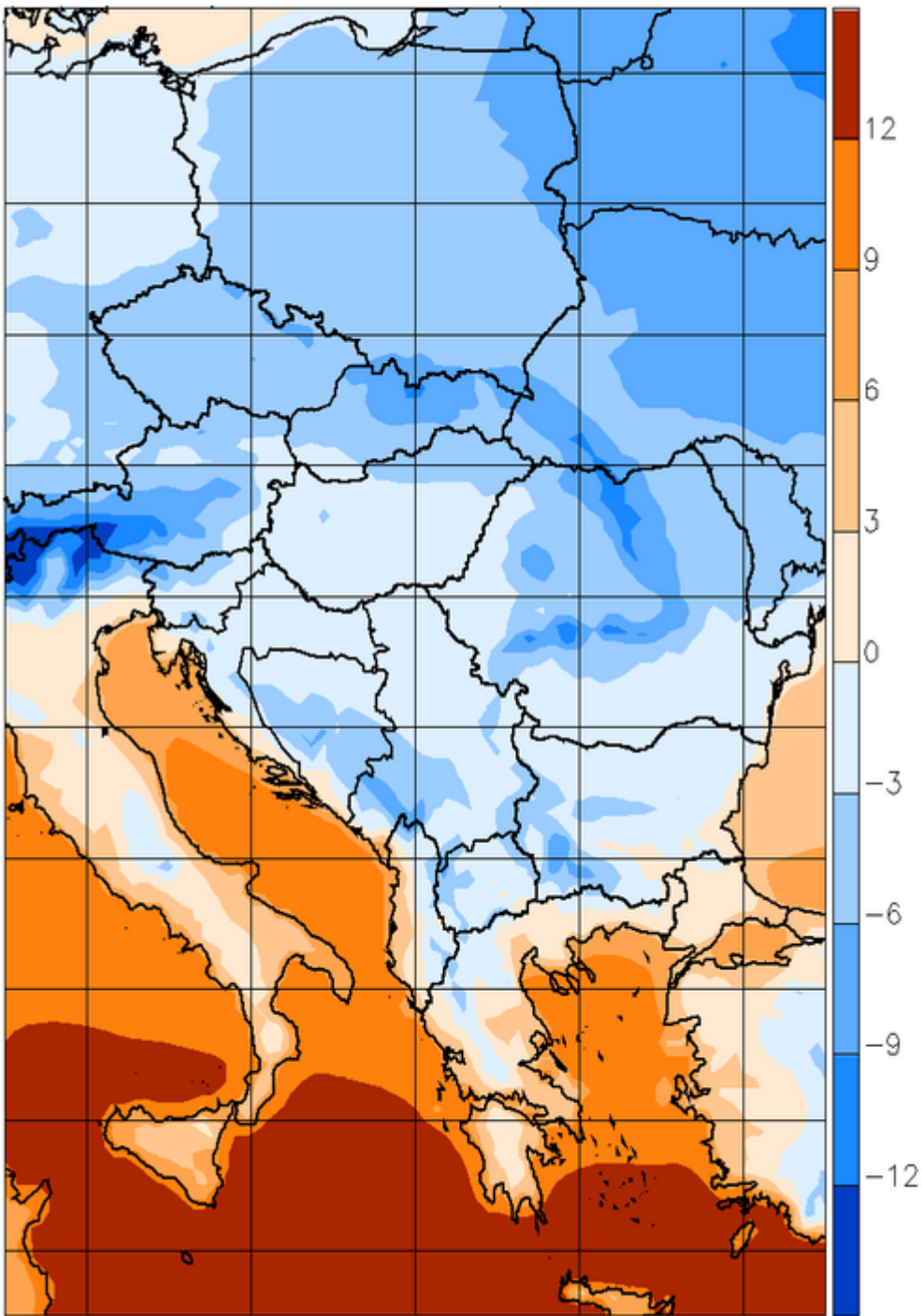
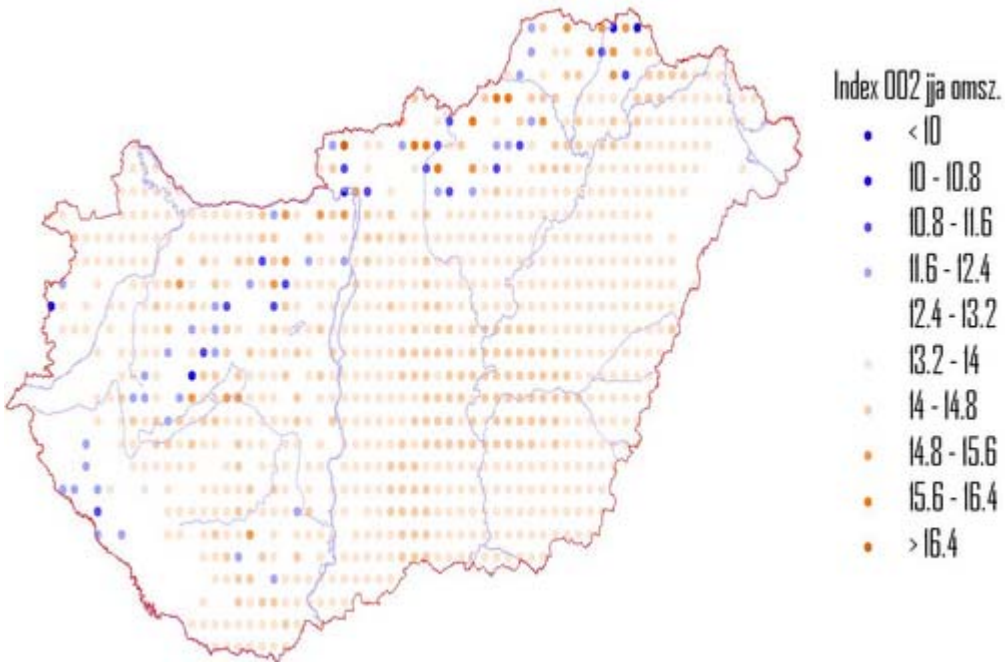
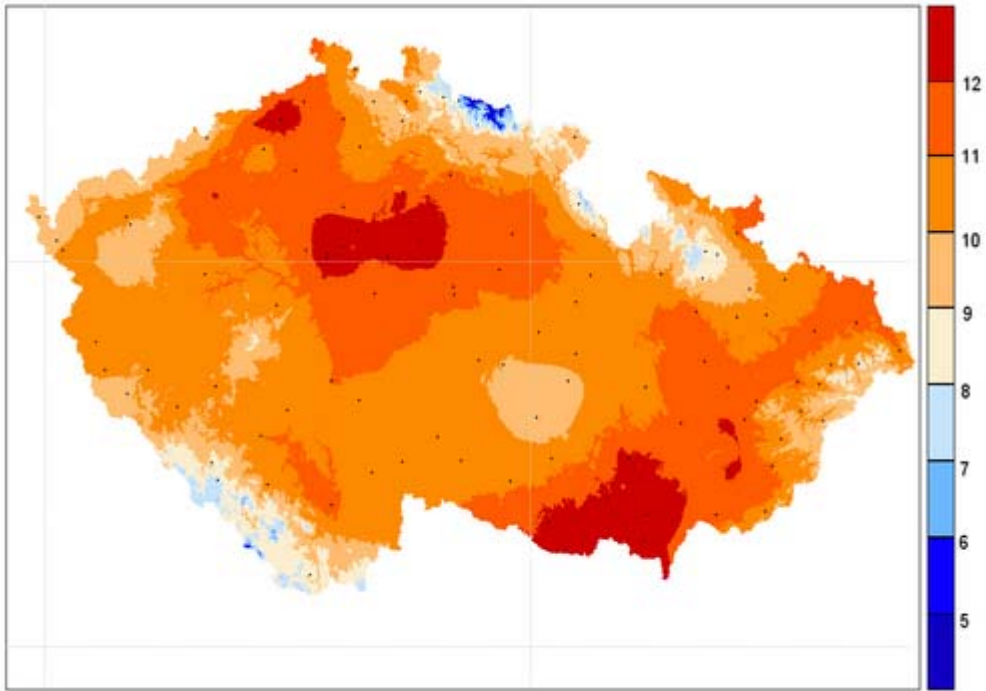
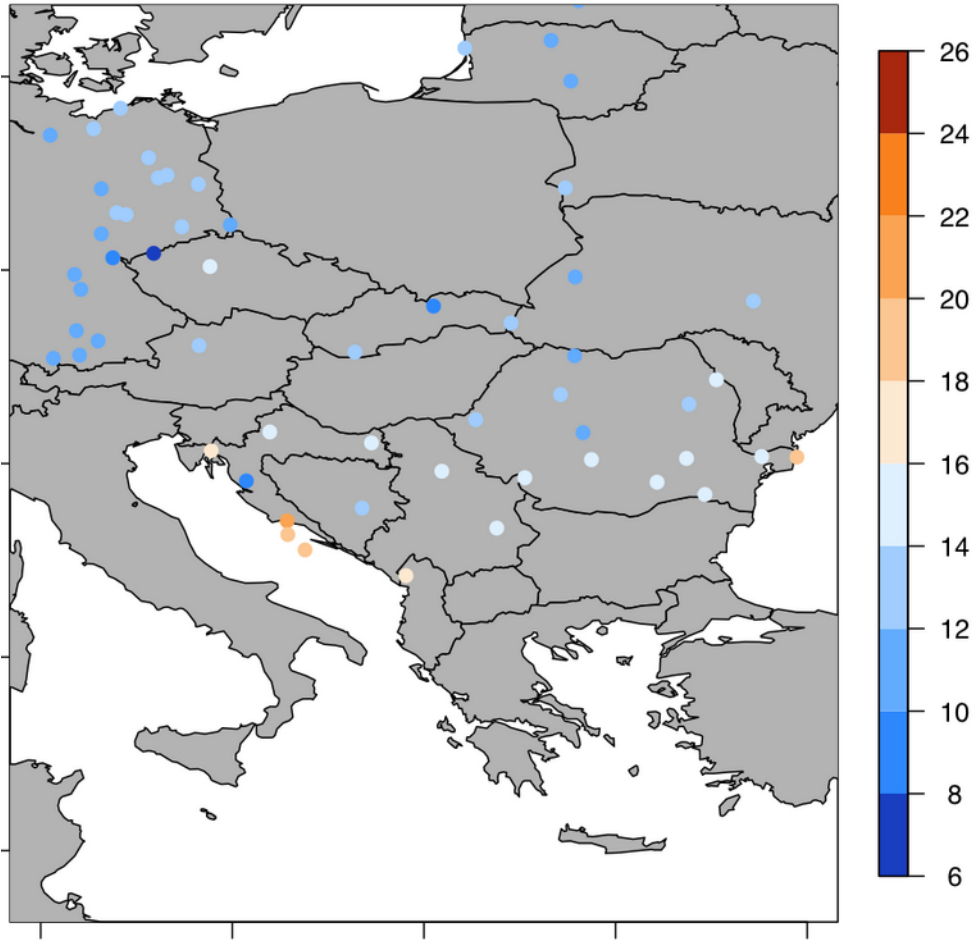
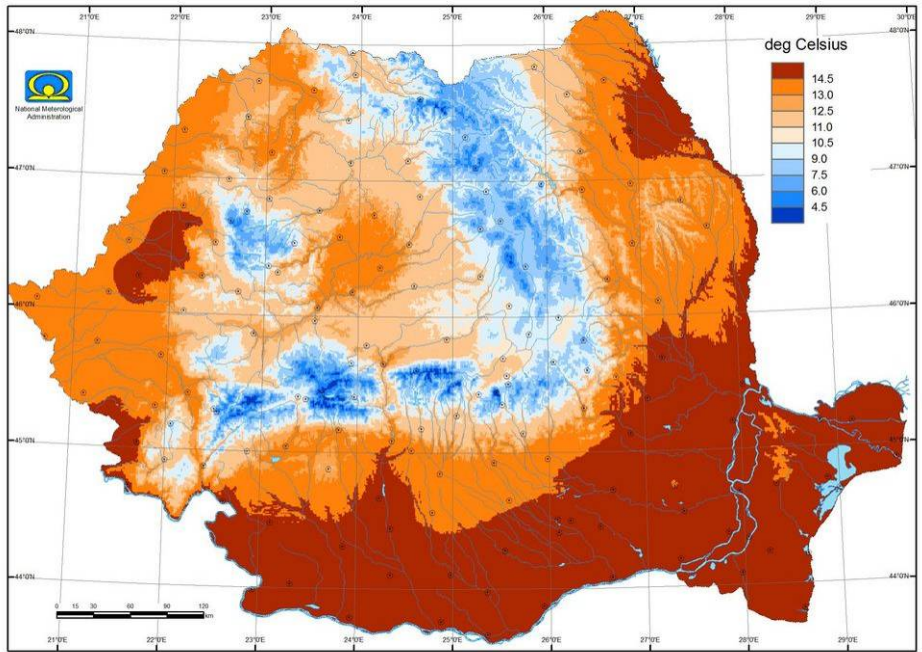


Figure B3 Mean daily-minimum temperature for winter (DJF) for the period 1961-1990. Panels like the previous figure.



INDEX 002 JJA ROMANIA 1961 - 1990



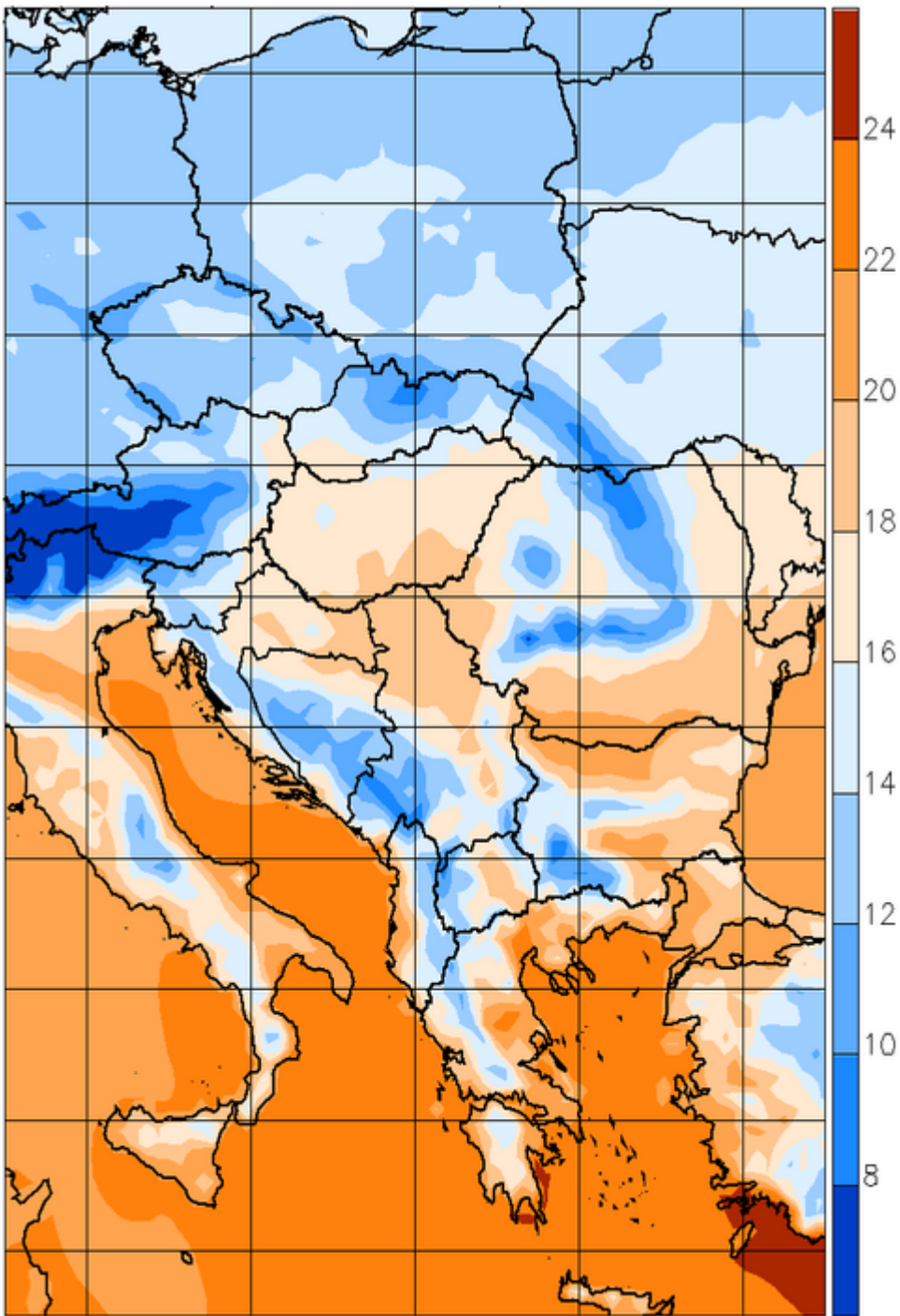
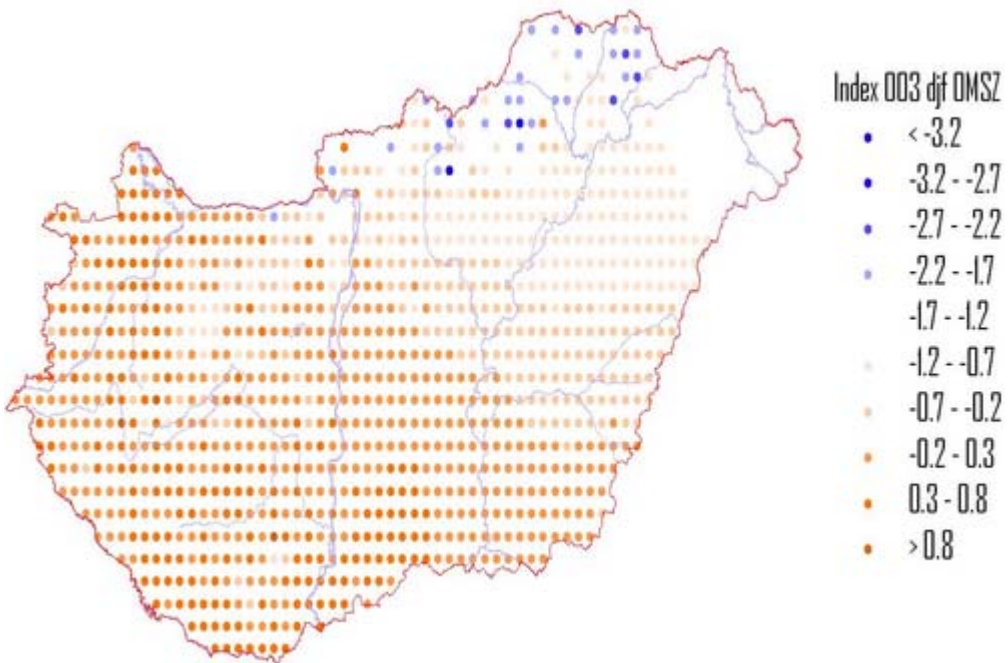
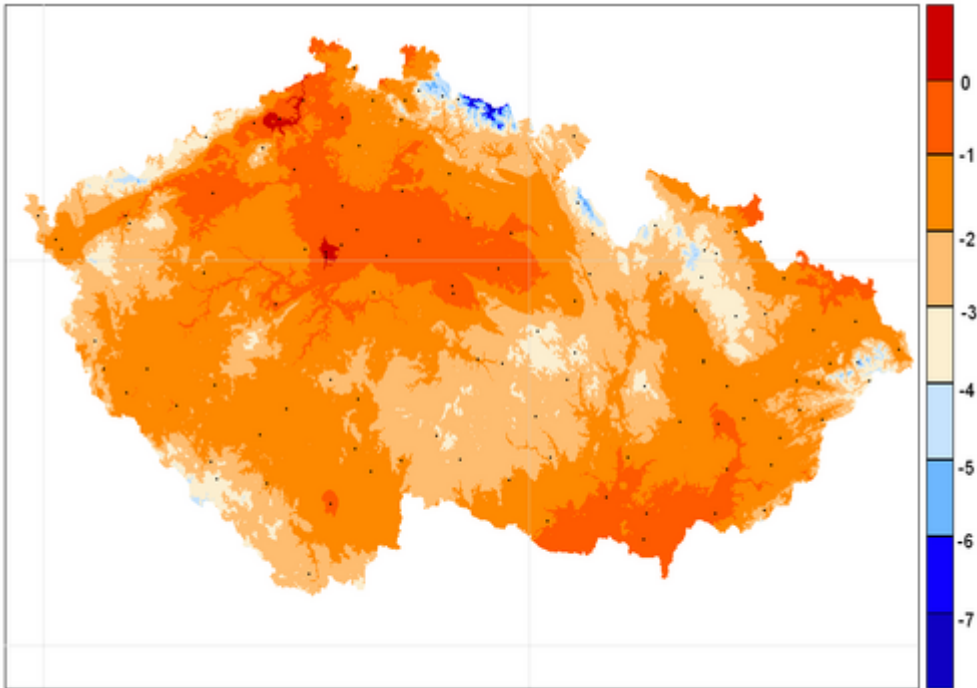
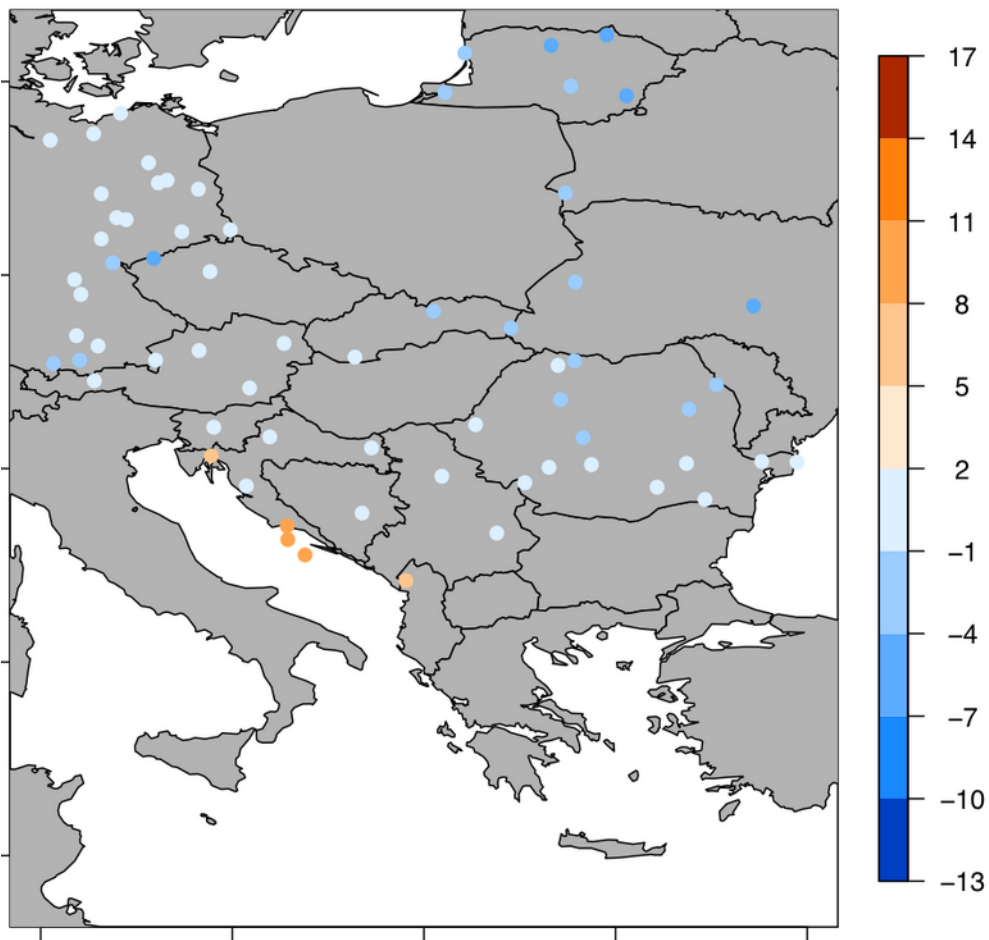
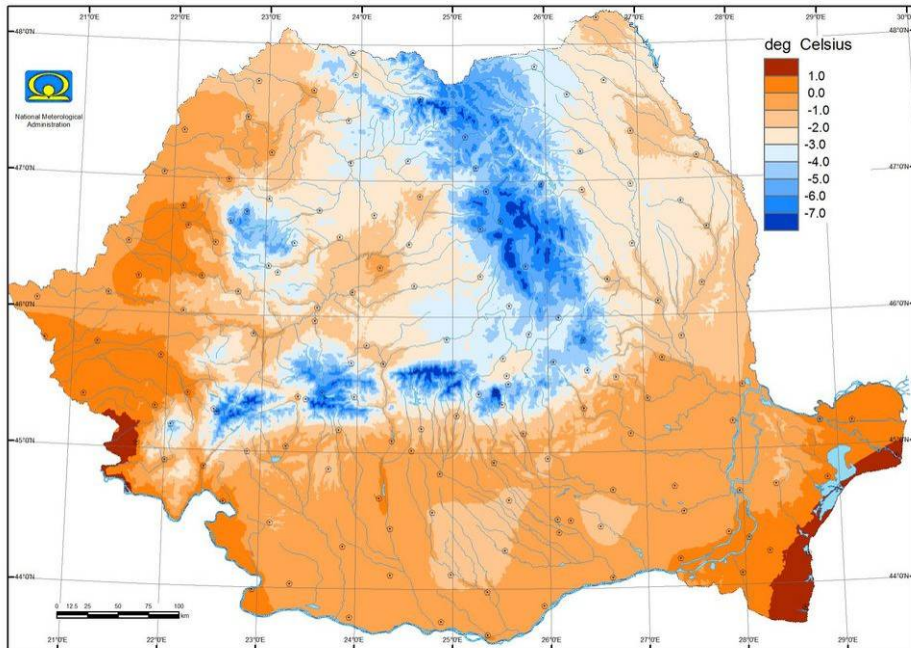


Figure B4 Mean daily-minimum temperature for summer (JJA) for the period 1961-1990. Panels like the previous figure.



INDEX 003 DJF ROMANIA 1961 - 1990



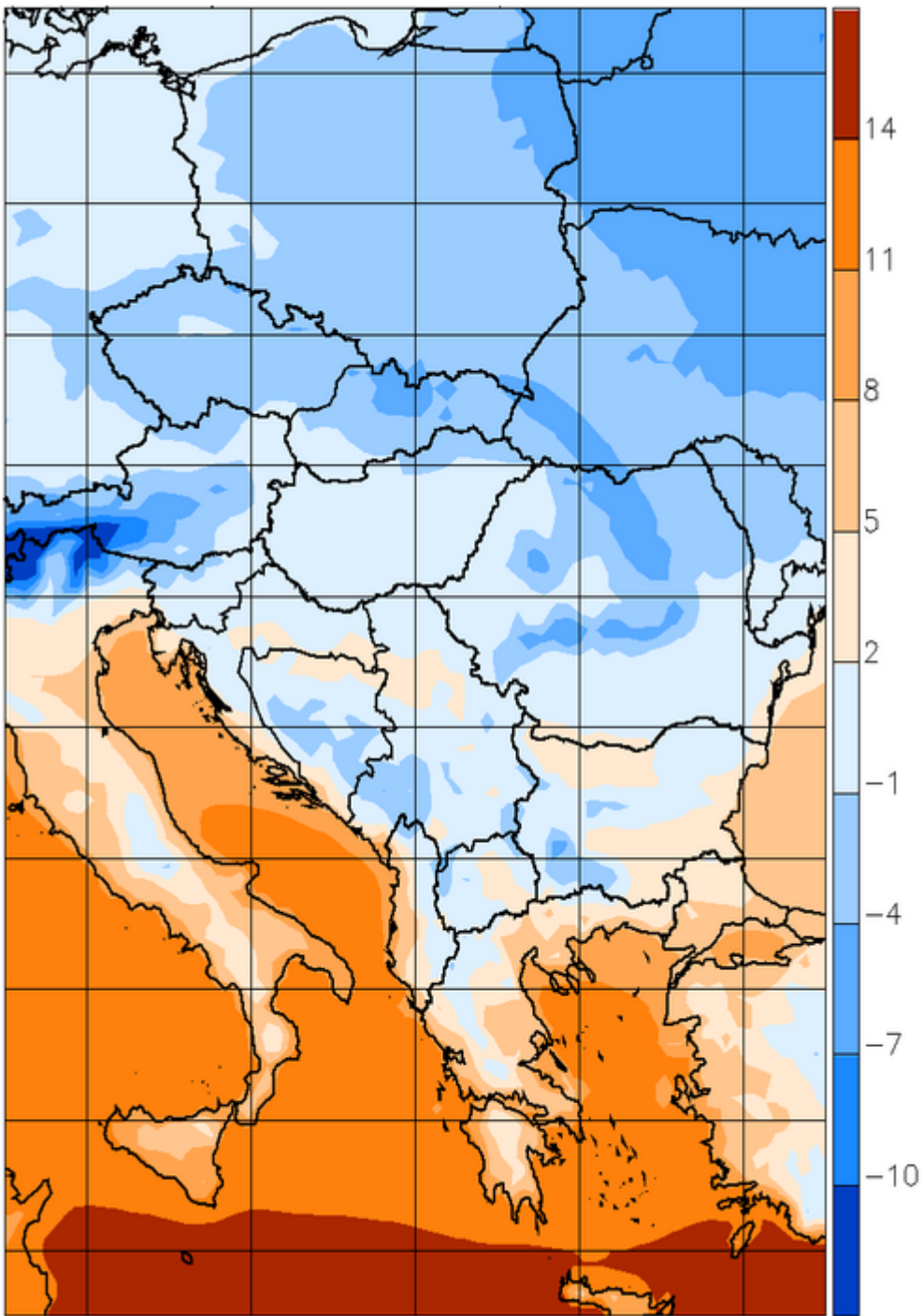
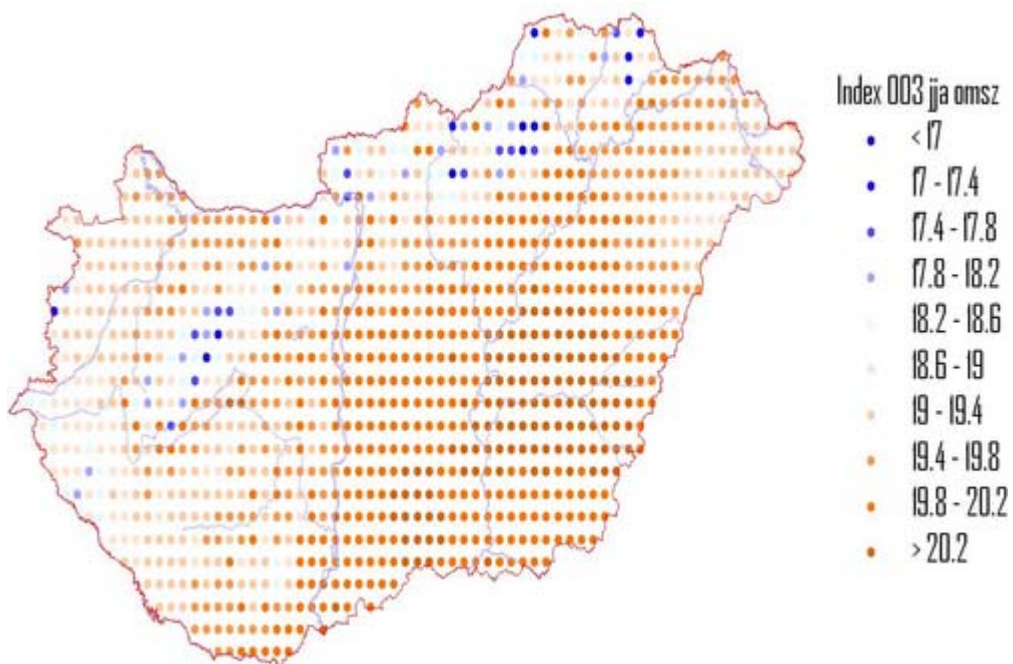
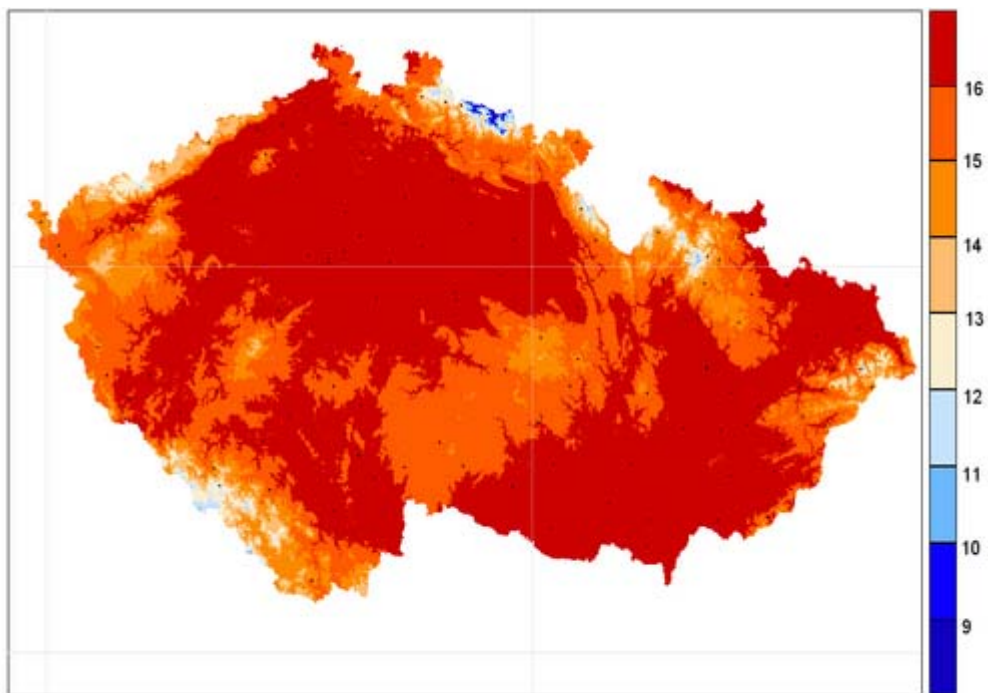
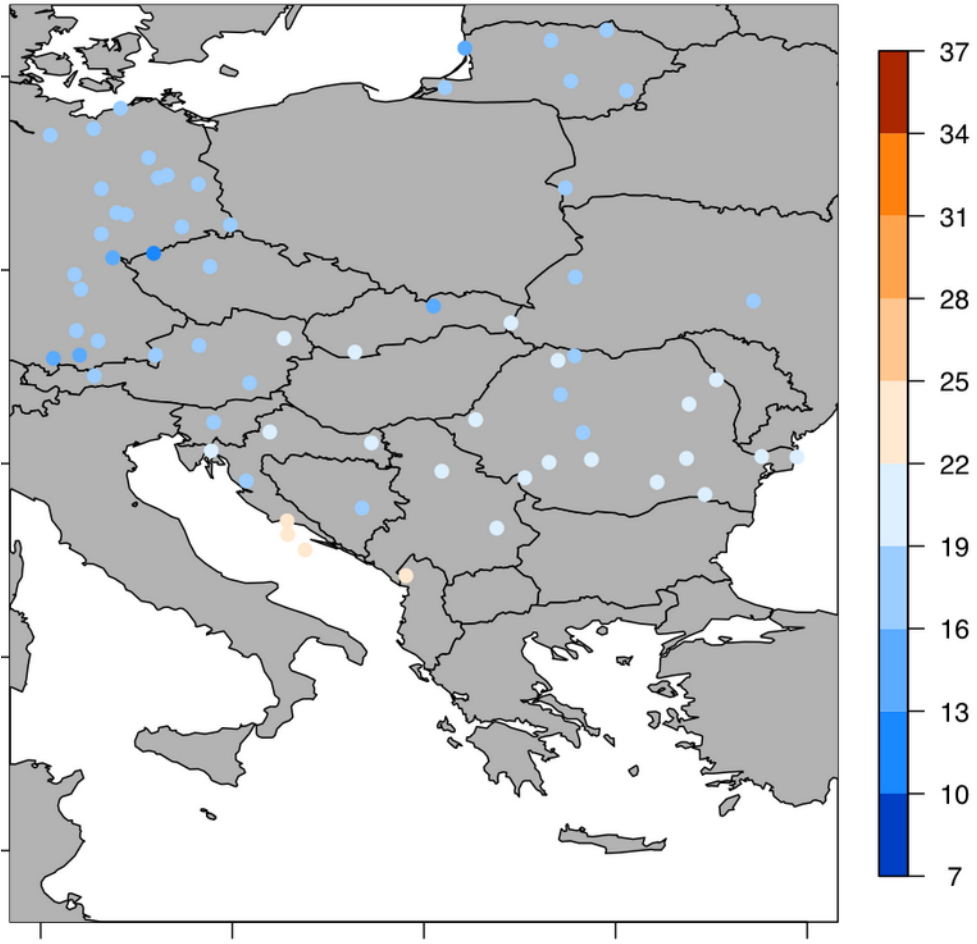
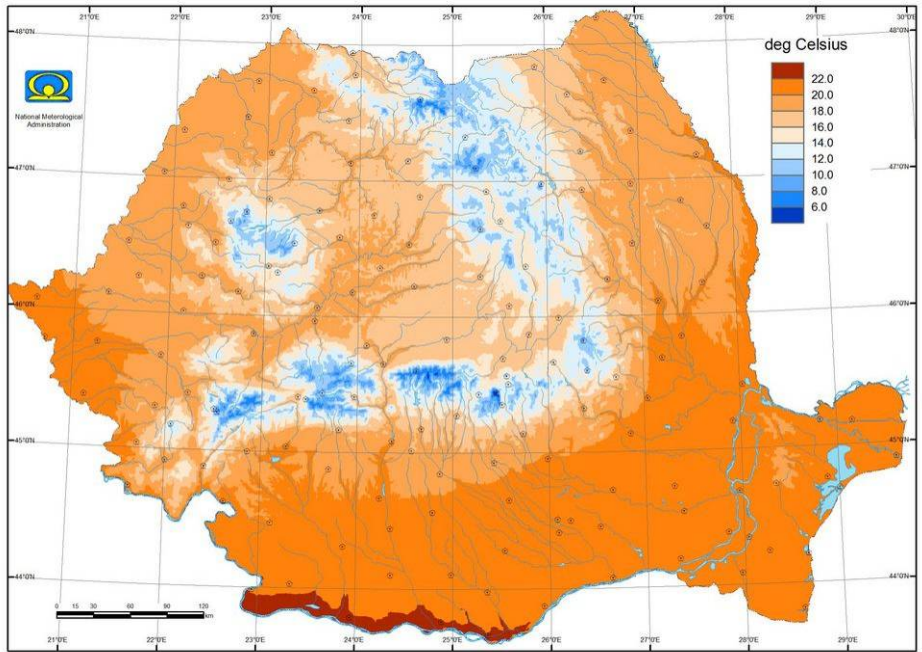


Figure B5 Mean daily average temperature for winter (DJF) for the period 1961-1990. Panels like the previous figure.



INDEX 003 JJA ROMANIA 1961 - 1990



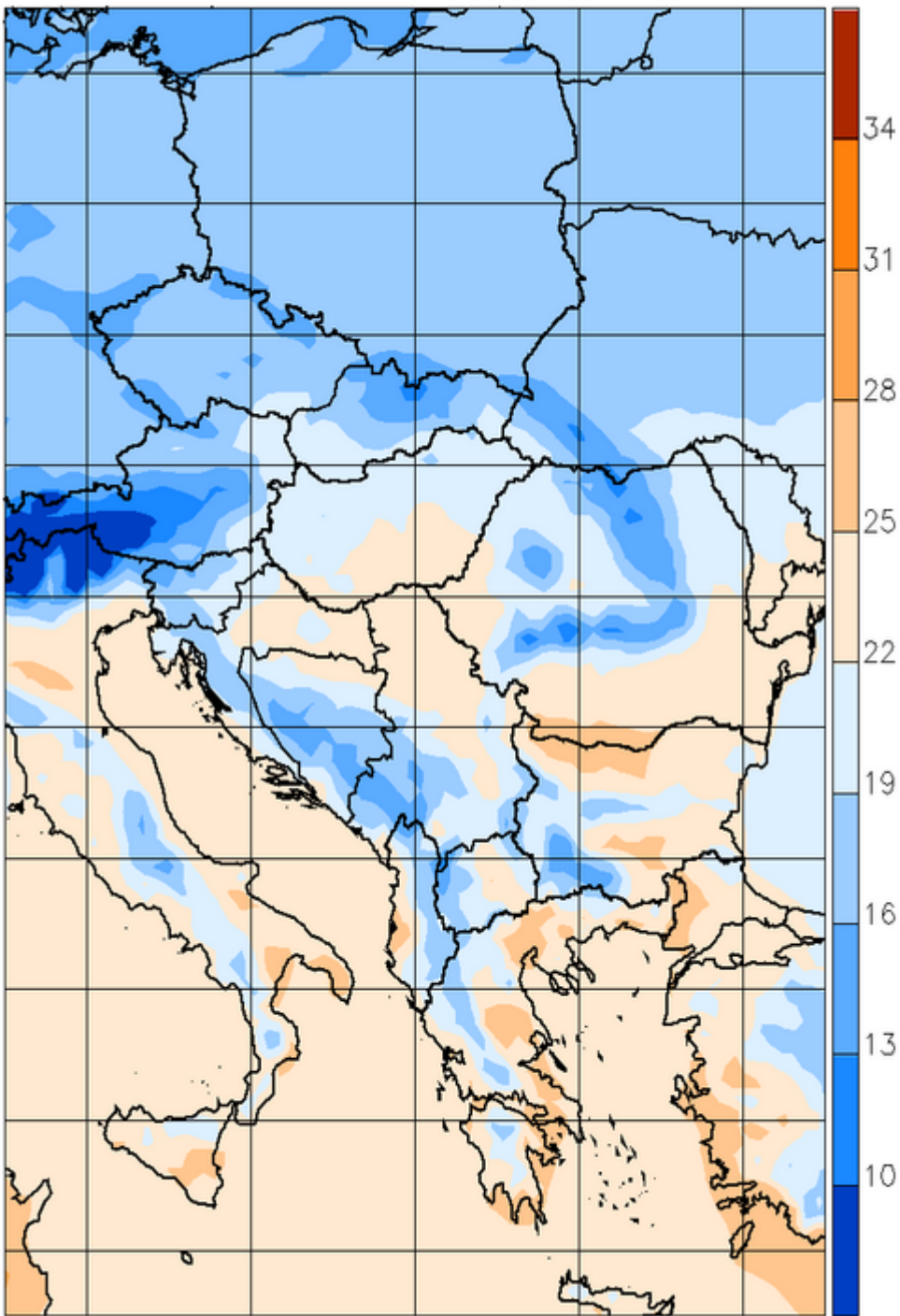
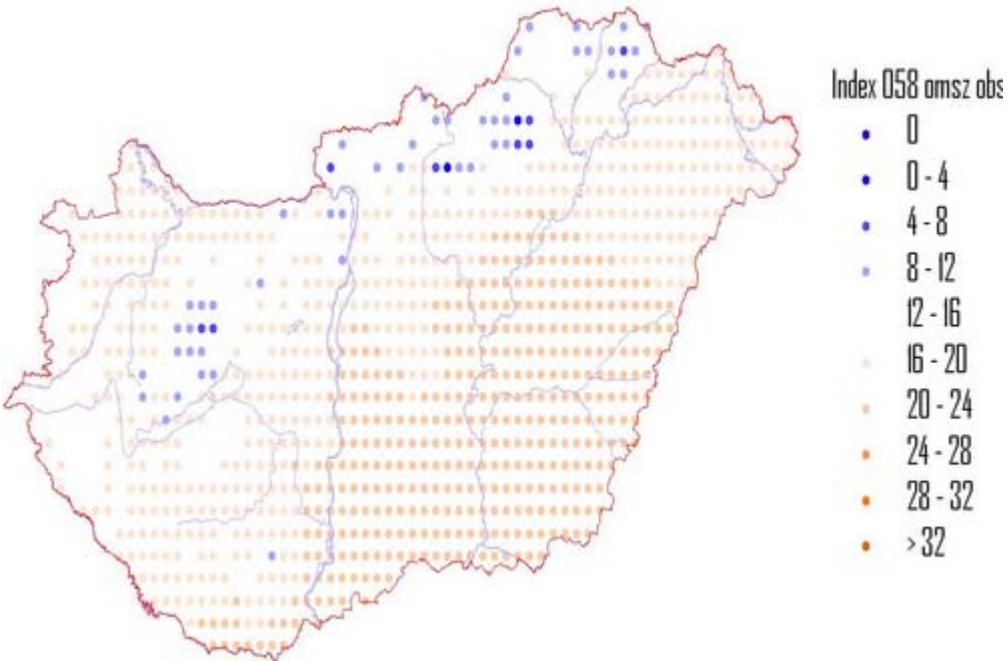
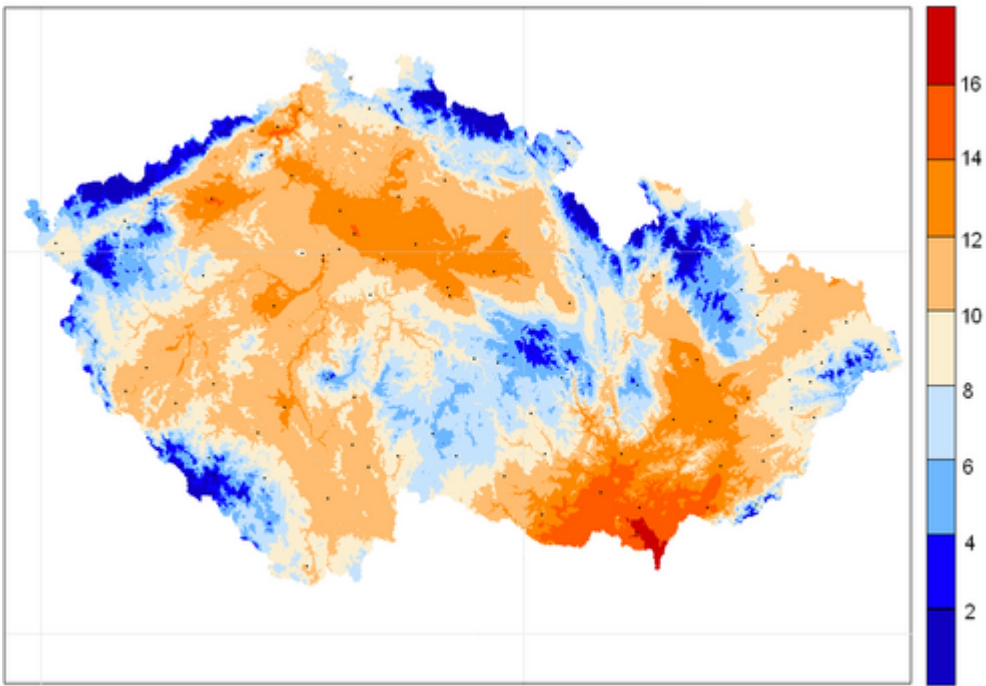
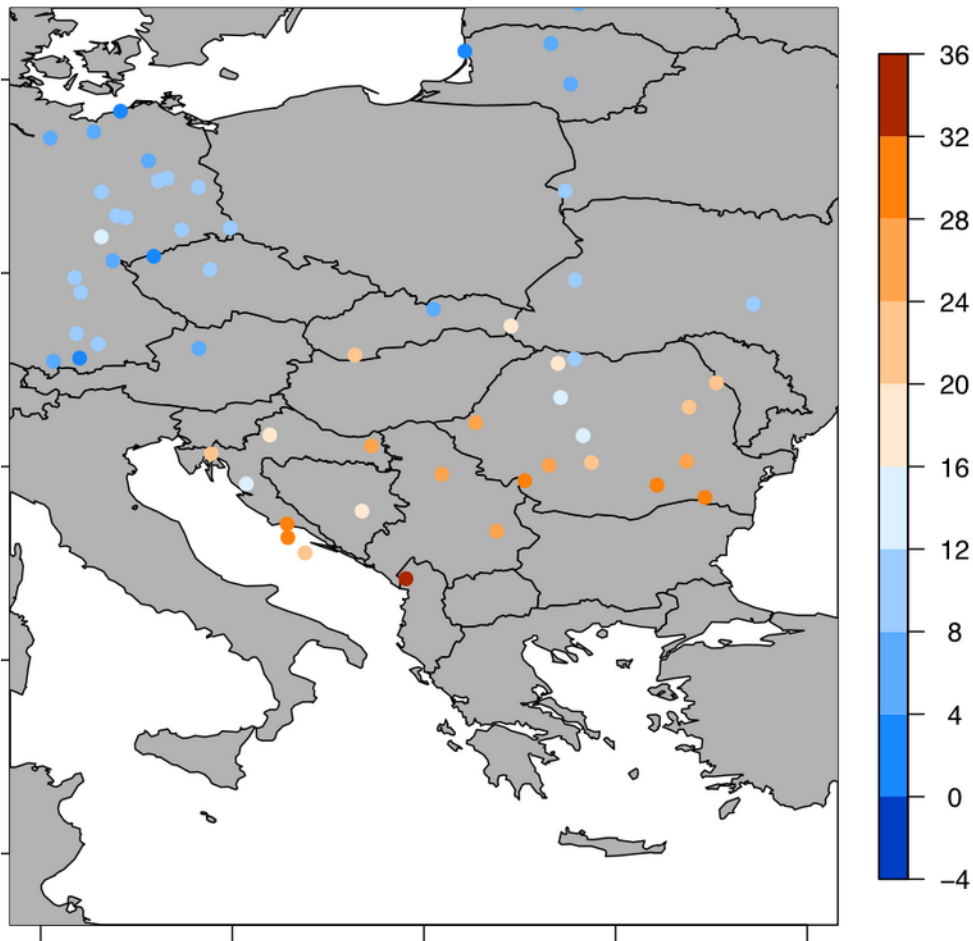
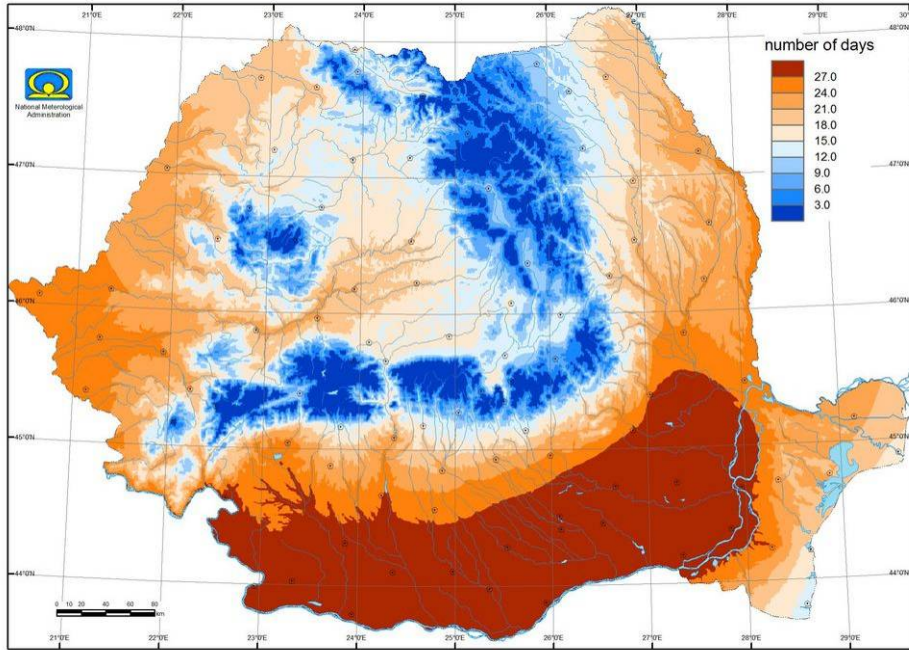


Figure B6 Mean daily average temperature for summer (JJA) for the period 1961-1990. Panels like the previous figure.

INDEX 058 TERN GLEBOFFNY 058



INDEX 058 ANN ROMANIA 1961 - 1990



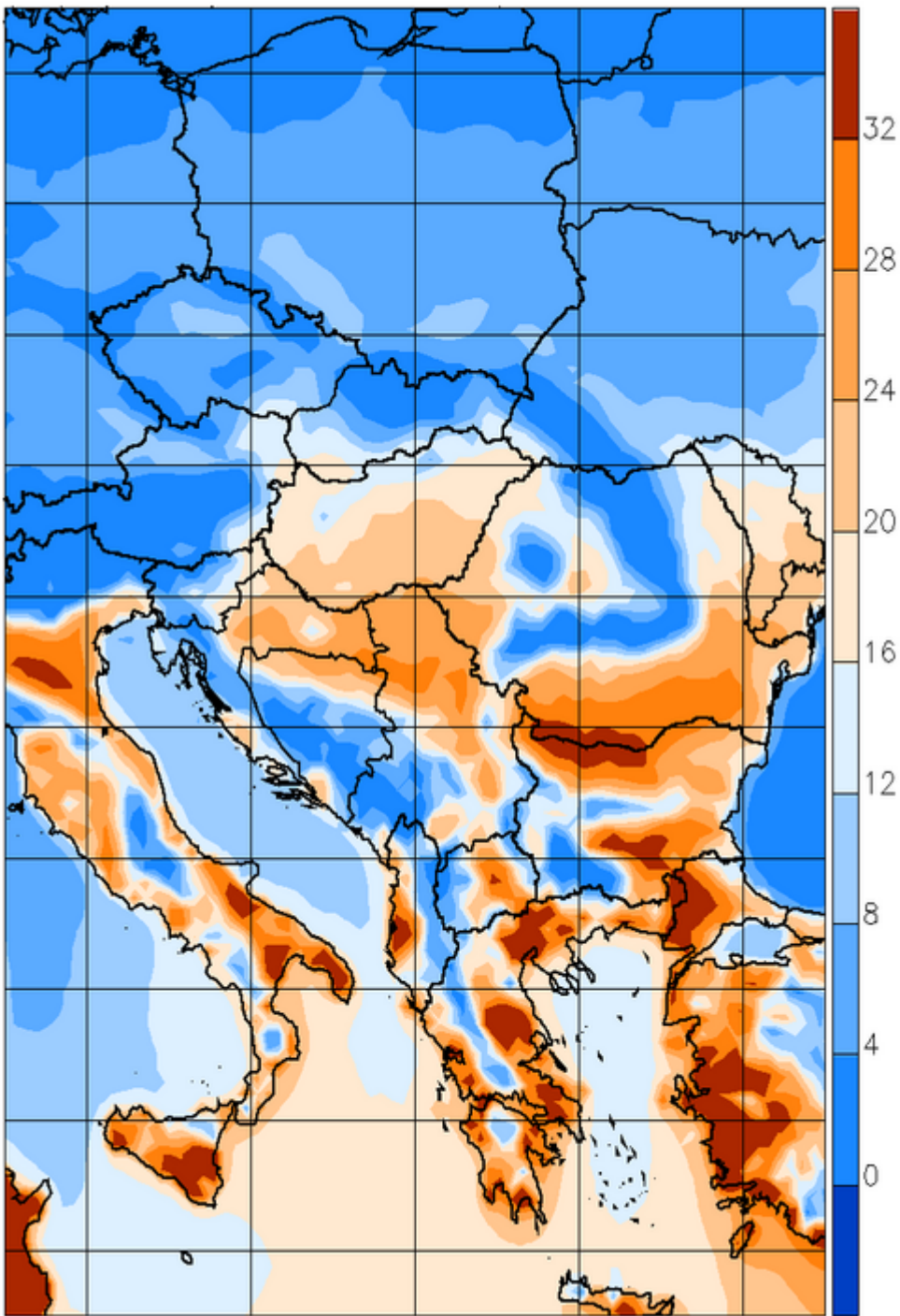
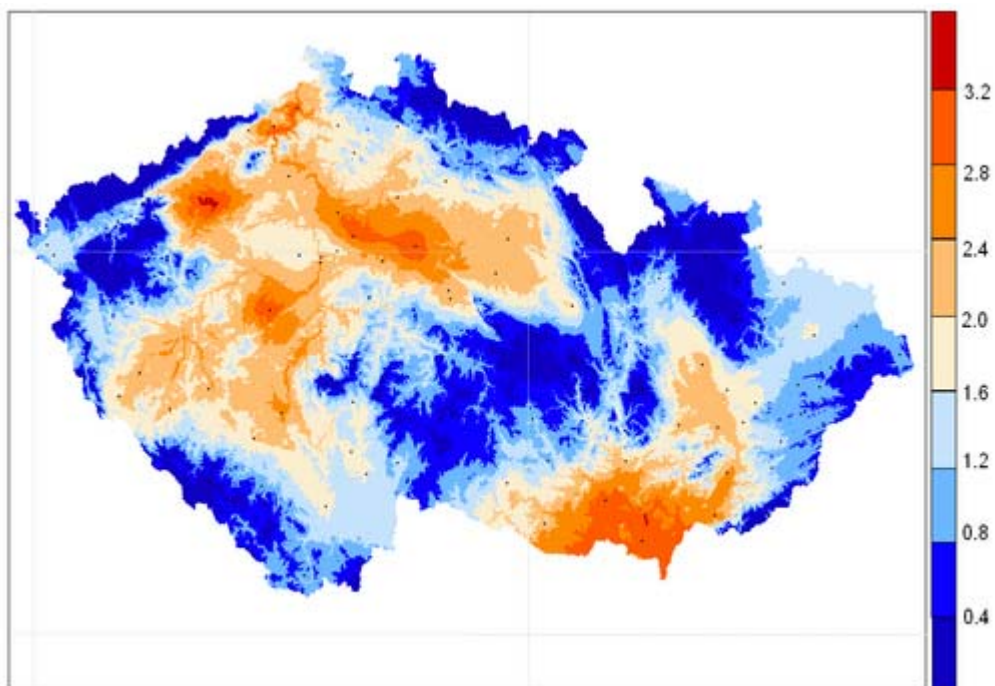
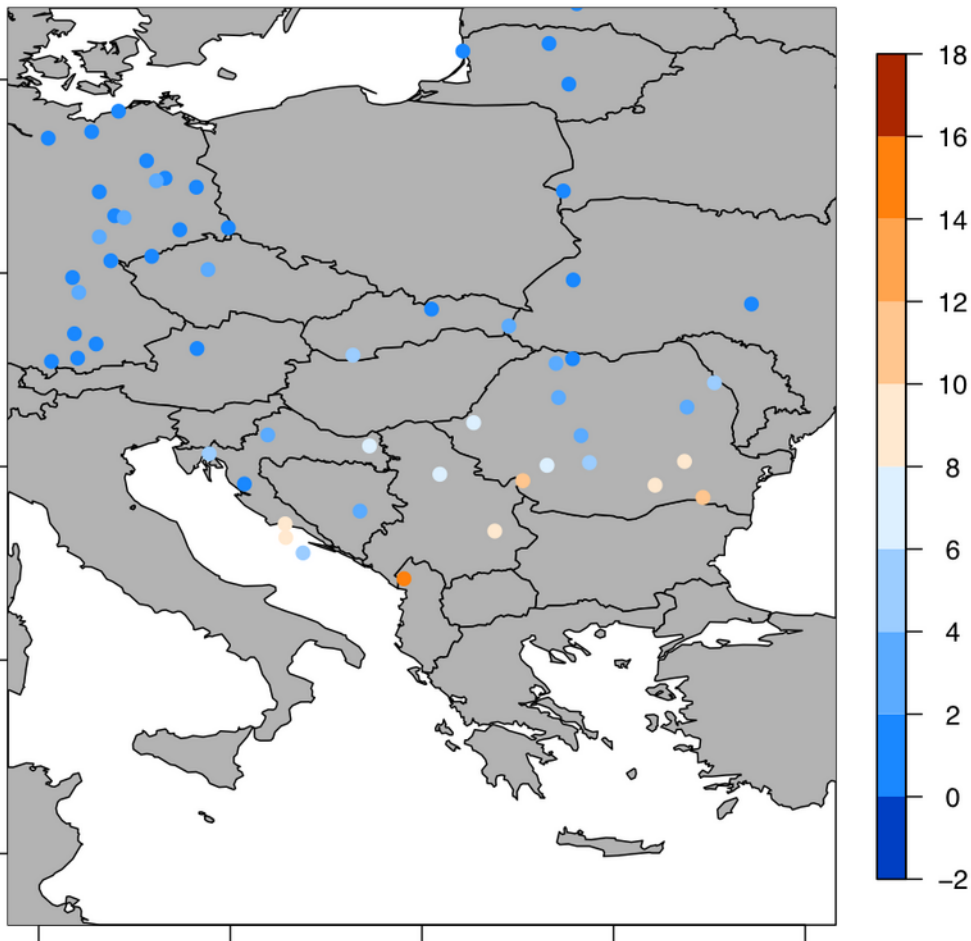
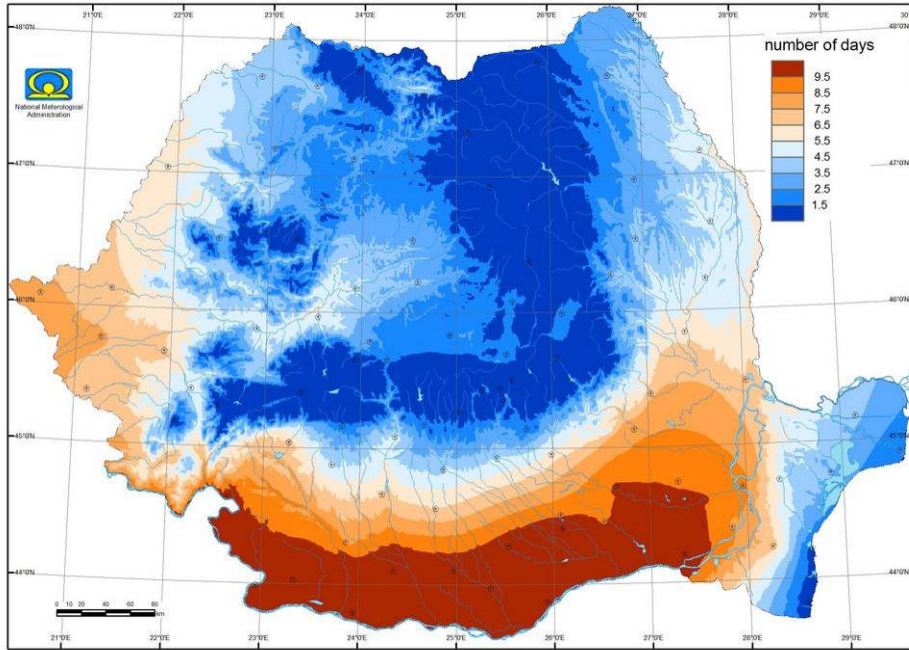


Figure B7 Percentage of days in the year with maximum temperature above 25C. Panels like the previous figure.



INDEX 066 ANN ROMANIA 1961 - 1990



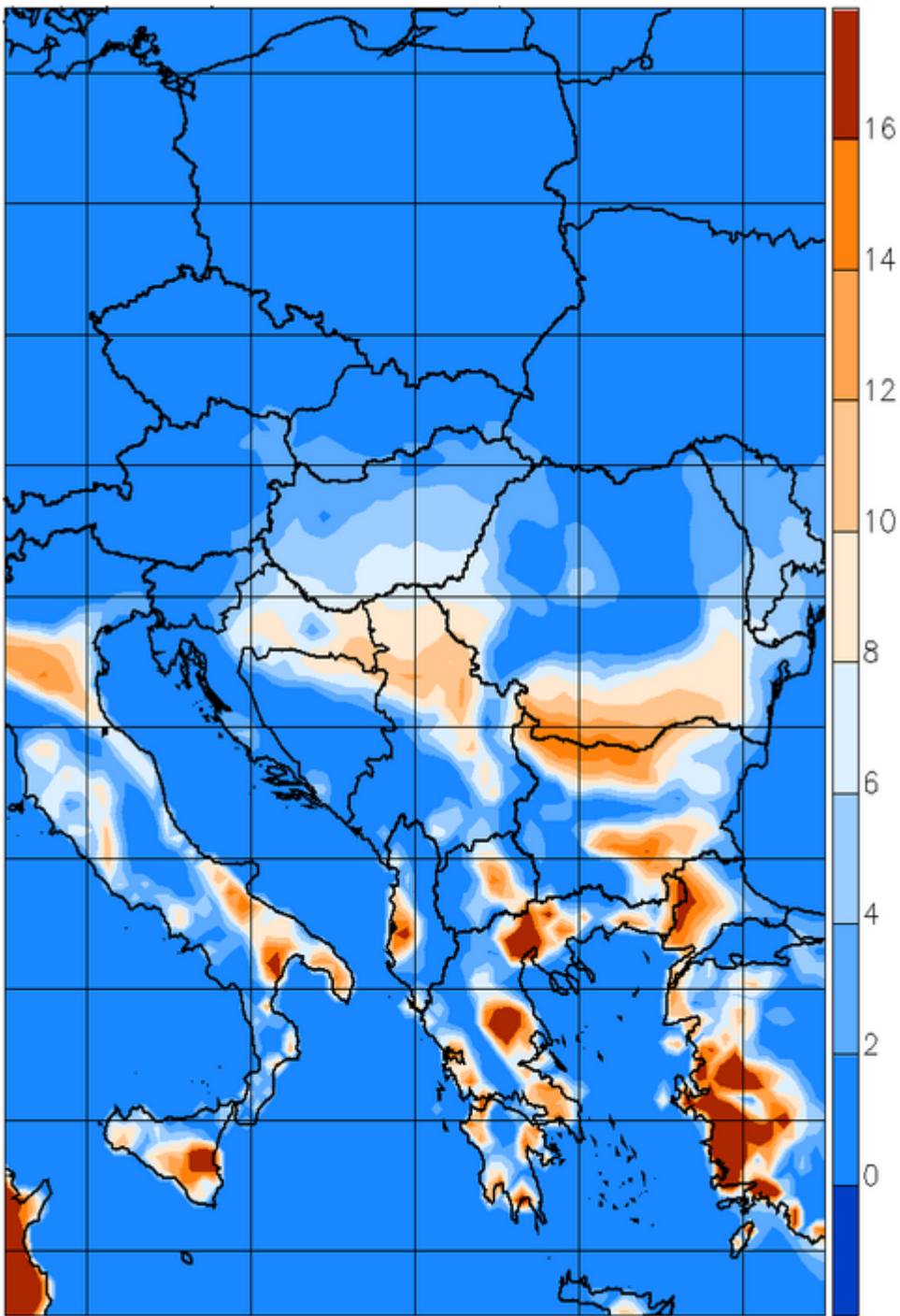
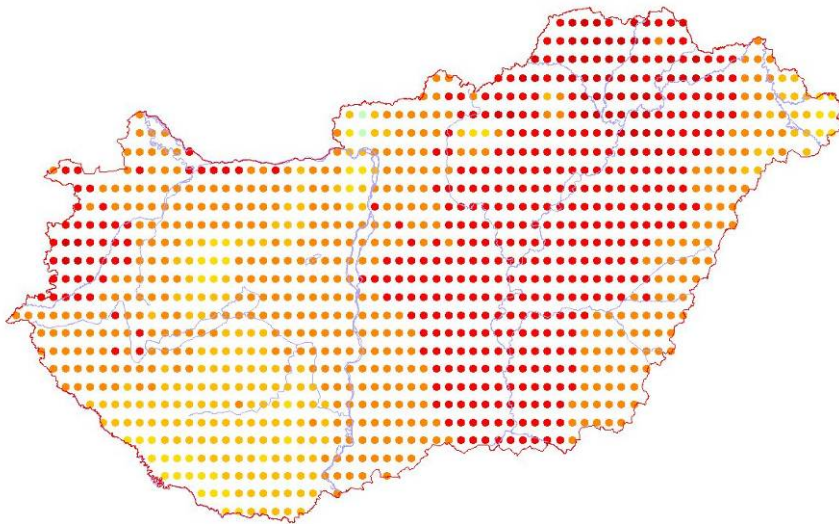
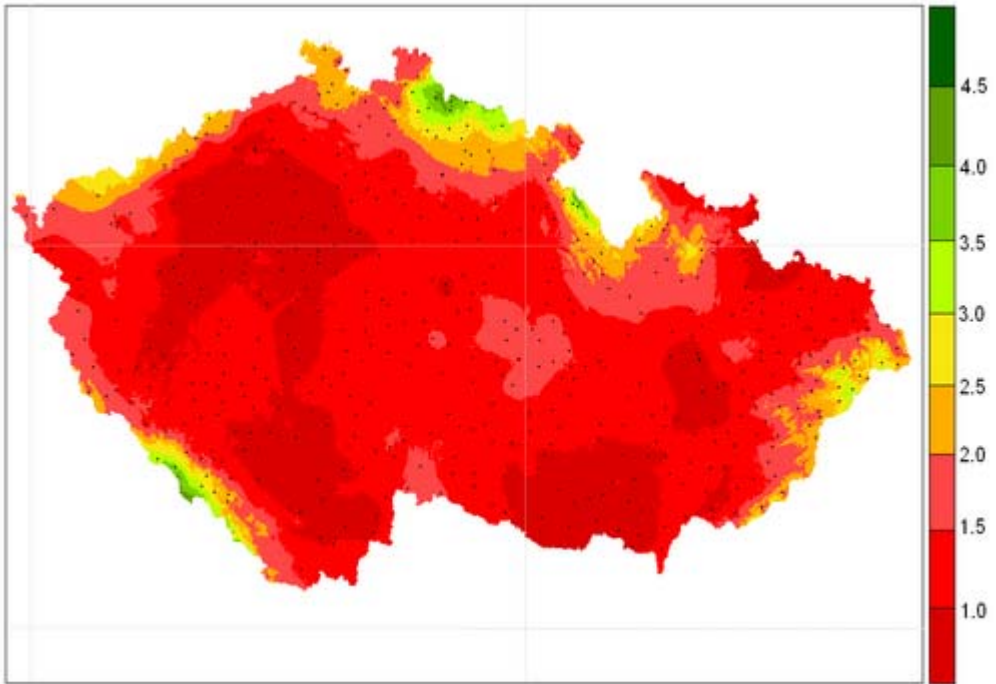
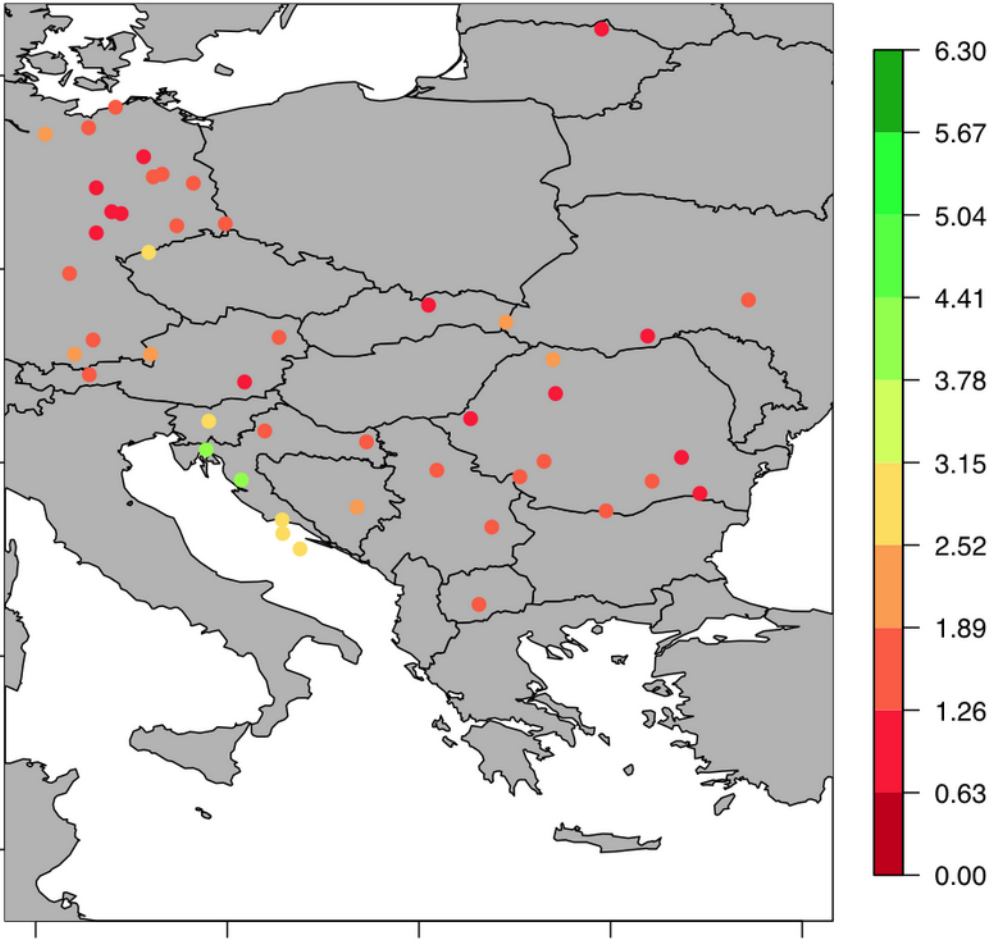


Figure B8 Percentage of days in the year with maximum temperature above 30C. Panels like the previous figure



Index 76 djf omsz c

- <1
- 1-1.2
- 1.2-1.4
- 1.4-1.6
- 1.6-1.8
- 1.8-2
- 2-2.2
- 2.2-2.4
- 2.4-2.6
- >2.6



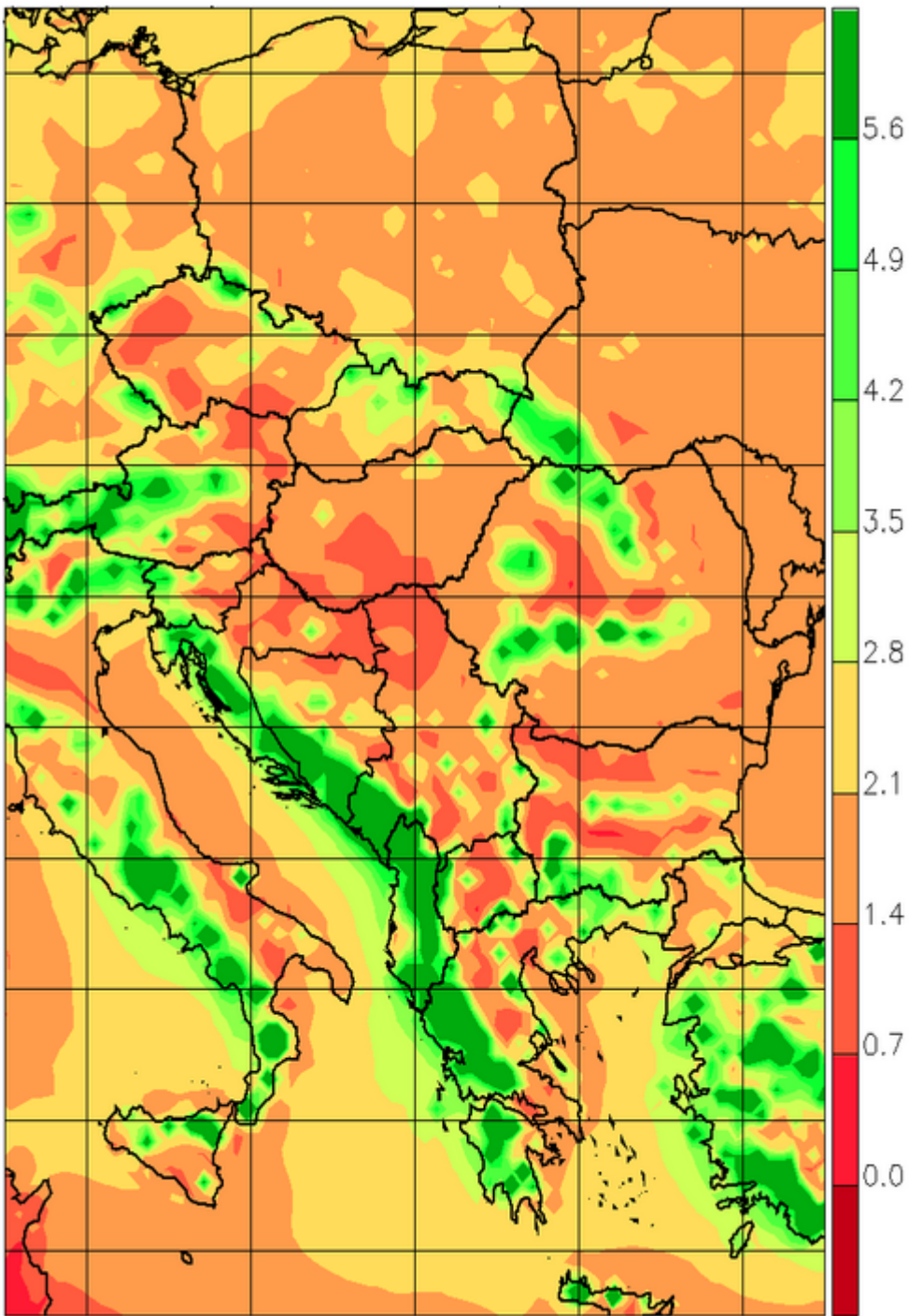
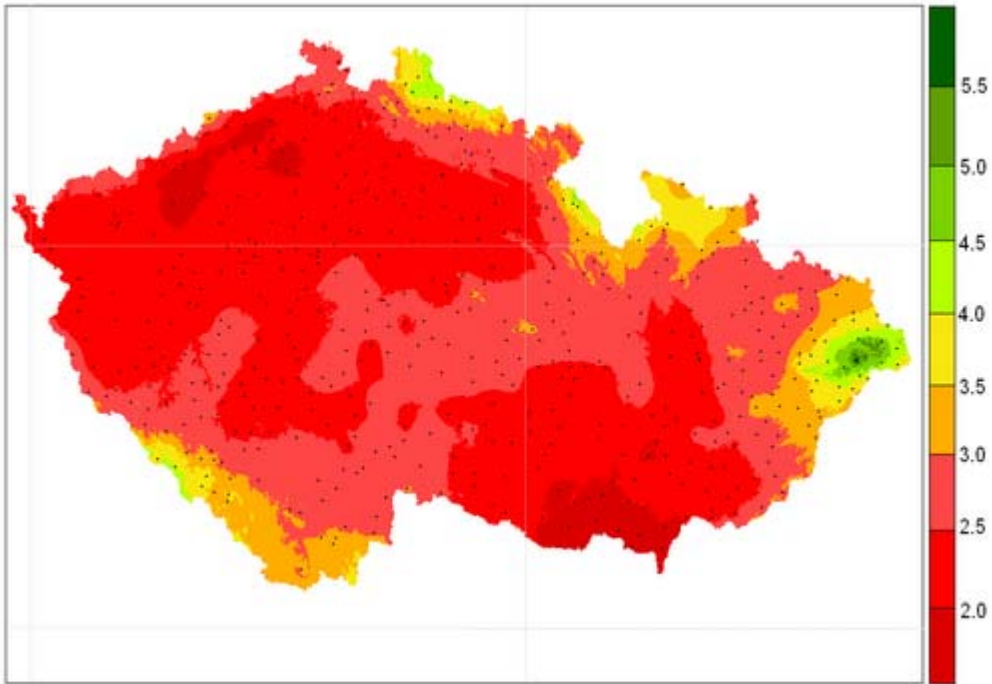
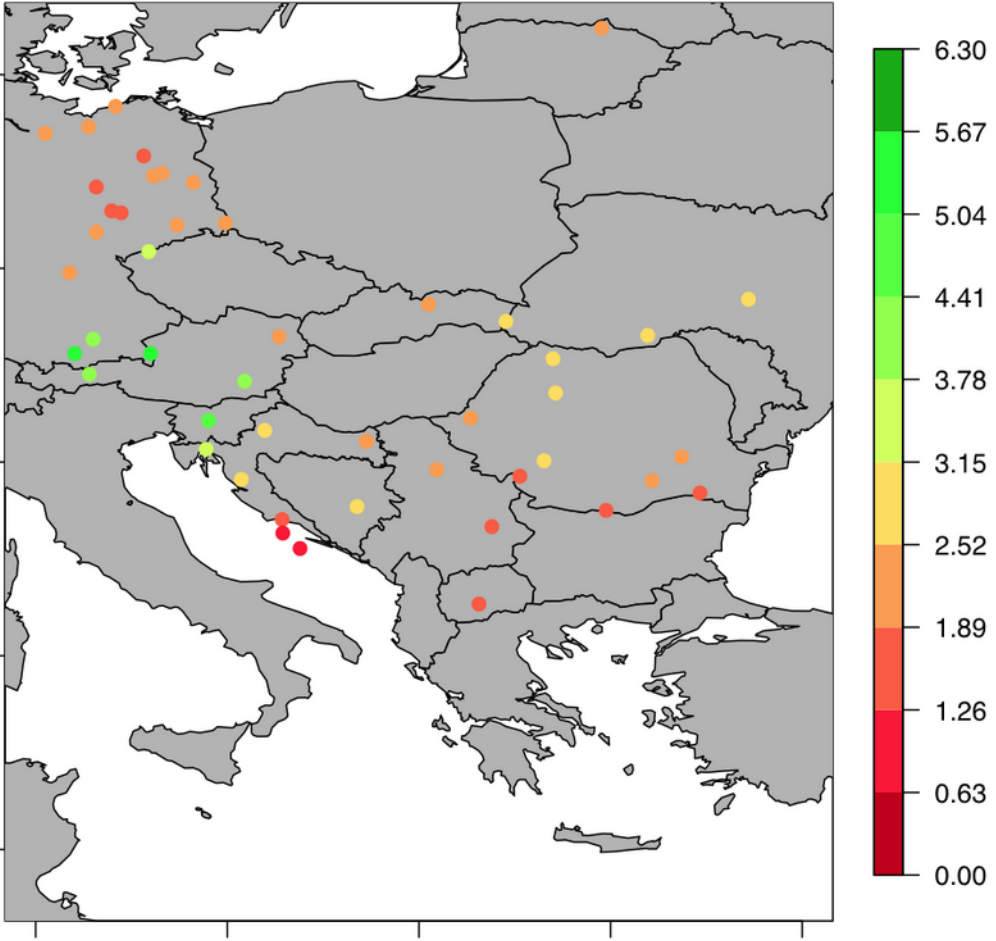


Figure B9 Average precipitation winter (DJF) in mm/day. From top to bottom: observations from the Czech Republic; observations from Hungary; observations from the ECA&D dataset; regional model output from the ENSEMBLES reanalysis-based HIRHAM5-experiment performed at the DMI.



Index 76 djf omsz t

- <1
- 1-1.2
- 1.2-1.4
- 1.4-1.6
- 1.6-1.8
- 1.8-2
- 2-2.2
- 2.2-2.4
- 2.4-2.6
- >2.6



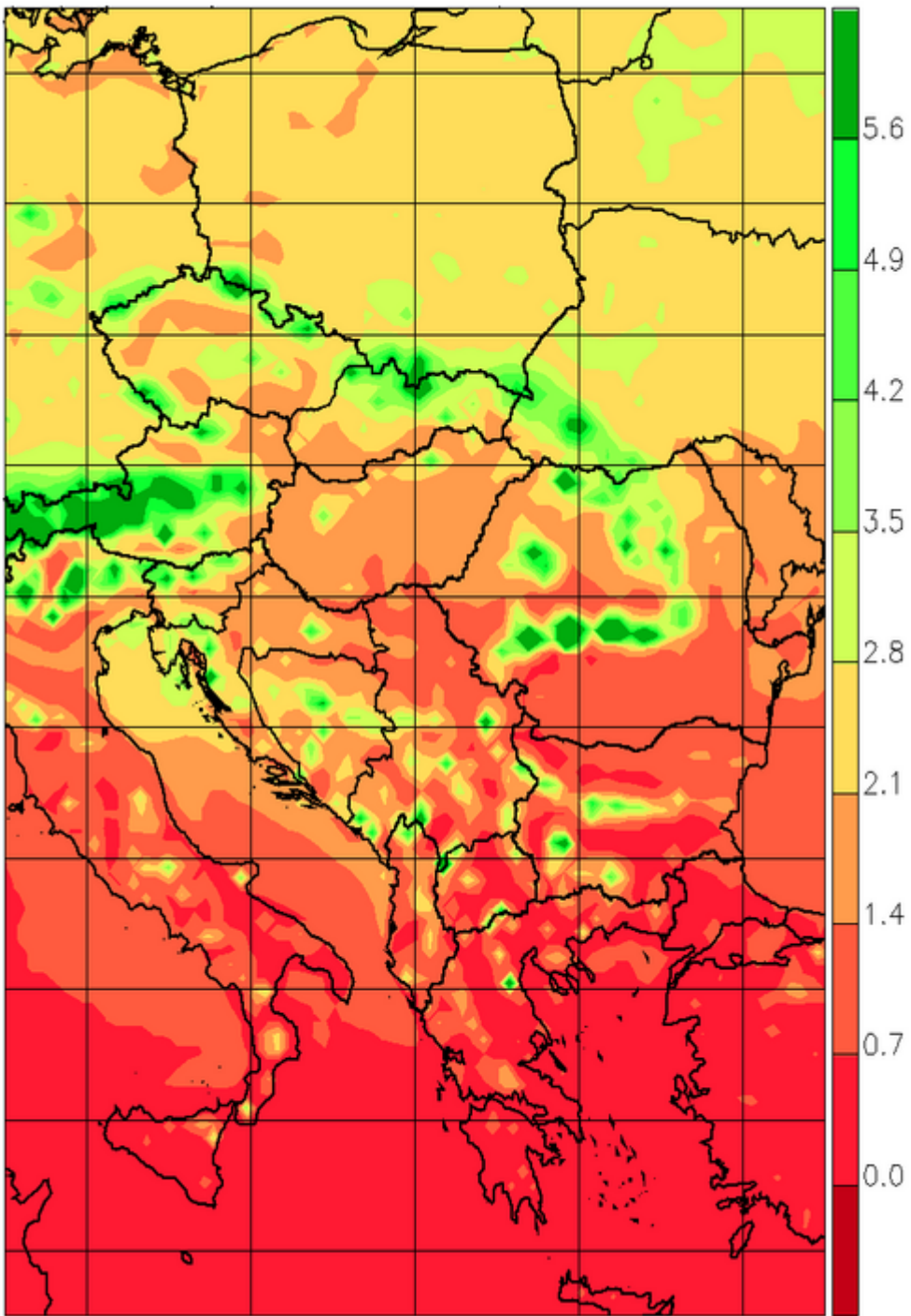
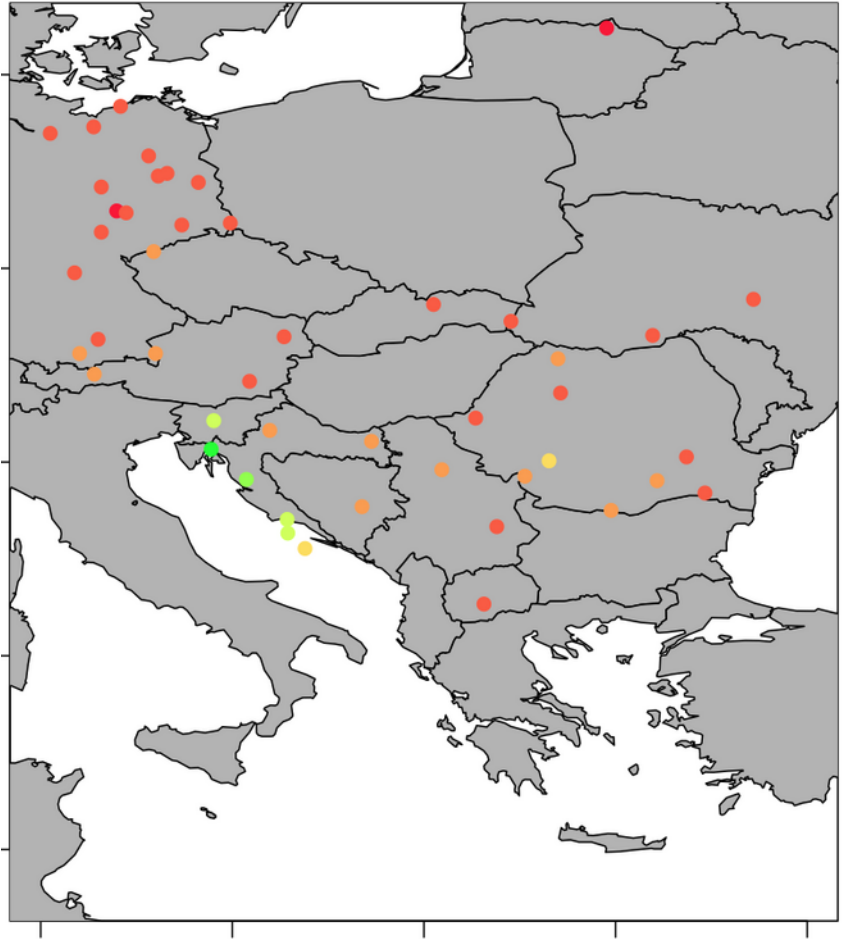
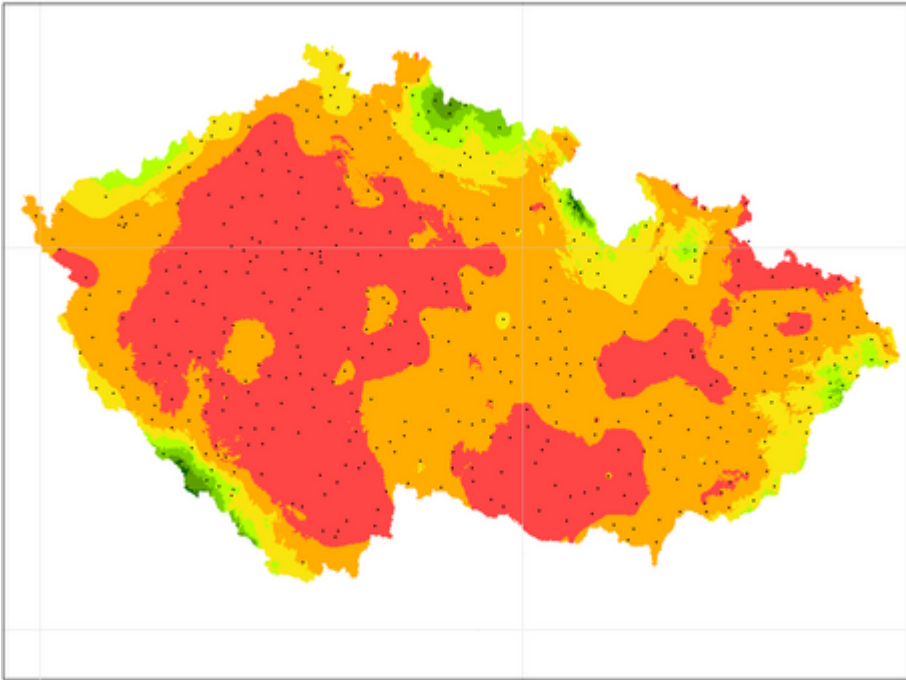


Figure B10 Average precipitation in summer (JJA) in mm/day. Panels like the previous figure.

INDEX OF BIOGEOGRAPHIC CELLS



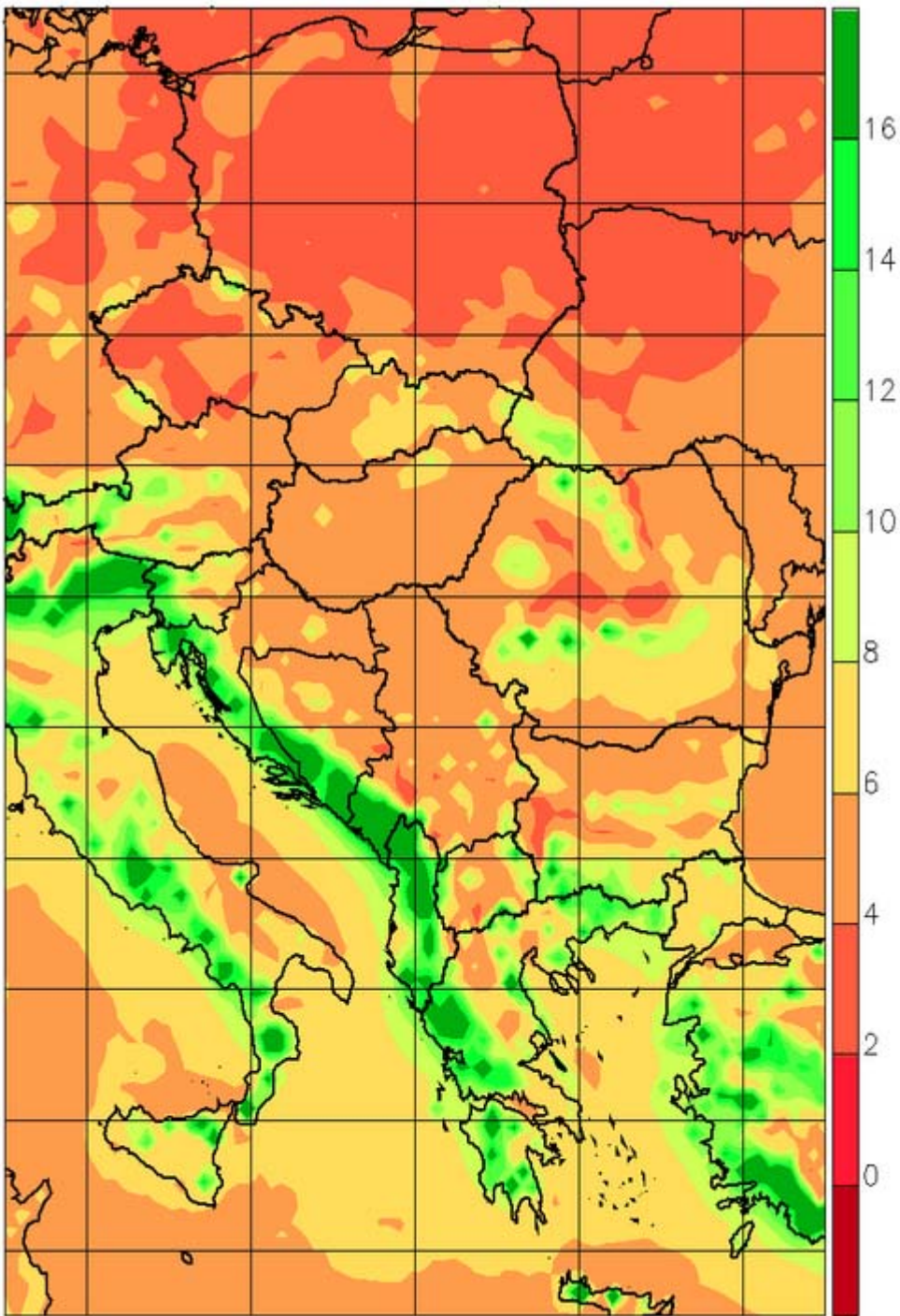
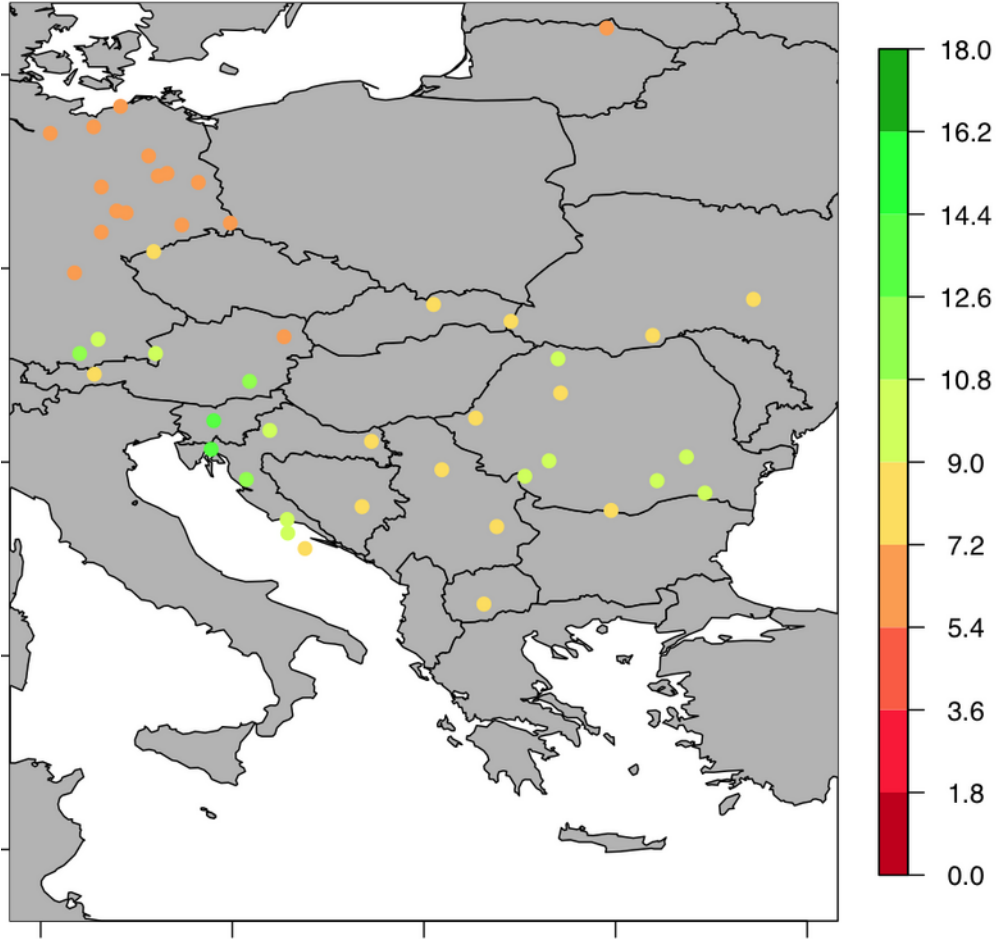
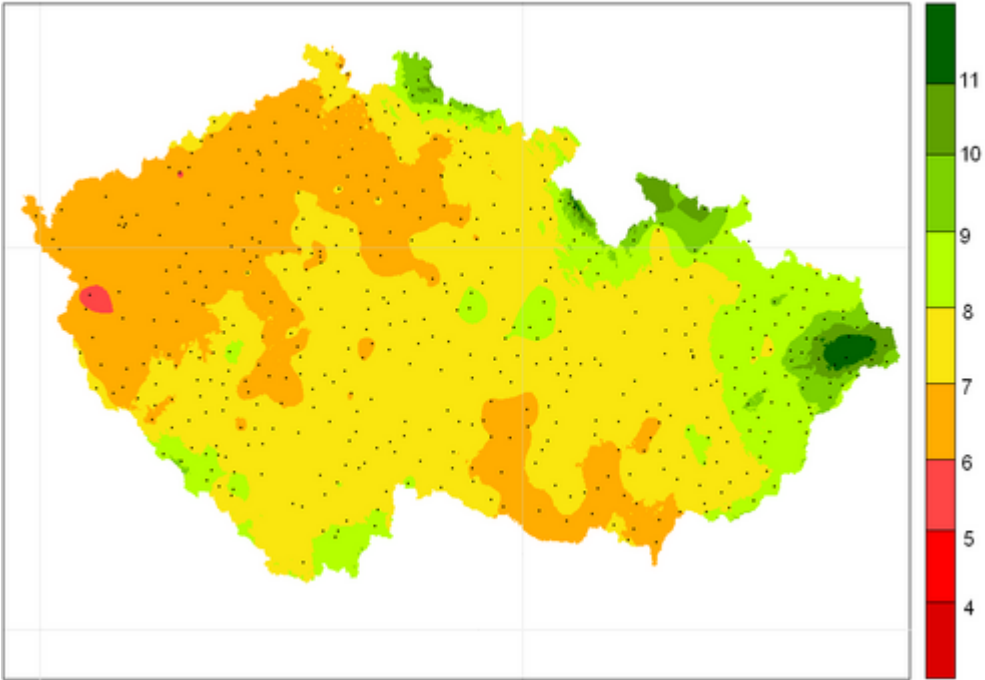


Figure B11 Average wet-day precipitation in winter (DJF) in mm/day. Panels like the previous figure.

INDEX OF SOY GROWING DAYS



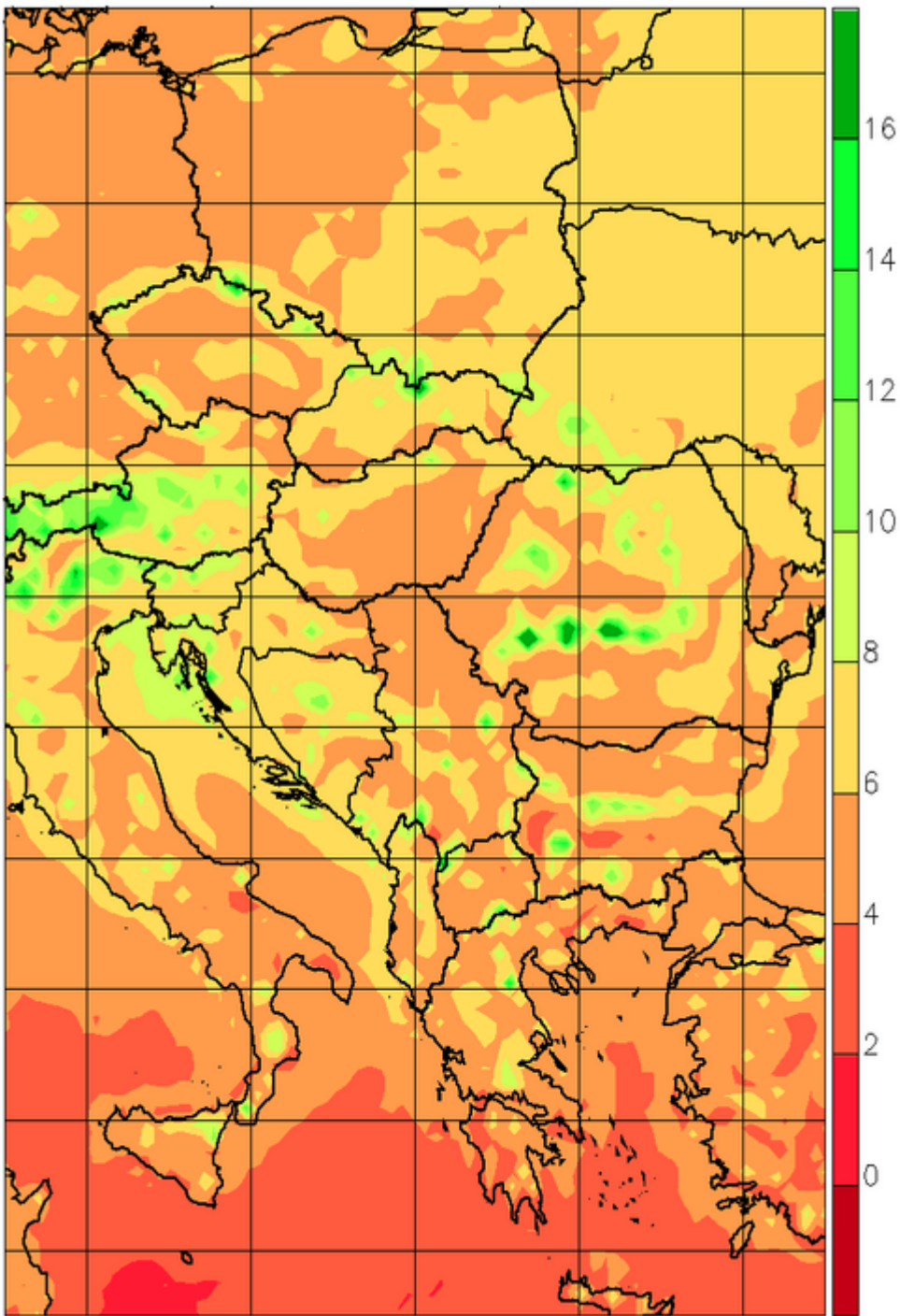
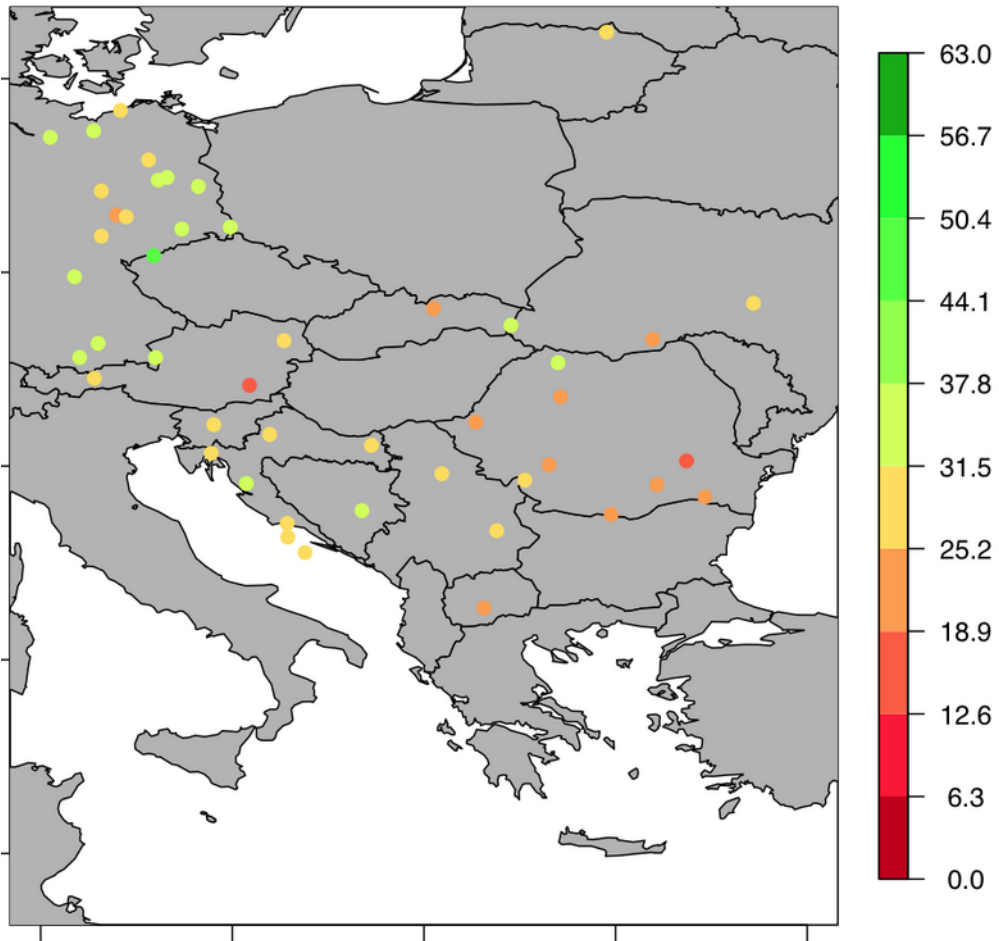
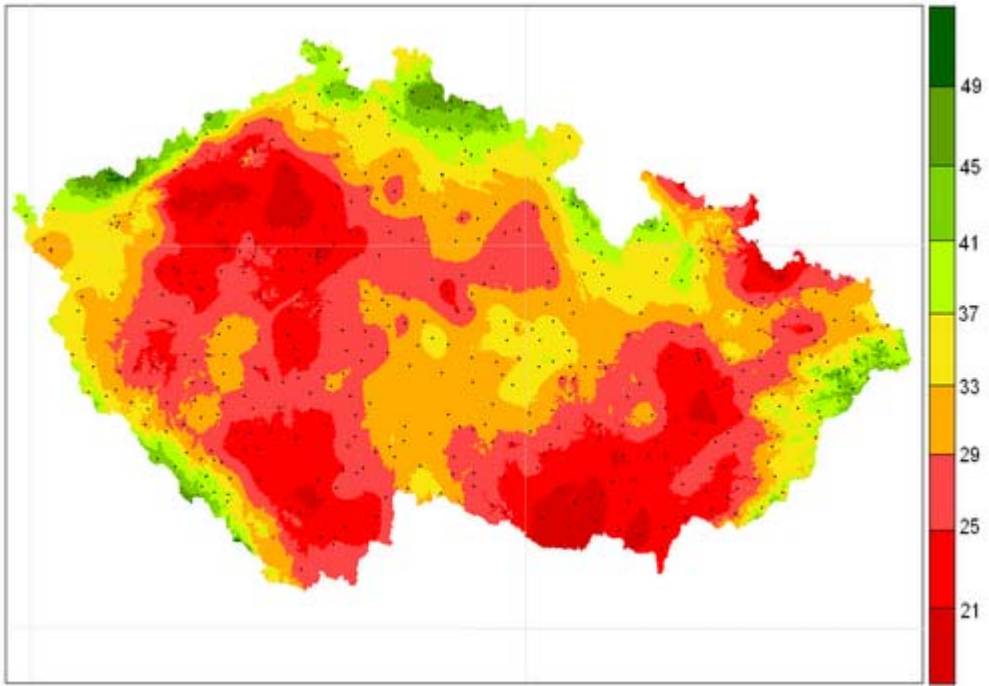


Figure B12 Average wet-day precipitation in summer (JJA) in mm/day. Panels like the previous figure.



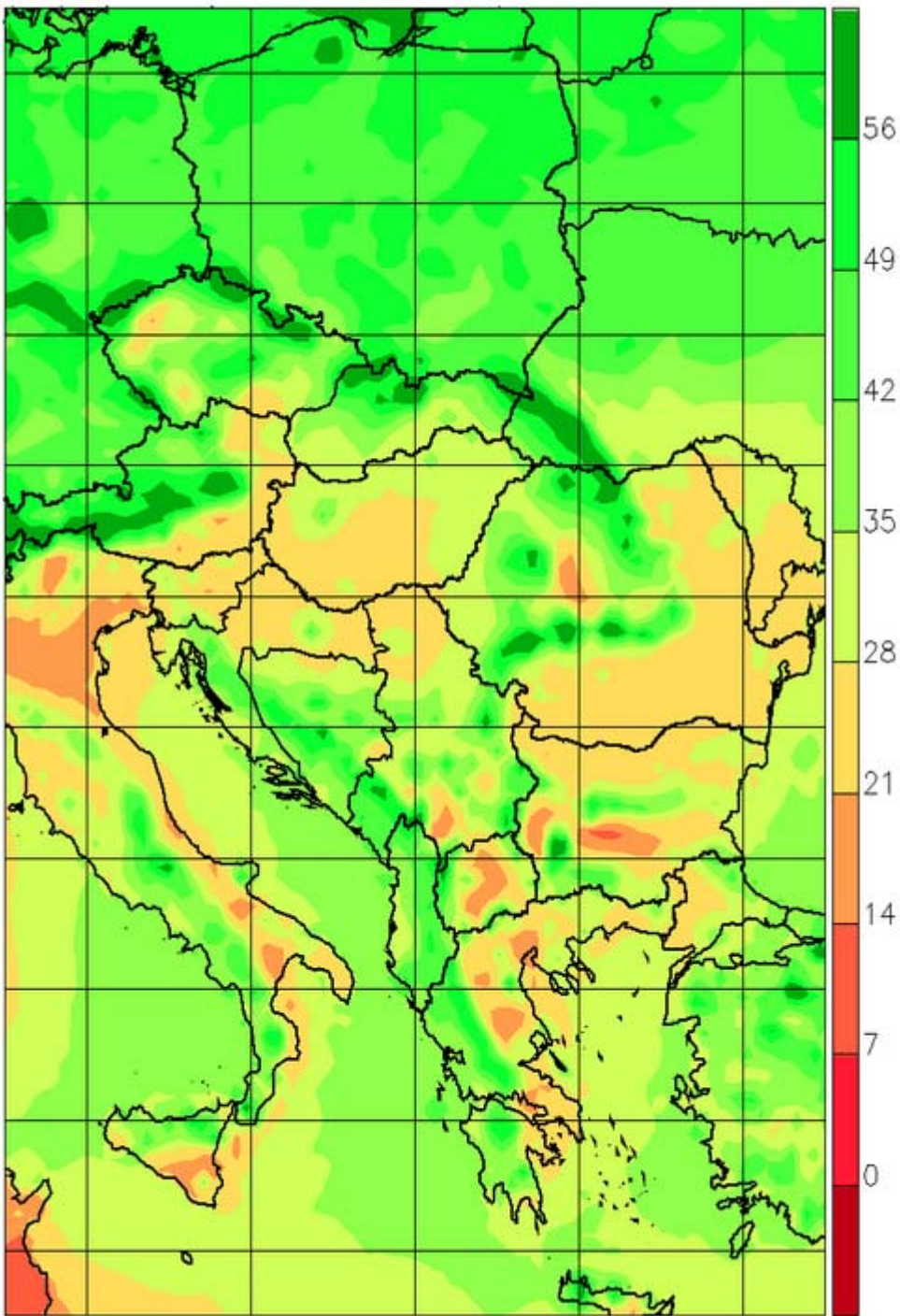
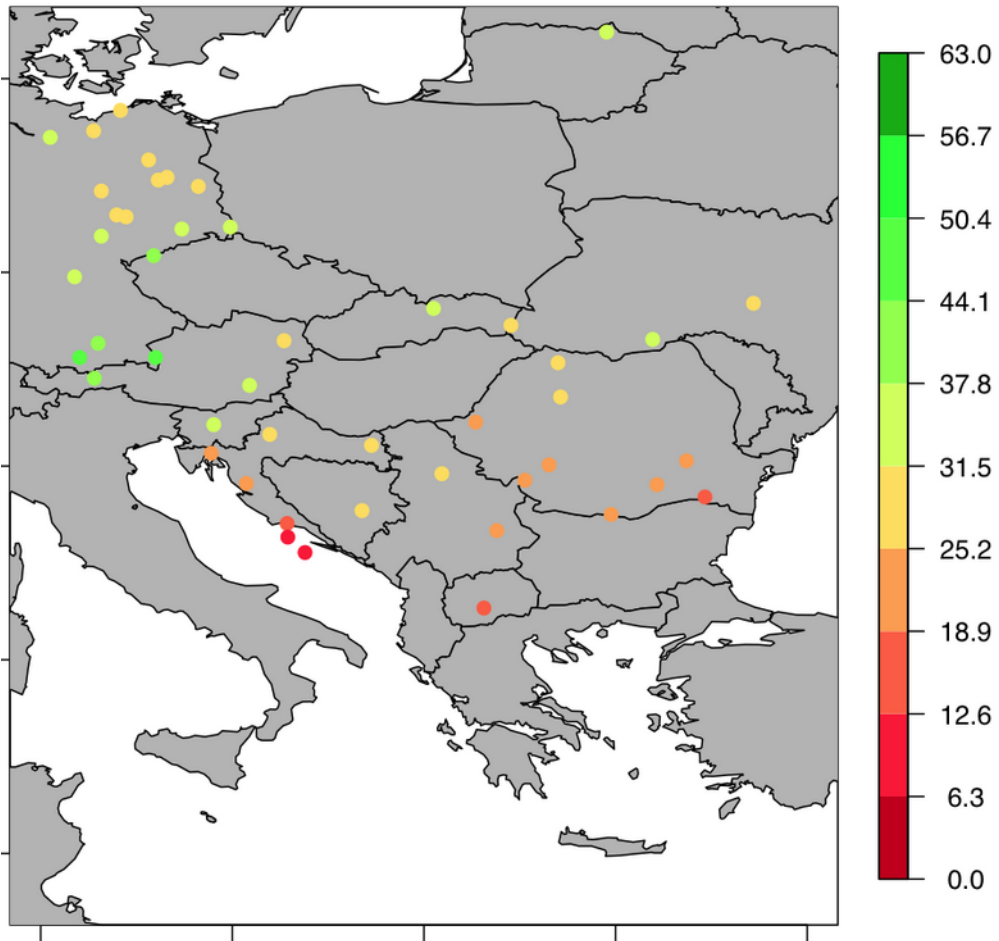
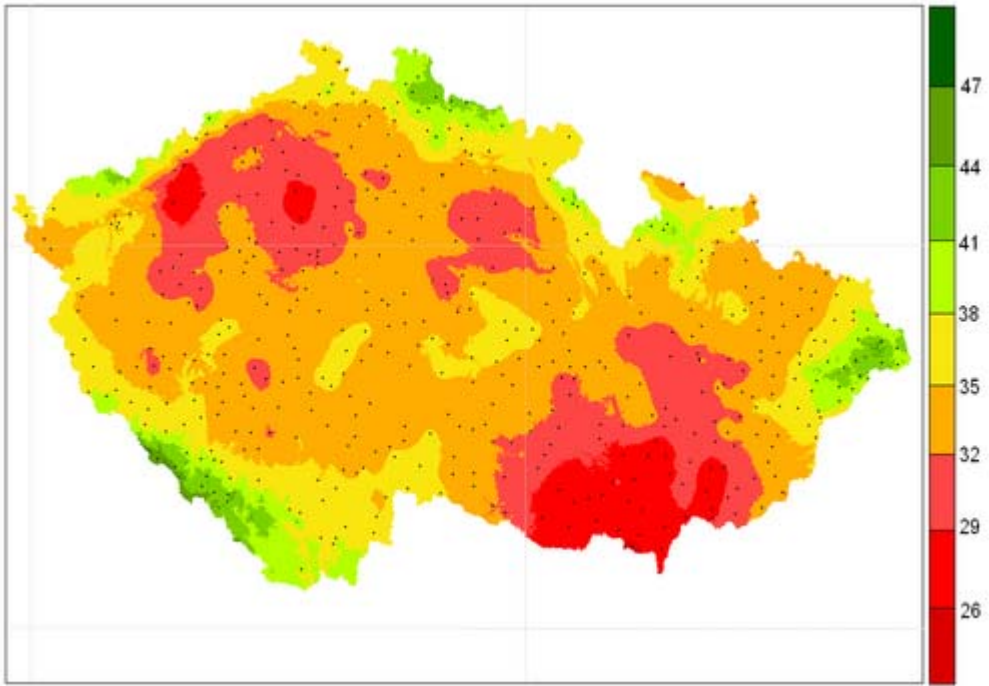


Figure B13 Percentage of wet days, winter (DJF). Panels like the previous figure.



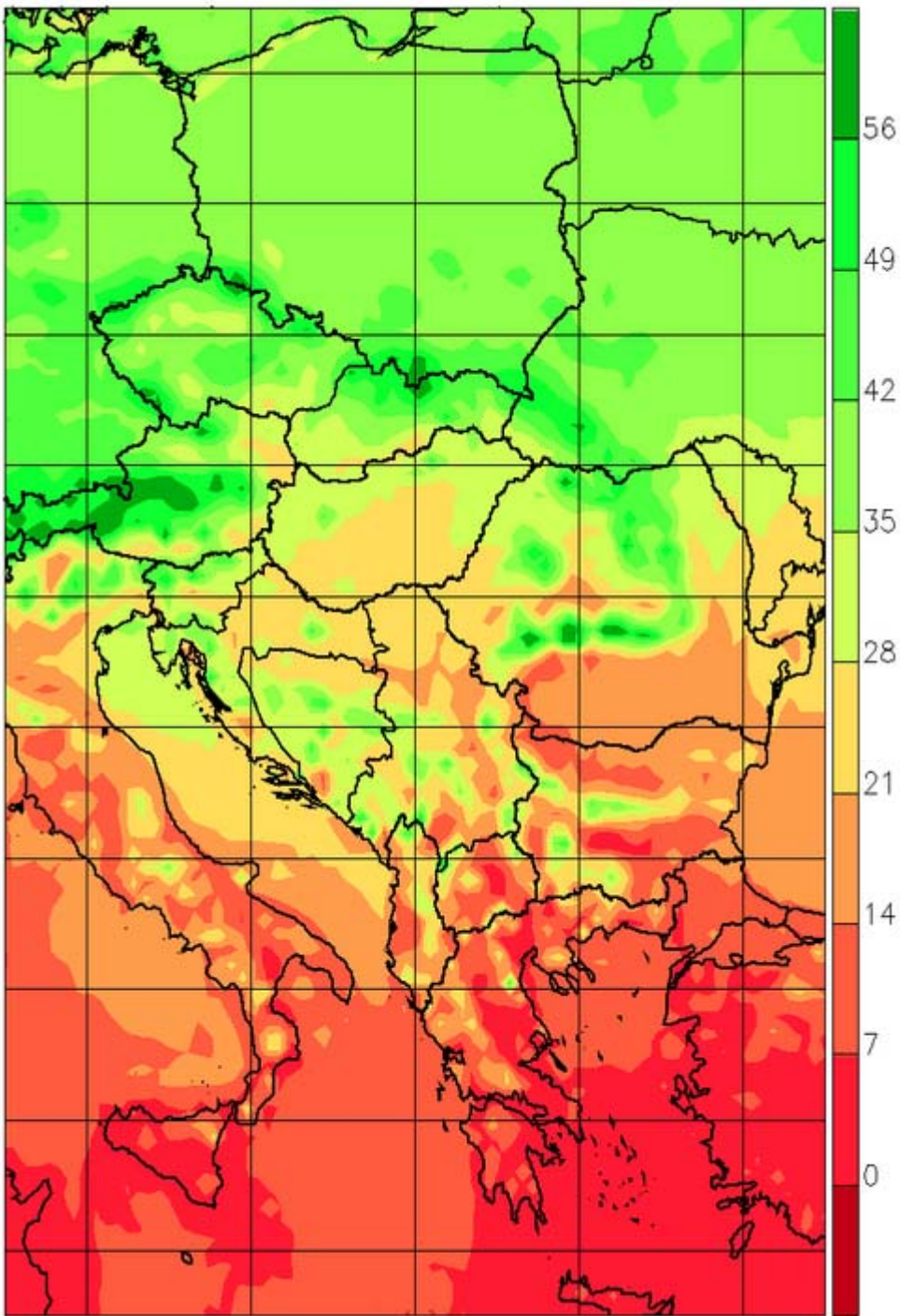
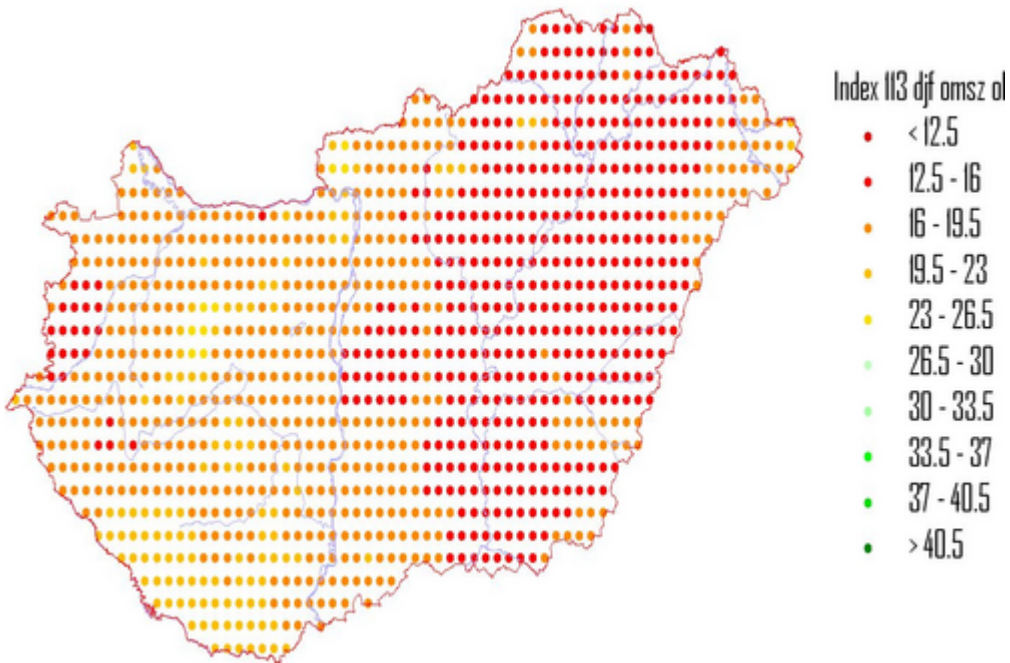
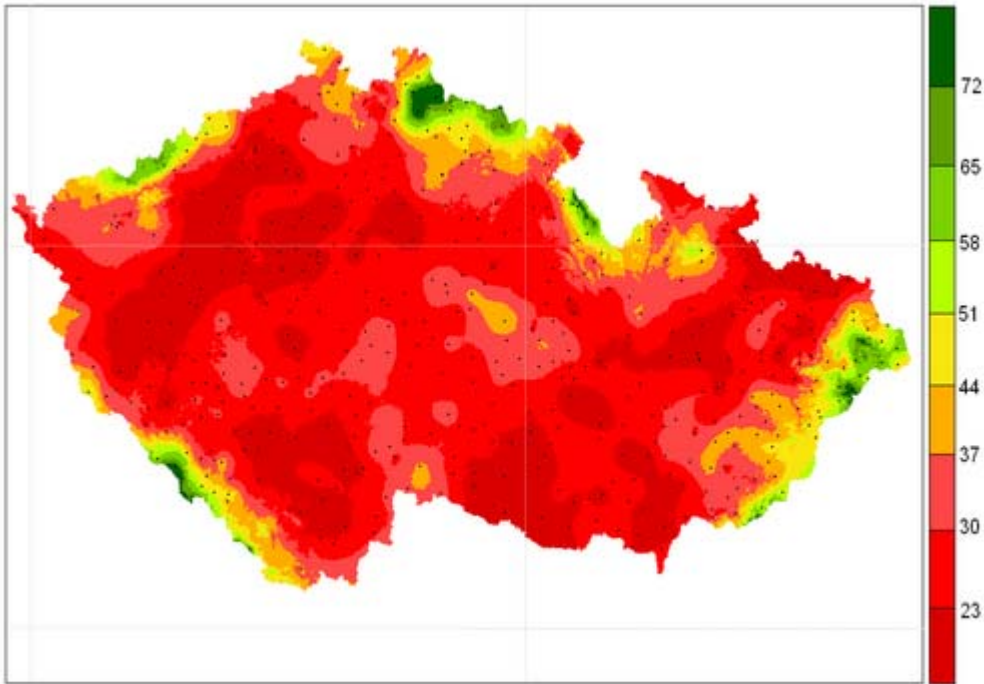
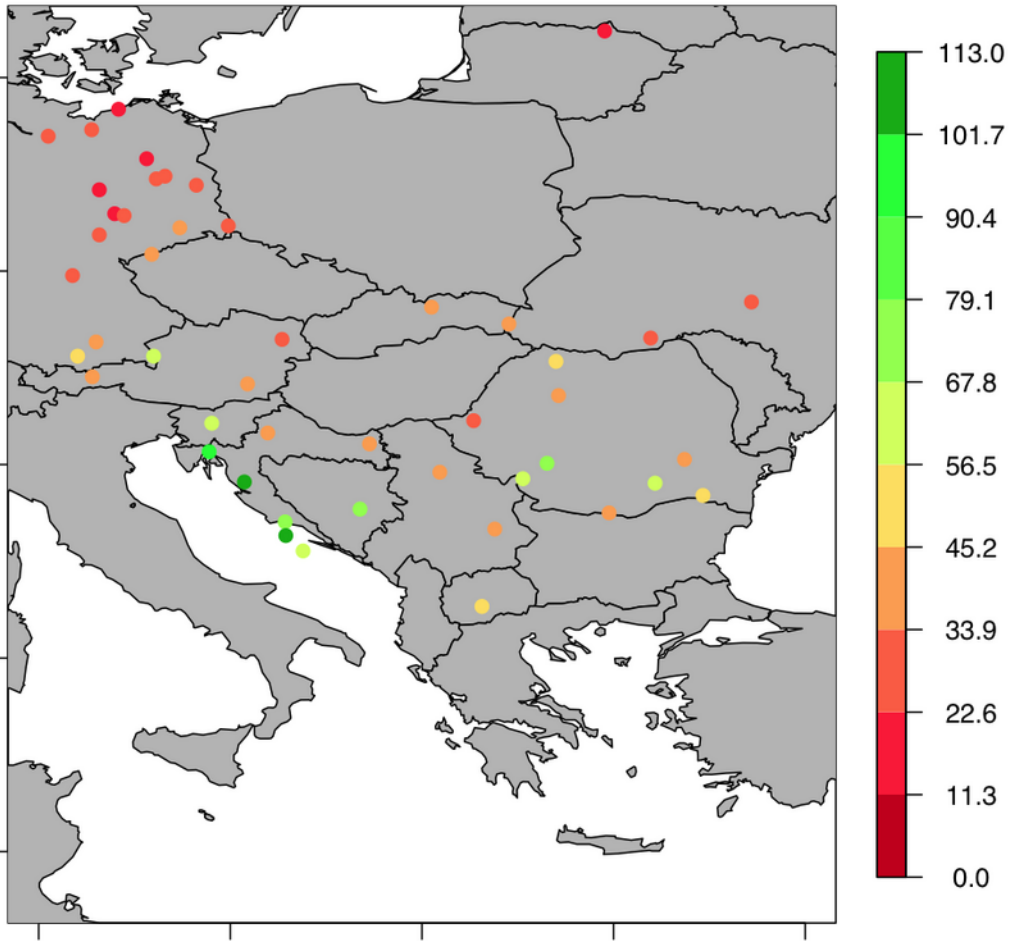


Figure B14 Percentage of wet days, summer (JJA). Panels like the previous figure.





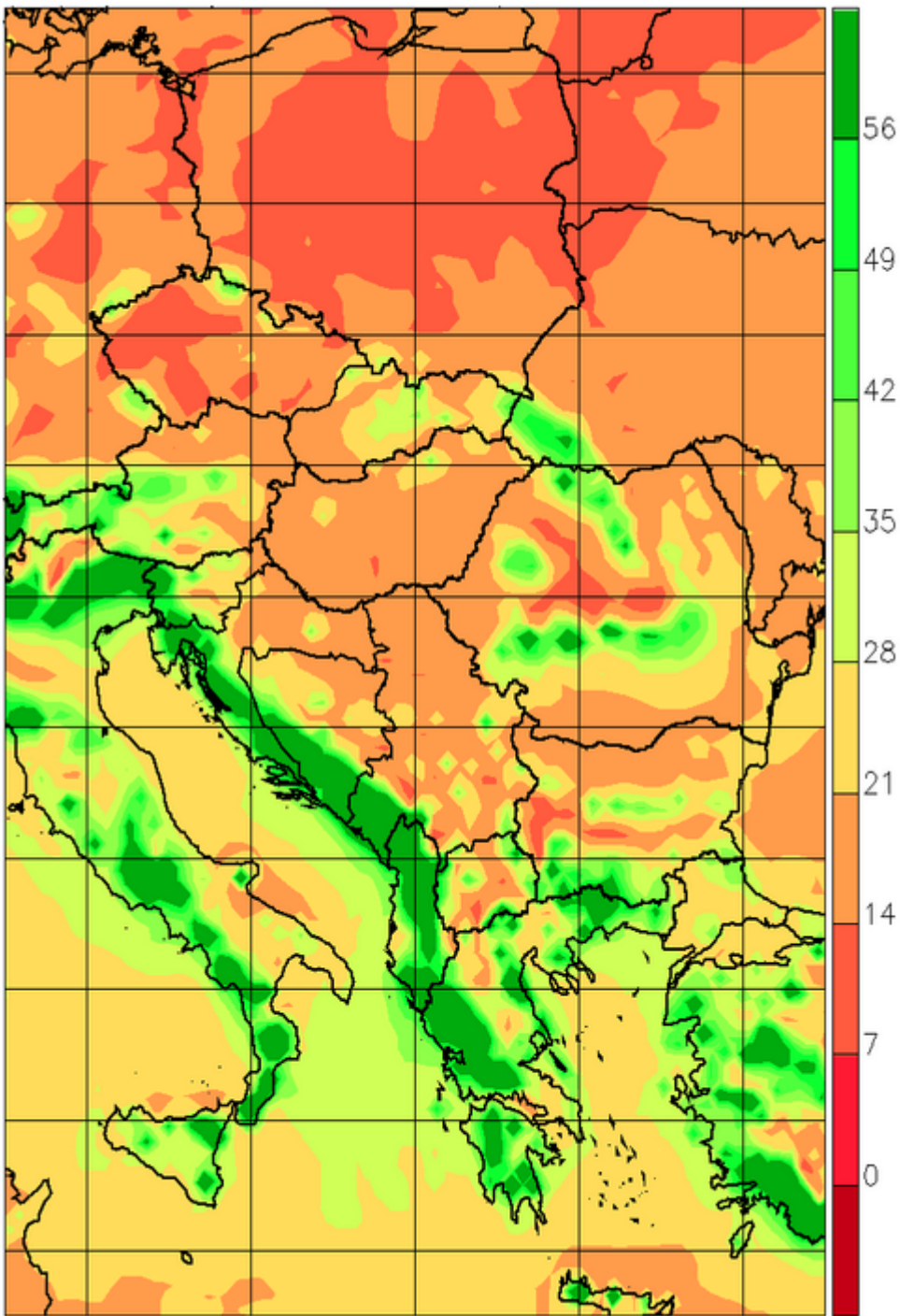
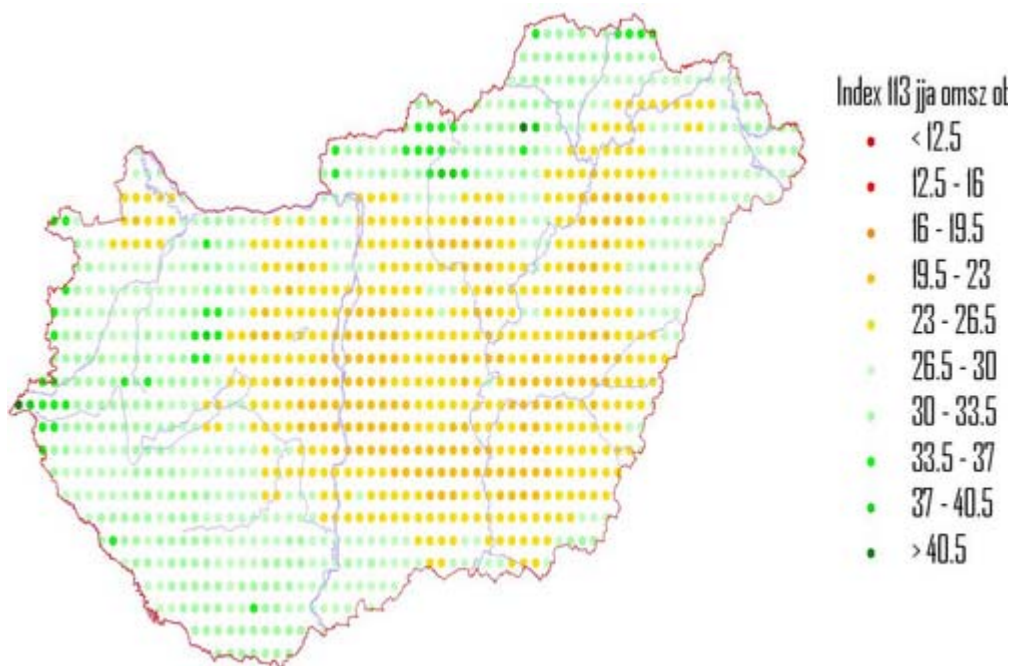
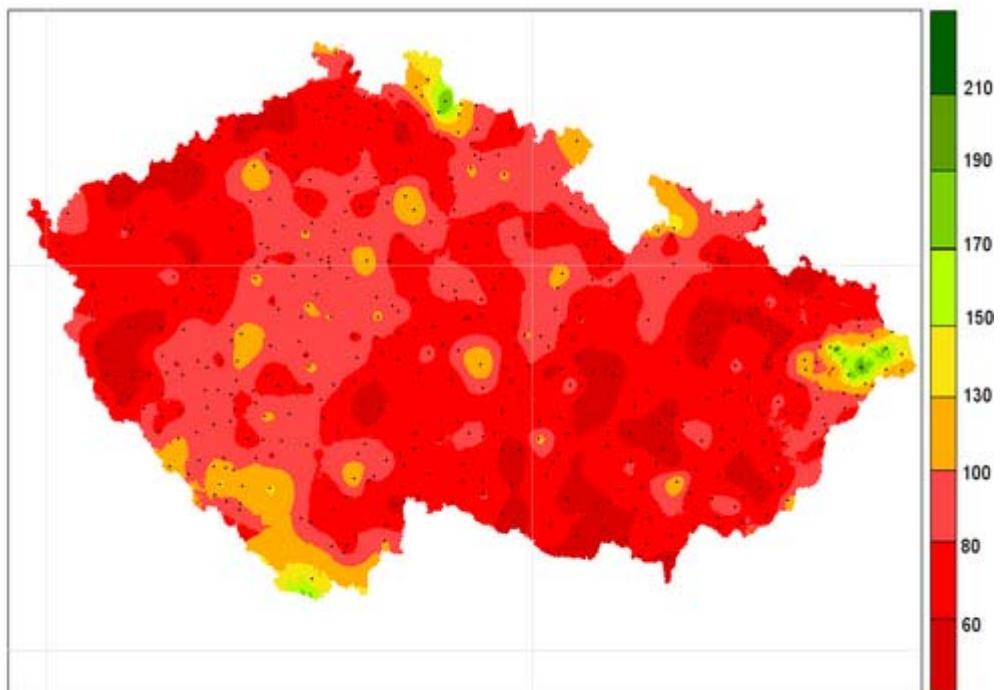
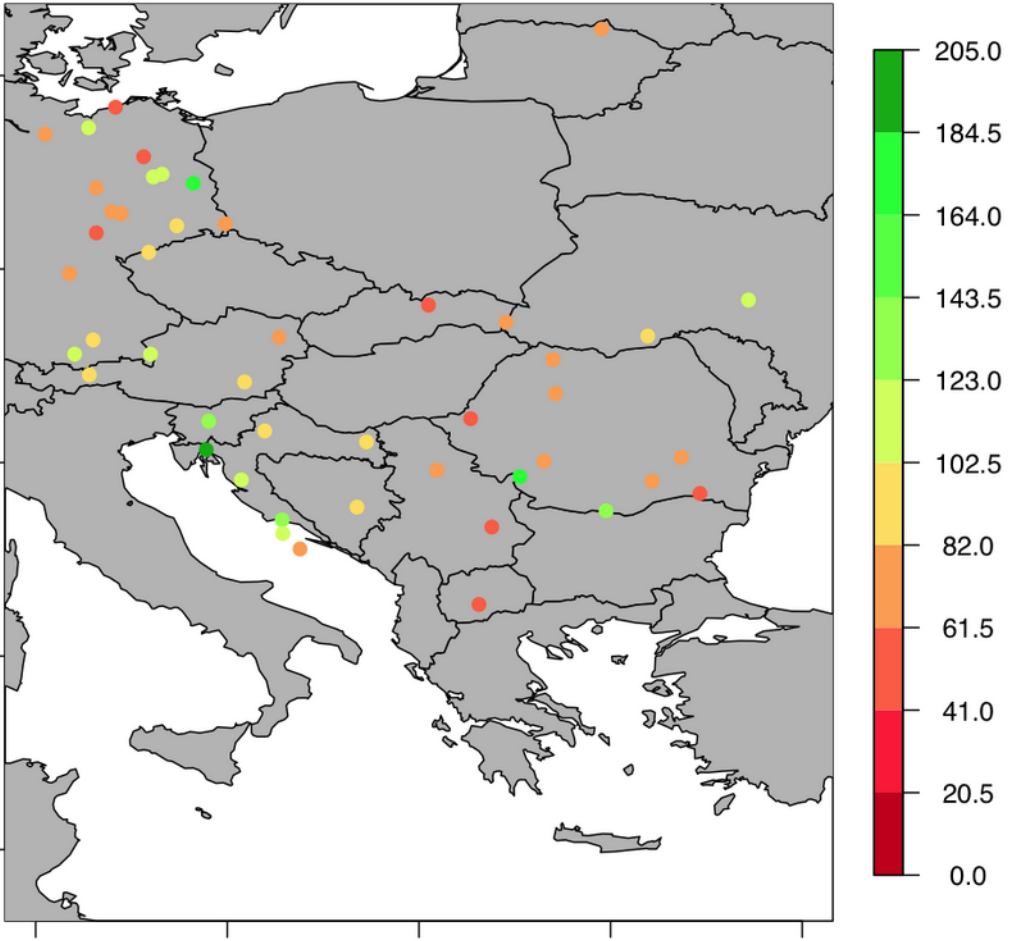


Figure B15 Greatest 1-day rainfall in winter (DJF), mm. Panels like the previous figure.





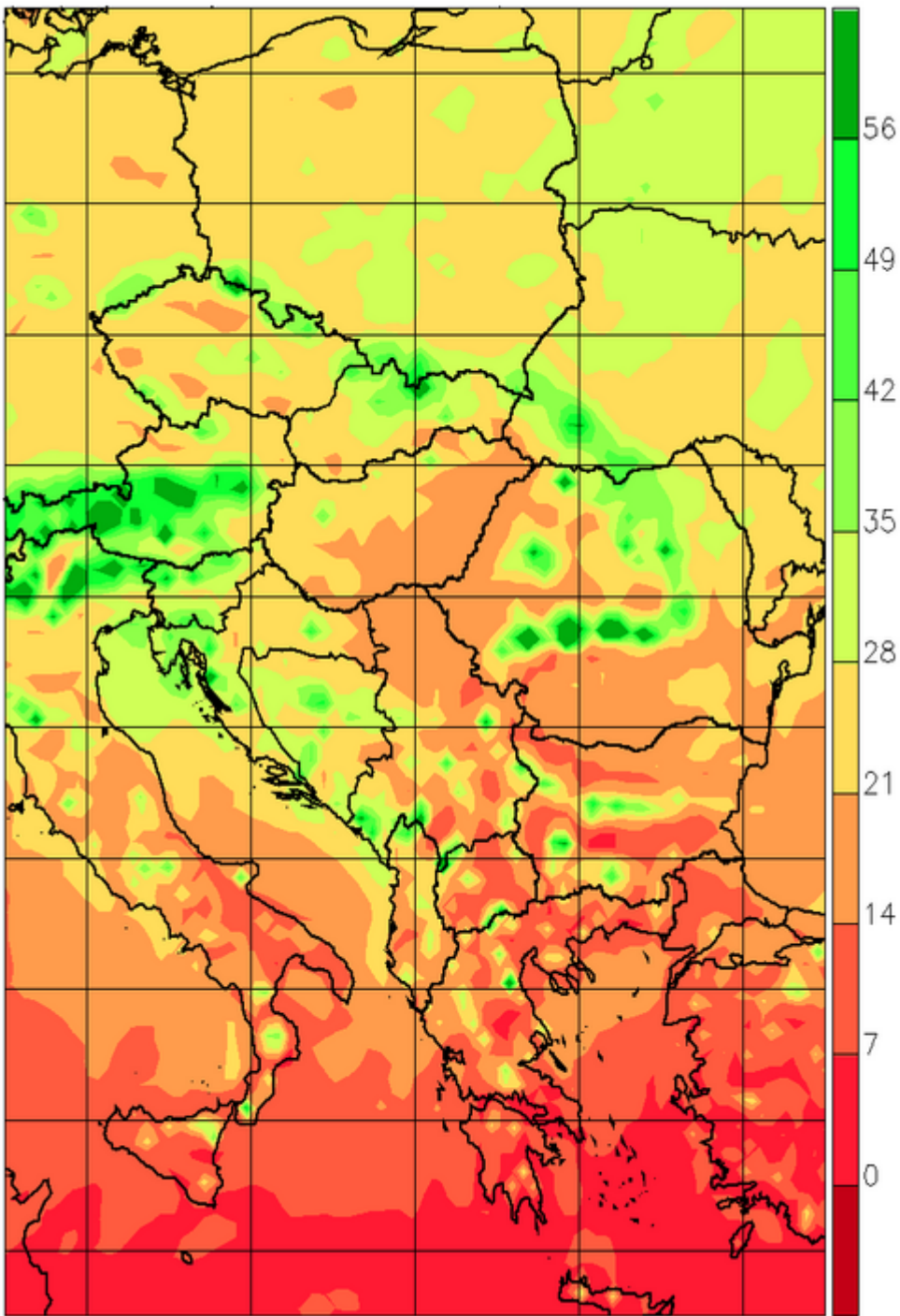
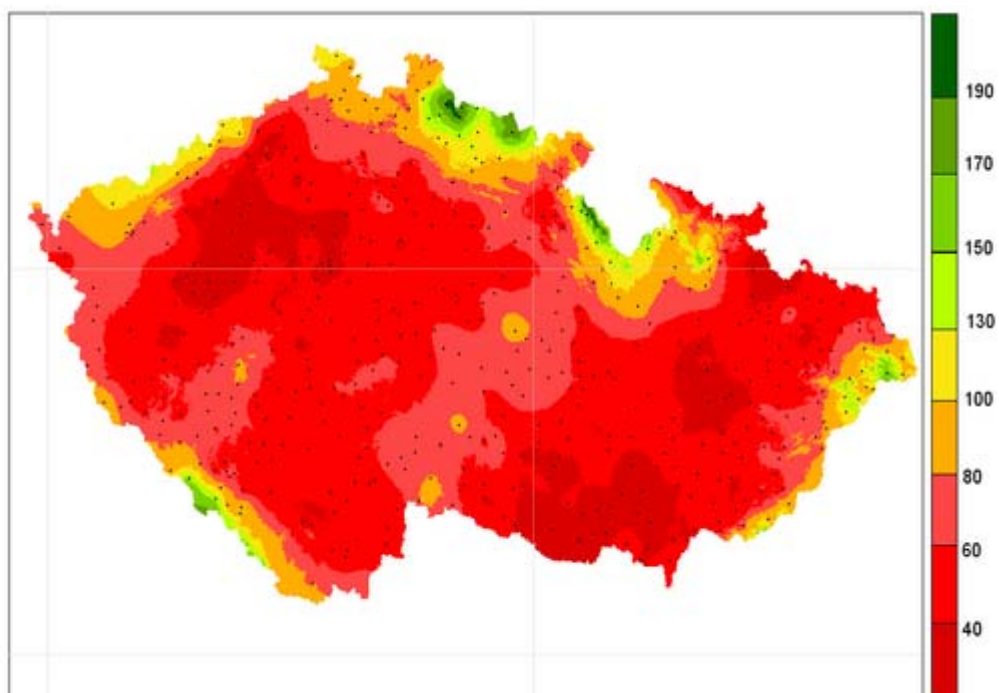
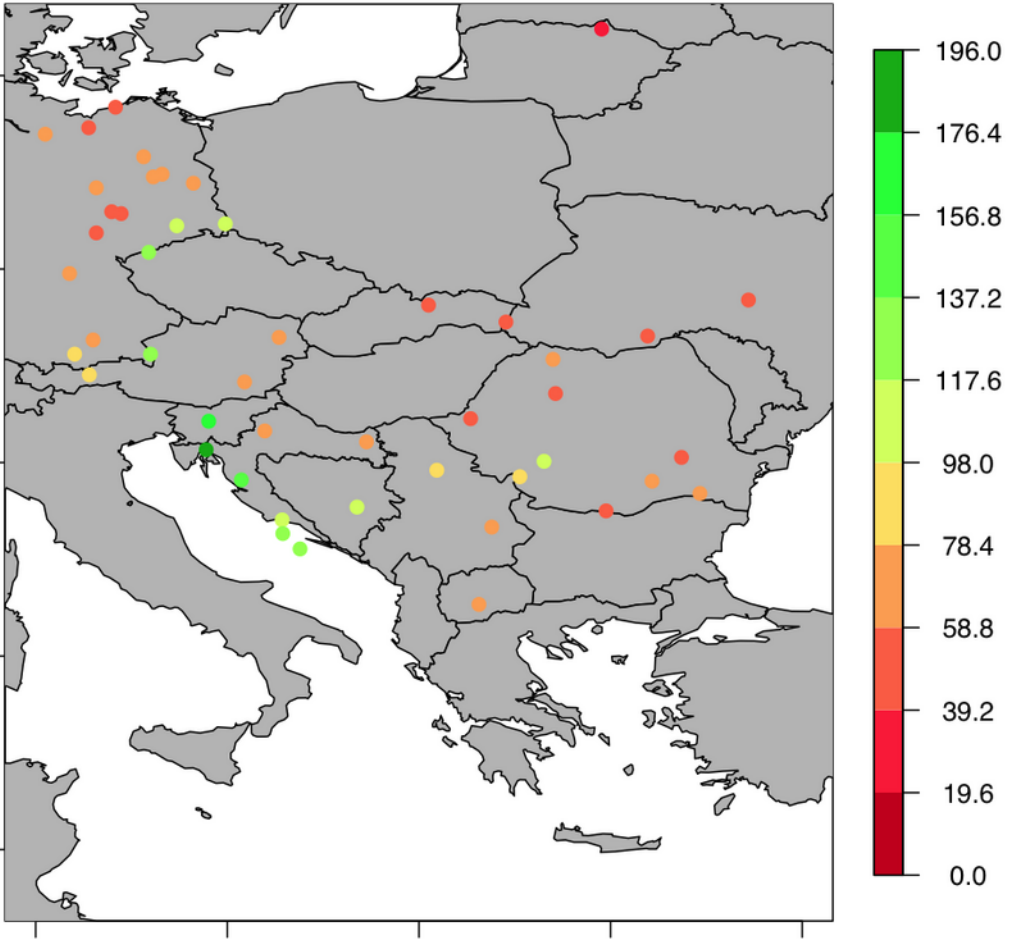


Figure B16 Greatest 1-day rainfall in summer (JJA), mm. Panels like the previous figure.





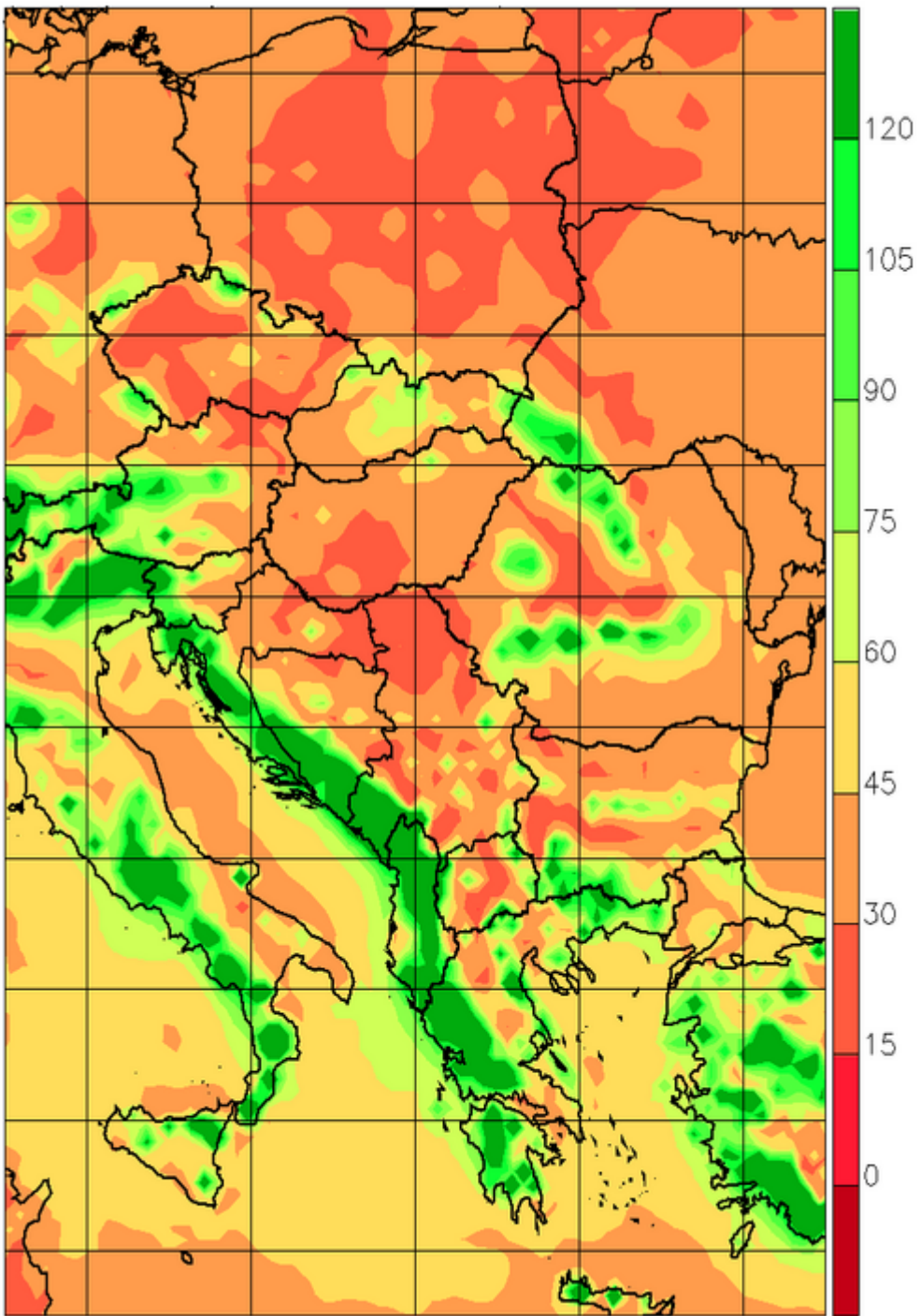
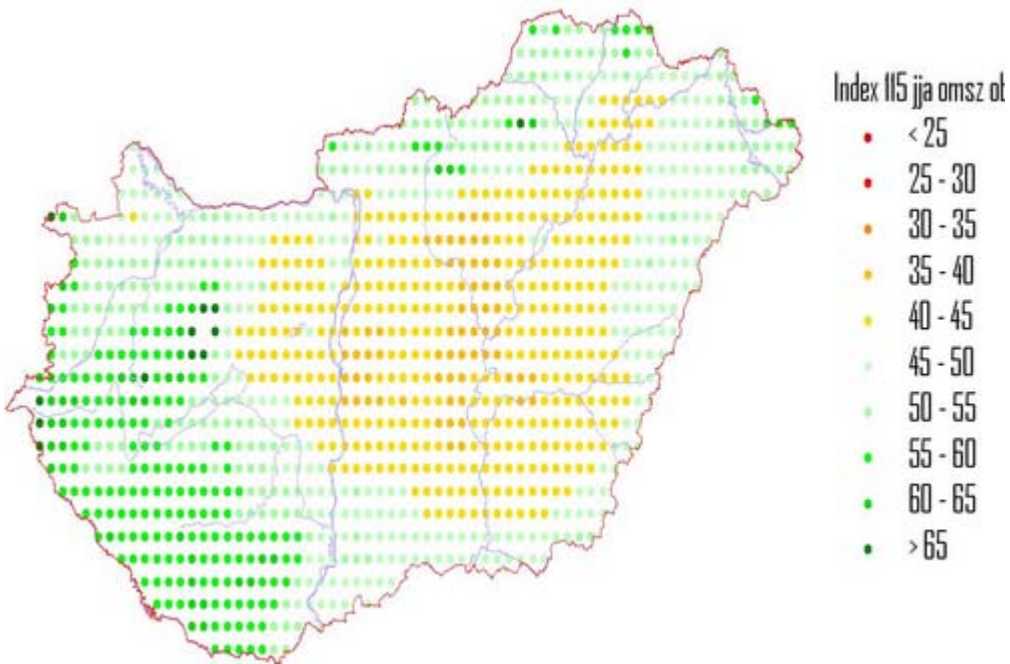
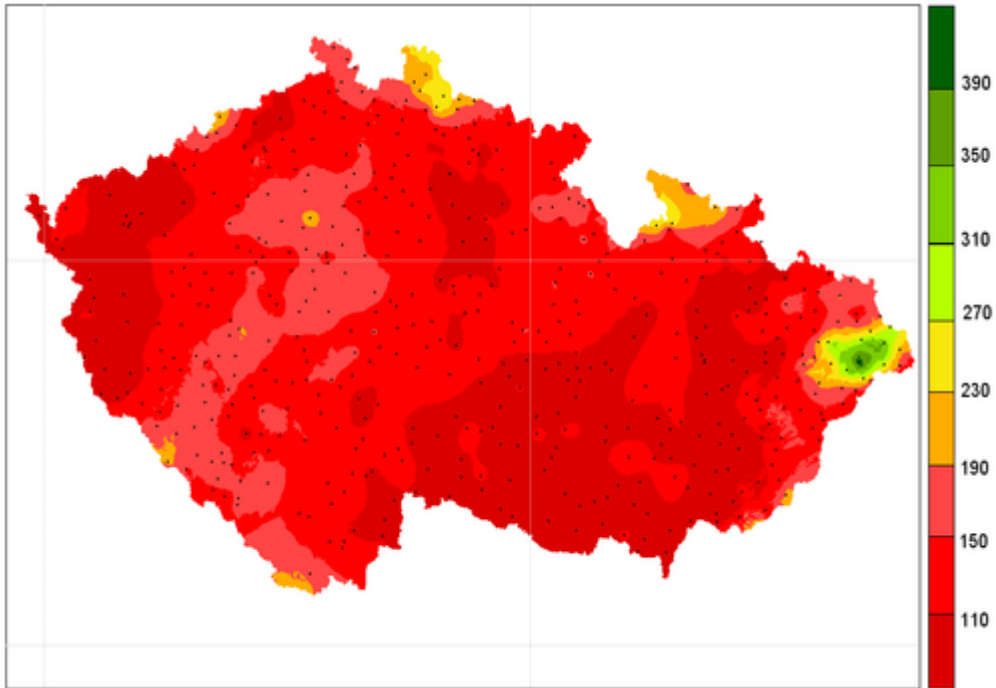
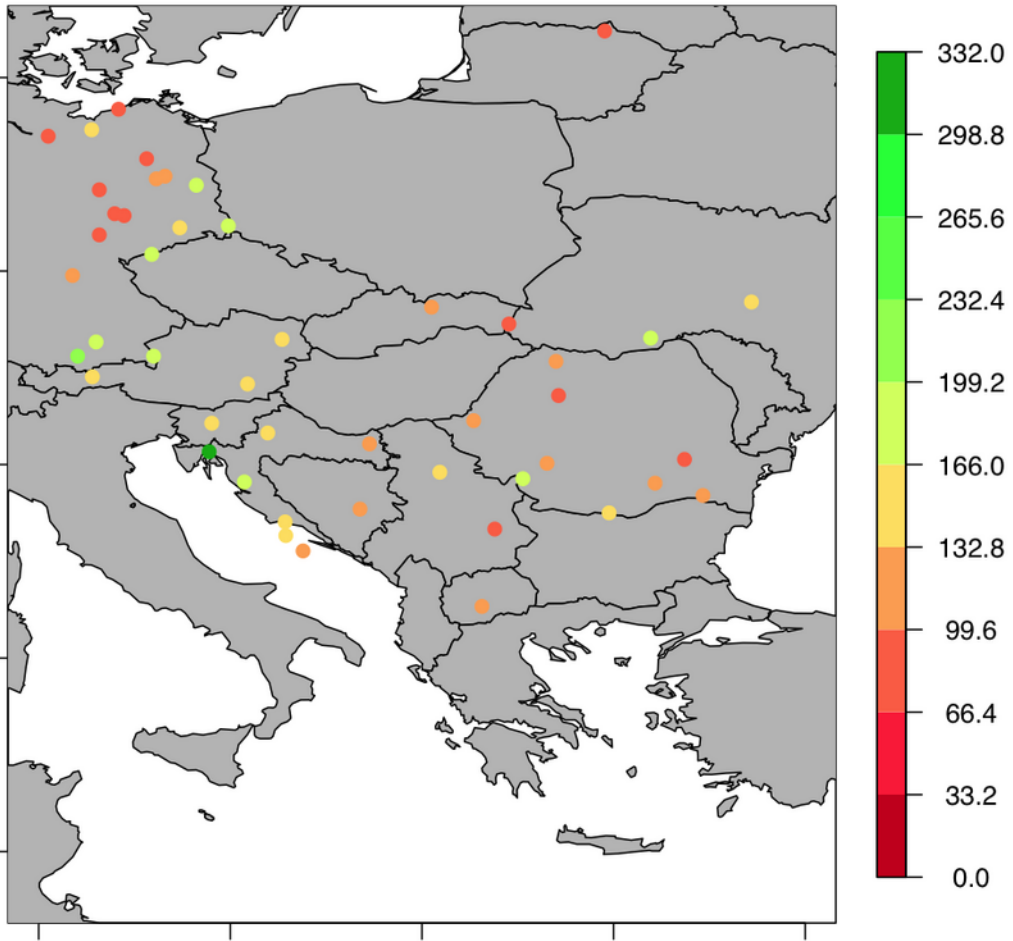


Figure B17 Greatest 5-day rainfall in winter (DJF), mm. Panels like the previous figure.





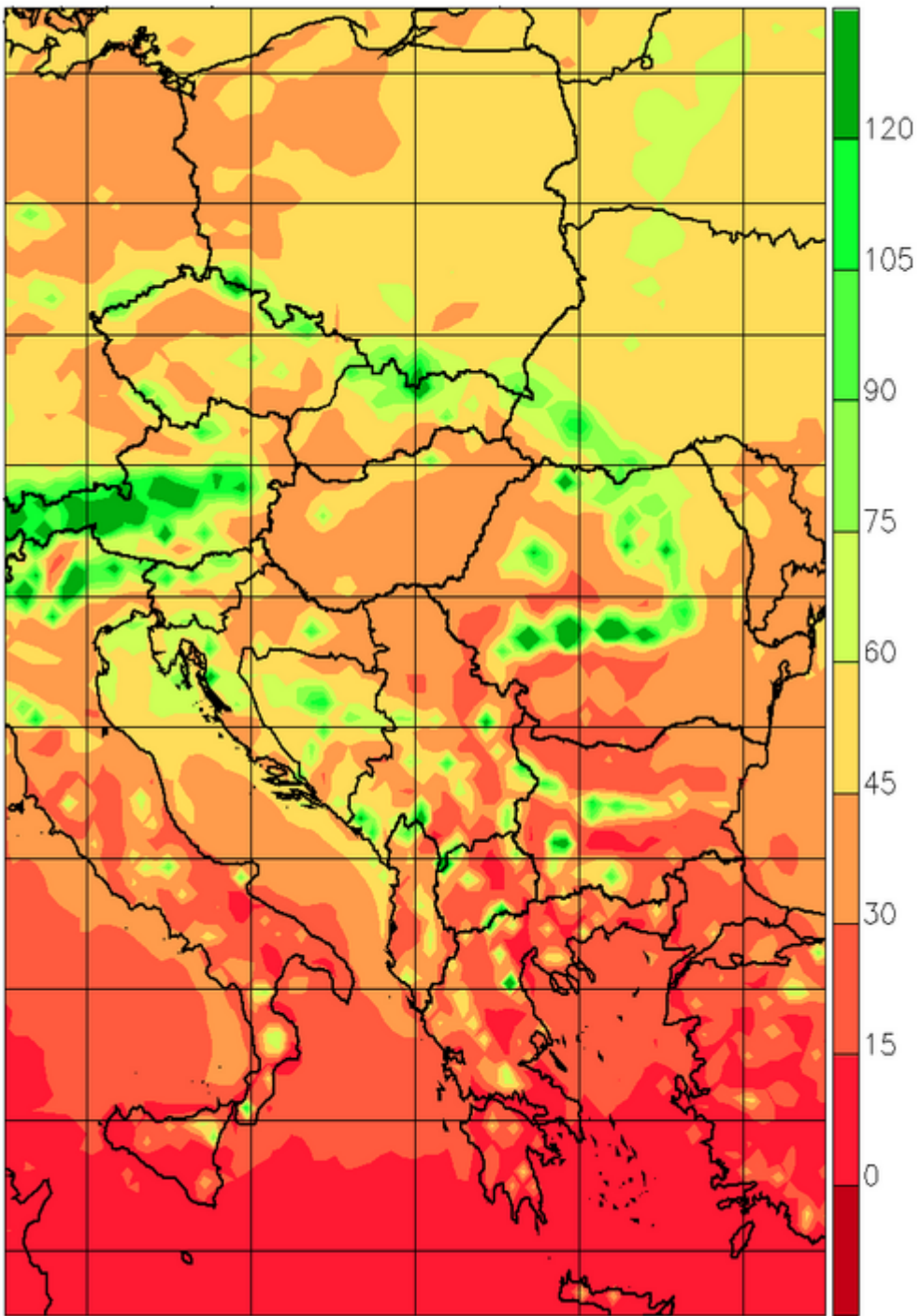


Figure B18 Greatest 5-day rainfall in summer (JJA), mm. Panels like the previous figure.